ERDC/GSL TR-03-12

US Army Corps
of Engineers®
Engineer Research and
Development Center

A Study of Effective Moment of Inertia Models for Full-Scale Reinforced Concrete T-Beams Subjected to a Tandem-Axle Load Configuration

Joseph E. Wickline, Thomas E. Cousins,
and Yazmin Seda-Sanabria

August 2003

Geotechnical and Structures Laboratory

ERDC/GSL TR-03-12
August 2003

A Study of Effective Moment of Inertia Models for Full-Scale Reinforced Concrete T-Beams Subjected to a Tandem-Axle Load Configuration

Joseph E. Wickline, Thomas E. Cousins

Virginia Polytechnic Institute and State University
Blacksburg, VA 24061

Yazmin Seda-Sanabria

Geotechnical and Structures Laboratory
U.S. Army Engineer Research and Development Center
3909 Halls Ferry Road
Vicksburg, MS 39180-6199

Final report

Prepared for U.S. Army Corps of Engineers
Washington, DC 20314-1000

ABSTRACT: This study focuses on some of the research efforts from the U.S. Army Engineer Research and Development Center (ERDC) in developing more accurate procedures for the estimation of the load-carrying capacity of in-service fixed bridges, in particular, of reinforced concrete T-beam bridges. This bridge type represents a stumbling block for U.S. Army field engineers whenever they are faced with unknown important parameters for load capacity estimation such as the amount and location of the flexural reinforcement in the T-beam girder cross sections.

Research personnel from the ERDC in collaboration with personnel from the Virginia Polytechnic Institute and State University worked in the development of a procedure that is potentially more accurate, can be quickly executed in the field, and is relatively easy to use by military engineers. The evaluation procedure presented herein provides a methodology for transition between the quantity of flexural reinforcement in a reinforced concrete T-beam and the member's actual moment of inertia.

This report is aimed at the evaluation of the accuracy of selected, effective moment of inertia models as a component in the proposed evaluation procedure. The accuracy of the selected models is evaluated using laboratory test data generated from an experimental program detailed herein, which included the load testing of full-scale reinforced concrete T-beams. The test specimens were subjected to a closely spaced, tandem-axle load configuration, which represents a typical load configuration in military equipment.

Contents

List of Figures

List of Tables

Preface

This report describes a research study developed by the Virginia Polytechnic Institute and State University (Virginia Tech) in collaboration with the U.S. Army Engineer Research and Development Center (ERDC) for the selection of an appropriate effective of inertia model to accurately define the stiffness behavior of reinforced concrete members. This model will have a key role as part of a load capacity evaluation procedure for reinforced concrete T-beam bridges that is currently being developed at the ERDC. The study was part of the AT40 Direct-Alloted 159T Tele-Engineering Development RDT&E Work Package, Work-Unit TE004 "Rapid Load Capacity Assessment of Reinforced Concrete Bridges," which is sponsored by Headquarters, U.S. Army Corps of Engineers.

This publication was prepared by personnel from Virginia Tech and the ERDC, Geotechnical and Structures Laboratory (GSL), Vicksburg, MS. The research described herein was conducted by Mr. Joseph Wickline and Prof. Thomas E. Cousins, Virginia Tech, and by Ms. Yazmin Seda-Sanabria, Structural Engineering Branch (StEB), GSL. Ms. Seda-Sanabria prepared this publication under the general supervision of Dr. David W. Pittman, Acting Director, GSL; Dr. Robert L. Hall, Chief, Geosciences & Structures Division, GSL; and Mr. James S. Shore, Chief, StEB, GSL.

At the time of publication of this report, COL James R. Rowan, EN, was Commander and Executive Director of ERDC, and Dr. James R. Houston was Director.

1 Introduction

1.1 General

Bridges are one of the most essential links of the communication and logistic systems in military theater-of-operations. Many types of ground military operations frequently require the rapid deployment of personnel and the movement of heavy equipment through an existing transportation network. This network is typically constituted by an assemblage of routes, which in turn are comprised of numerous segments, each of which may include various types of highway structures, such as reinforced-concrete bridges.

The feasibility of the deployment and/or redistribution of ground military forces through a region strongly depends on the capability of the existing bridges to carry heavy military-vehicle loads. Therefore, for the successful accomplishment of such military operations, it becomes crucial that the load-carrying capacity (or load rating) of existing bridges be estimated as accurately as possible. The ability to determine the load rating of all bridge structures comprised within the area of operations undoubtedly plays a strategic role in the selection of the most effective and appropriate route for any given operation. If a bridge on an otherwise desirable route is unable to support the required loads, then alternative routes must be considered. This may highly complicate a ground operation, forcing the relocation of resources and potentially increasing the risks associated with the safety of military personnel and equipment.

In critical operational situations, such as those concerned with rapid deployment of vehicles and troops, the effective recollection of the required information is of paramount concern. Usually, under highly stressful conditions and with very severe time constraints, field reconnaissance teams will rapidly approach the bridge under consideration and retrieve as many crucial configuration parameters as possible. The level and quality of the field information retrieved will be crucial in determining the degree of accuracy of the final assessment of the structural capacity. In many instances, the level of information available for the analysis of the bridges along the selected route is very limited. Some of the most important bridge design parameters are unknown, making it very difficult to reasonably estimate their load capacity. Conservative assumptions based on engineering experience must be considered in the rating analysis in order to obtain a gross estimate of the structural capacity the bridge under consideration. Because of the nature of the assumptions involved, these assessments may result in a severe underestimation of the actual capacity of the bridge, limiting their use

well below the full-service load capacity for which they were originally designed. This situation becomes especially challenging in the case of bridge structures having reinforced-concrete superstructures. In reinforced-concrete T-beam bridges, for example, the girders are among the main components controlling the load capacity of the structure. If the amount of steel reinforcement in the girders is unknown, a good approximation of the actual structural capacity of the bridge will be difficult to determine.

Whenever the military needs to move cargo supplies and personnel through the United States transportation network, the task of determining the load-capacity characteristics of existing reinforced-concrete bridges can be determined fairly accurately. All the necessary information required for the load rating analysis can be obtained from the design specifications and plans of the bridges under consideration. Their complete information is typically well-documented and available through sources such as the National Bridge Inventory (NBI) and local state agencies. However, whenever there is the need to deploy military forces in foreign scenarios, the task of evaluating the capacity of a bridge becomes more complex. Some bridges in foreign countries have cast-in-place reinforced-concrete superstructures, as is the case of T-beam bridges, and specifications related to their design loads, material properties and construction practices are frequently unavailable. While simplified methods based on engineering principles for the load rating of this type of bridges are presently available for the military engineer, they provide a very conservative assessment especially when not all the parameters of the bridge are known. Information such as the amount of steel reinforcement is of critical importance in the determination of the capacity of the bridge main components. If the information on the amount of reinforcement of the T-beam member is lacking, conservative estimates based on design requirements can lead to overly conservative results in its rating analysis.

In recent years, the U.S. Army Engineer Research and Development Center (ERDC) has been working in the development of a rapid evaluation procedure to accurately assess the load-carrying capacity of reinforced concrete T-beam bridges in the military theater of operations. This procedure is aimed at providing an accurate methodology that can be executed in a quick and easy way by military field engineers. As part of these efforts, researchers at ERDC have collaborated with faculty and staff from Virginia Tech in the development of a methodology that incorporates a more accurate definition of the load-deflection behavior of reinforced concrete T-beam members. The study described herein was developed with the goal of assisting these research efforts by providing an evaluation of various effective moment of inertia models currently available in the literature.

1.2 Proposed Evaluation Procedure

The load-carrying capacity of a reinforced concrete T-beam bridge (see Figure 1.1) will strongly depend in the amount of flexural reinforcement of its main load-supporting members, as well as on the mechanical properties of the

materials that constitute them. Typically, under in-service conditions these properties are either partially or completely unknown.

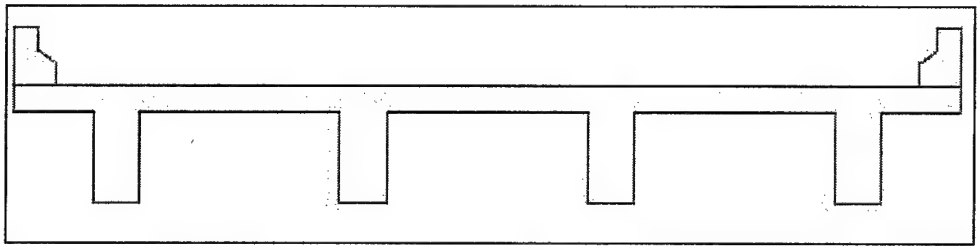

Figure 1.1. Typical T-beam Bridge Cross Section

1.2.1 Study Focus

The focus of this study is to accurately estimate the unknown amount of flexural reinforcement of a reinforced concrete T-beam member. The effects related to the concrete material properties on the load capacity of the member are not addressed by this study under the assumption that compressive strength and, in turn, modulus of elasticity can be reasonably estimated from knowledge pertaining to materials and practices of the region. In addition, this study will evaluate various effective moment of inertia models and their accuracy in defining the stiffness behavior of T-beam members subjected to a tandem-axle load configuration. Proper selection of this model is key in the development of the proposed load capacity evaluation procedure. The proposed procedure, as depicted in the flowchart of Figure 1.2, is aimed at providing a rapid methodology that uses field measurements to estimate parameters typically unknown (such as steel reinforcement) that are key for the determination of the load-carrying capacity of a member.

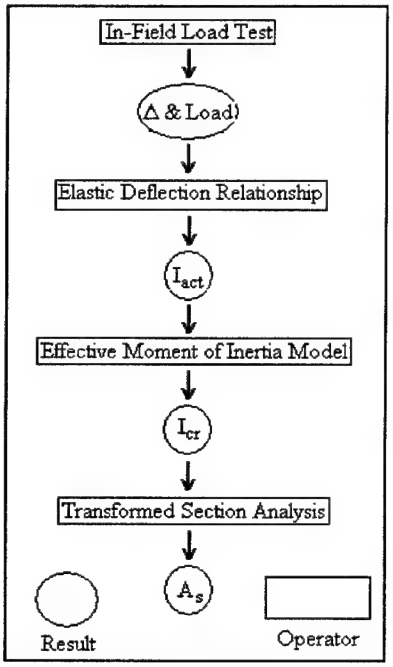

Figure 1.2 Proposed Evaluation Procedure Flow Chart

In this flowchart shown, the term Δ represents the in-field test deflection, I_{act} is the actual moment of inertia, I_{cr} is the cracked moment of inertia, and A_s is the area of flexural reinforcement.

One of the key aspects of this load capacity evaluation procedure is the definition of the load-deflection characteristics (or stiffness behavior) of the reinforced concrete member. Typically, this behavior is represented using semi-empirical approximations to define the transition between the moment of inertia (or stiffness) of the loaded member between its pre-cracked and cracked condition. In design practice, one of the models most commonly used to define this transition has been adopted by the American Concrete Institute (ACI) Building Code and is known as the Branson equation (ACI 2002). This equation, also known as the effective moment of inertia, (I_e), represents an "average" value of the moment of inertia along the length of the member and is given as:

$$I_e = (M_{cr}/M_a)^3 I_g + [1-(M_{cr}/M_a)^3] I_{cr} \leq I_g \tag{1.1}$$

where

I_e = effective moment of inertia
M_a = maximum applied moment
I_g = gross moment of inertia
I_{cr} = cracked moment of inertia of the member

The Branson model, along with three other effective moment of inertia models, are evaluated as part of this study using experimental data obtained as part of the testing program described in Chapter 3.

1.2.2 Procedure Limitations

The accuracy involved in the results of a reinforced concrete T-beam bridge load-capacity evaluation procedure can be affected by many factors. Some of these factors include the magnitude of the vehicle loads, the vehicular wheel configuration, as well as the way that loads are distributed into the main carrying members. Thus, it is of utmost importance to select an effective moment of inertia model that accurately represents the load-deformation behavior of the main load-carrying members.

1.3 Objective

The objective of this study is to identify an effective moment of inertia model that can accurately represent the stiffness behavior of a reinforced concrete T-beam bridge girder subject to a typical military load configuration. This model will be used as part of a load-capacity evaluation procedure or T-beam bridges currently under development at ERDC.

2 Literature Review

2.1 Introduction

The control of deflections experienced by reinforced concrete members during service load conditions was not of concern until the late 1950s (Yu and Winter 1960). During that period, material manufactures began producing higher strength concrete and reinforcing steel and the reinforced concrete design community accepted the ultimate strength design philosophy. The combination of these factors resulted in the design of significantly shallower, reinforced concrete members for the same prescribed loads. The shallower members provided significant cost savings, but a drawback to the developments was the significant deflections that the shallower members experienced under service load that the earlier, bulky members did not. Therefore, the need for a reliable means of calculating the deflection a reinforced concrete member would experience under service load conditions was created.

2.2 Early Reinforced Concrete Design

2.2.1 General

The only mention of deflection in all editions of the American Concrete Institute (ACI) Building Code prior to the 1963 edition was the maximum allowable deflection limits printed under the "Loading and Criteria of Acceptability" section of the Code (ACI 1956). No further guidelines or methodology for calculating deflections was given. Designers calculated member deflection, then as now, with an elastic deflection relationship that could be derived from any one of numerous structural analysis methods. A stumbling block for designers of that time and a source of debate in the academic community was which moment of inertia value to incorporate in the elastic deflection relationship (ACI 1966).

The moment of inertia combined with the modulus of elasticity represents the bending stiffness of a reinforced concrete member. Bending stiffness is easily defined for a true homogenous material like steel, but for a material like reinforced concrete it is, at best, an estimate that is controlled by cracking, creep, shrinkage, and load history (Grossman 1981). Prior to the early 1960s, researchers had developed relationships to accurately determine the modulus of elasticity

of concrete (ACI 1966), but an accurate method of determining the moment of inertia, as a function of the factors mentioned above, did not exist. Therefore, the only means of estimating the deflection that a reinforced concrete member may experience at service load was to conservatively use the cracked moment of inertia (I_{cr}) or unconservatively use the gross moment of inertia (I_g) of the cross-section.

2.2.2 Early Deflection Models

One of the earliest deflection models was developed by Maney in 1914 (Equation 2.1) and was based on the assumption that I_{cr} represents the moment of inertia throughout the length of the member (ACI 1966).

$$\Delta = kL^2(f_s + \eta f_c^{'} / E_s d) \tag{2.1}$$

where

Δ = member deflection
k = constant (function of loading configuration and end constraints)
L = length of the member
f_s = stress in the reinforcing steel
$f_c^{'}$ = compressive stress of concrete
n = modular ratio
E_s = reinforcing steel modulus of elasticity
d = depth of the reinforcement centroid measured from the compression face of the section

T. Myrlea, chairman of ACI Committee 307 (an early committee formed by ACI to study the deflection of reinforced concrete members) suggested the adoption of Equation 2.1 by the ACI Building Code (ACI 1931). In 1940 Murashev proposed increasing the elastic modulus of the steel reinforcement in Equation 2.1 to account for the portion of concrete in the tension region not yet cracked, which adds to the flexural stiffness of the reinforced concrete member (ACI 1966). This modification can be expressed as:

$$E_s = E_s / \psi \tag{2.2}$$

where E_s is the reinforcing steel modulus of elasticity, and

$$\Psi = 1 - (2/3)(M_{cr} / M_a)^2 \leq 1.0 \tag{2.2a}$$

where

M_{cr} = cracking moment
M_a = applied moment in the member

The ACI Code adopted neither form of Maney's equation, nor any other equations developed during those early years, probably due to the lack of

significance of service load deflections rather than for the validity of any of these expressions.

2.3 Effective Moment of Inertia

The increase in concrete and steel strengths and the acceptance of ultimate strength design during the late 1950s and the early 1960s prompted many efforts to develop an easy, reliable way of calculating the service load deflections experienced by a reinforced concrete member. The new information on the subject combined with the existing information, arguing the use of I_g or I_{cr}, prompted ACI Committee 318 in 1957 to form ACI Committee 435 to research the methods and literature regarding the deflection of reinforced concrete members. The members of ACI Committee 435 published a comprehensive study detailing their research in the June 1966 edition of the ACI Journal Proceedings (ACI 1966). A portion of that report detailed the performance of two relatively new procedures for calculating the deflection of reinforced concrete members; both procedures were based on an "effective" moment of inertia that provided a transition between the gross and cracked moments of inertia and is assumed to be constant along the length of the member.

2.3.1 Yu and Winter Research

In 1960 Yu and Winter published the findings of their extensive research that studied the deflection of rectangular and flanged reinforced concrete members under working loads (Yu and Winter 1960). Their research was two-fold, investigating both short-time and long-time deflections of rectangular and flanged cross-sections subjected to uniform load. The authors compared theoretical deflections, calculated by two different methods, to deflection data acquired from six independent investigations by other individuals. The first method (Method A) used to compute defections simply used I_{cr} in the appropriate elastic deflection equation. The second means of calculating deflections (Method B) accounts for the flexural rigidity supplied by un-cracked concrete on the tension face of the member. The supplemental rigidity was accounted for by multiplying the deflection obtained in Method A by a correction factor. The correction factor was applied directly to the elastic deflection equation by replacing I_{cr} with I_{eff} calculated with Equation 2.3.

$$I_{eff} = I_{cr} / (1 - b * (M_1 / M_a)) \tag{2.3}$$

where

b = width of beam on the tension side
I_{eff} = effective moment of inertia
I_{cr} = cracked moment of inertia
M_a = applied moment

$$M_1 = 0.1(f_c')^{2/3} h(h - kd) \tag{2.3a}$$

where

f_c' = concrete compressive strength
h = total height of member
k = constant (function of loading configuration and end restraint)
d = effective depth

Ideally, Equation 2.3 yields a value between I_g and I_{cr}. The values obtained from Method B gave slightly better results than Method A when compared to the experimental deflection data. Yu and Winter were the first researchers to publish any form of an effective moment of inertia model.

2.3.2 Branson's Model

Dan E. Branson published the most notable reinforced concrete deflection study in 1963 (Branson 1963). The purpose of Branson's study was to determine if an "effective" moment of inertia model developed by him was accurate and reliable. Like Yu and Winter (1960), Branson tested the validity of his model by comparing it to deflection data obtained during other investigations of rectangular and flanged cross-sections subjected to uniform load. The model, given by Equation 1.1, is in the form of applied load and inherently bounded by I_{cr} and by a logical upper bound of I_g. The cubic exponent was empirically determined by applying the model to rectangular and flanged cross-sectioned beams subjected to uniform loading. This exponent allowed the model to inherently account for the permanent deflection sustained by a reinforced concrete member due to the inelastic effects of tensile cracking (PCA 1999). Equation 1.1 was found to be accurate and reliable for the purpose of estimating the immediate deflections of a reinforced concrete member when compared to test data available at that point in time.

The ACI Building Code adopted Branson's equation in its 1971 edition as the acceptable model for the computation of effective moment of inertia. It remains until today as the recommended approach for the calculation of immediate deflections in a reinforced concrete member. Branson's effective moment of inertia equation, unlike Yu and Winter's model, is inherently bounded by I_{cr} and is void of any terms that would associate it to the allowable stress design philosophy.

2.4 Moment-Curvature Relationships

An alternative to the effective moment of inertia approach of calculating reinforced concrete member deflections is the integration of curvatures method (Ghali 1993). Integration of curvatures involves calculating the curvature due to a given load (Equation 2.4) at various points along a member and integrating the curvatures over the member's length to obtain the deflection at a desired location (Kassimali 1995).

$$\psi = M/(EI) \tag{2.4}$$

where

ψ = the curvature
M = applied moment
E = modulus of elasticity
I = moment of inertia

Equation 2.5 gives the basic integral for calculating member deflection (Kassimali 1995).

$$\Delta = \int \psi x \, dx \tag{2.5}$$

where Δ is the deflection, and x is the location of desired deflection value.

This procedure shows to be a more accurate representation than previous models because the variation in stiffness along the length of the member is accounted for and not assumed constant (Ghali 1993). An "effective" stiffness must be obtained to account for the portion of uncracked concrete in the tension region that contributes to the flexural rigidity of the member. This effect is handled in the European Building Code (CEB-FIP 1990) for reinforced concrete by Equation 2.6, which gives an expression to calculate a mean curvature to be used in Equation 2.5.

$$\psi_m = (1-\zeta)\psi_1 + \zeta\psi_2 \tag{2.6}$$

where

ψ_m = mean curvature (at a specific location)
ψ_1 = curvature at uncracked section
ψ_2 = curvature at cracked section
ζ = interpolation coefficient

Like the effective moment of inertia models presented above, the mean curvature expression is empirical. The empirical nature lies in the interpolation coefficient (ζ) in Equation 2.6 (Sherif and Dilger 1998). The major downfall of this method is the time required for its execution. In most instances, a computer is required to expedite the procedure.

2.5 Other Effective Moment of Inertia Models

Since its adoption by the ACI Code in 1971, Branson's model has been continually opposed. The reasons vary, but center around the accuracy of the model. Design engineers argue that the cumbersome calculation of I_{cr}, especially for flanged sections, is complex and time consuming (Grossman 1981). They also argue that the final product does not justify the effort required. Grossman (1981)

states that the estimated deflection obtained by using Branson's model is, at best, within ±20 percent of experimental deflections obtained in a controlled lab setting. Another argument against Branson's model is that its empirical nature can produce gross errors when applied to beams that are either lightly or heavily reinforced and/or subjected to non-uniform loads. Researchers have shown, that in some instances, Branson's model can produce values that are 100 percent in error (Fikry and Thomas 1998).

These arguments and concerns prompted various researchers to study the validity of Branson's equation. The subsequent research produced numerous simplifications and enhancements to the Branson model.

2.5.1 Branson Simplified

A study by Grossman (1981) determined that Branson's model could be simplified such that the computation of I_{cr} was not needed, therefore allowing an estimation of I_e to be made before the quantity and placement of steel reinforcement was determined (Grossman 1981). The procedure can be stated as follows:

$$\text{For } M_a/M_{cr} < 1.6: \qquad I_e/I_g = (M_{cr}/M_a)^2 \leq 1.0 \tag{2.7a}$$

$$\text{For } M_a/M_{cr} > 1.6: \qquad I_e/I_g = 0.1(M_a/M_{cr}) \tag{2.7b}$$

where

I_e = effective moment of inertia
I_g = gross moment of inertia
M_a = applied moment
M_{cr} = cracked moment of inertia

A lower bound of I_e/I_g equal to 0.35 is to be applied to both relationships.

The above relationships were obtained from a parametric study conducted by Grossman (1981) that applied Branson's equation to numerous design situations in which reinforced concrete members had increasing loads applied to them. Grossman's study was based on the assumption that Branson's equation was correct in all instances.

2.5.2 Graphical representations of Branson's model

A few researchers succeeded in graphically representing Branson's model. One such researcher was Lutz (1973), who developed two sets of curves that allowed I_g, I_e, and M_{cr} to be determined from the cross-section geometry, reinforcement ratio, and the concrete properties of a given member.

These graphical methods may have proved useful in the pre-computer reinforced concrete design community, but their usefulness waned in the wake of programmable calculators and personal computers.

2.5.3 Effect of Loading Configuration on the Effective Moment of Inertia

In 1991 scholars from King Saud University in Riyadh, Saudi Arabia, published findings from research conducted aimed at determining if non-uniform load configurations are accurately accounted for by Branson's effective moment of inertia model (Al-Zaid, Al-Shaikh, and Abu-Hussein 1991). Their research compared theoretical moment of inertia values to experimental moment of inertia values obtained from subjecting reinforced concrete members of rectangular cross-section to a uniform load, a mid-span concentrated load, a third-point load, and a mid-span concentrated load combined with a uniform load. The service load moment applied to the member was the same for each load configuration. It was observed that the experimental moment of inertia values for a member subjected to a mid-span concentrated load was 12 percent greater than that experienced by a member subjected to a third-point load, and 20 percent greater than the experimental moment of inertia exhibited by a member subjected to uniform loading.

The experimental values proved that Branson's model is not accurate enough for all loading cases. Equation 1.1 returns a value comparable to the experimentally-obtained value for the uniform loading case, which means that if the member is loaded with a concentrated load at mid-span the stiffness of the member would be significantly underestimated.

Al-Zaid et al. addressed this discrepancy by suggesting that Branson's model be generalized by modifying it to the form of Equation 2.8.

$$I_e = (M_{cr}/M_a)^m * I_g + [1-(M_{cr}/M_a)^m] * I_{cr} < I_g \qquad (2.8)$$

where

m = experimentally determined exponent
I_e = effective moment of inertia
I_{cr} = cracked moment of inertia
I_g = gross moment of inertia
M_a = applied moment
M_{cr} = cracking moment

Their study also showed that for each load case the discrepancy previously noted could be eliminated by generalizing Equation 1.1 and in turn solving for m as follows:

$$m = \log[(I_{\exp} - I_{cr})/(I_g - I_{cr})]/\log(M_{cr}/M_a) \qquad (2.9)$$

where $I_{\exp}$ is the experimental moment of inertia. They argued that the discrepancy revealed in Branson's model was caused by the various lengths over which a beam cracks under a specific load condition (Al-Zaid, et al. 1991). They suggested a model similar in form to Branson's model that incorporates the ratio

of cracked length to overall length and that inherently accounts for the variation in the effective moment of inertia caused by different cracked lengths as follows,

$$I_e = (L_{cr}/L)^{m'} * I_{cr} + [1-(L_{cr}/L)^{m'}] * I_g \quad (2.10)$$

where

I_e = effective moment of inertia
I_{cr} = cracked moment of inertia
I_g = gross moment of inertia
m' = experimentally determined exponent
L_{cr} = cracked length of the member
L = length of the member

The proposed model is bounded by $I_e = I_g$ when L_{cr} equals 0, and by $I_e = I_{cr}$ when the cracked length covers nearly the entire length of the member. The exponent m' is calculated using Equation 2.11. In theory, the exponent m' is solely a function of the reinforcement ratio. This theory was later expanded on another study (Al-Shaikh and Al-Zaid 1993).

$$m' = \log[(I_g - I_{exp})/(I_g - I_{cr})]/\log(L_{cr}/L) \quad (2.11)$$

where I_{exp} is the experimental moment of inertia. The authors concluded that the "modified" form of Branson's model together with the proposed model incorporating cracked length will produce effective moment of inertia values relatively close to experimental moment of inertia values whenever the proper exponent is employed.

2.5.4 Effect of Reinforcement Ratio on the Effective Moment of Inertia

As a continuation of the aforementioned study, two of the authors later executed an experimental program to study the effect that reinforcement ratio (ρ) plays on a reinforced concrete member's effective moment of inertia (Al-Shaikh and Al-Zaid 1993). The experimental program was conducted by applying a mid-span concentrated load to reinforced concrete beams, of rectangular cross-section, containing varying amounts of reinforcement. The test specimen labels and reinforcement quantities were:

Reinforcement Label	Reinforcement Ratio
Lightly	0.8
Normally	1.4
Heavily	2.0

This study revealed that Branson's model underestimated the effective moment of inertia of all test specimens. The underestimation of I_e was approximately 30 percent in the case of a heavily reinforced member, and 12 percent for a lightly reinforced specimen. Beyond the previously observed behavior of a reinforced concrete member subjected to a mid-span concentrated load

(Al-Shaikh and Al-Zaid 1993), it is obvious that reinforcement ratio affects the accuracy of Branson's model especially when the member is heavily reinforced. Therefore, by curve fitting, the authors derived an expression (Equation 2.12) to calculate the exponent m for use in Equation 2.8, which is given by the following expression:

$$m = 3 - 0.8\rho \tag{2.12}$$

where m is an experimentally determined exponent and ρ is the reinforcement ratio. The authors also applied the more general Equation 2.10, introduced in their earlier research, to the values obtained from this experiment. The experimental values were used to develop Equation 2.13 to determine the exponent m' for Equation 2.10.

$$m' = \beta M_{cr} / M_a \tag{2.13}$$

where m' is an experimentally determined exponent, and

$$\beta = 0.8\,\rho \tag{2.13a}$$

where ρ is the reinforcement ratio.

The use of Equation 2.10 may be better suited when considering the effects of reinforcement ratio on the effective moment of inertia, because the discrepancy created by load configuration is already taken into account by the cracked length term of the equation, which leaves the exponent m' dependent only on the reinforcement ratio.

2.5.5 A New Model

In 1998 researchers A. M. Fikry and C. Thomas (1998) published an article in which an effective moment of inertia model was derived from basic concrete flexural response theory. The authors were focused in developing an effective moment of inertia model that eliminated the laborious I_{cr} calculation associated with Branson's model, and that would account more accurately for variations in reinforcement ratio and load configuration. The derivation of the new model was based on an approximation for I_{cr}, which the authors called I_{cre}.

The authors began their derivation with a cracked, singly reinforced, rectangular cross-section concrete member. They derived I_{cr} as a function of two variables (η and ρ) and represented it in the form of Equation 2.14.

$$I_{cre} = (\alpha + \beta\eta\rho) * (bd^3 / 12) \tag{2.14}$$

where

I_{cre} = approximate moment of inertia
α = constant (given in literature)

β = constant (given in literature)
η = modular ratio
ρ = reinforcement ratio
b = width of the member
d = effective depth of the steel reinforcement

This derivation achieved their first goal, which was eliminating the I_{cr} calculation. The resulting approximations were found to lie within 6 percent of the cracked moment of inertia for all test specimens.

The cracked moment of inertia approximation was also expanded to flanged cross-sections and doubly reinforced, rectangular and flanged cross-sections. The expanded form of Equation 2.14 is given as:

$$I_{cre} = (\alpha + \beta\eta\rho_e) * (b' d^3 / 12) \tag{2.15}$$

where

$$\rho_e = \rho b_w / b' \tag{2.15a}$$

in which b_w is the web width of flanged member and b' is the equivalent width of the member. The term b' is detailed in the literature and accounts for a flanged cross-section and compression reinforcement.

The authors used the basic form of the I_{cre} equation, along with the assumption that uncracked concrete in the tension region of the cross-section can be thought of as a fictitious amount of steel reinforcement, and developed it into the following expression:

$$I_e = (\alpha + \beta\eta\rho \sim) * (bd^3 / 12) \tag{2.16}$$

where $\rho\tilde{}$ is the ρ_{actual} + fictitious amount of reinforcement required to achieve I_g. After applying the limits of $I_e = I_g$ when $M_a < M_{cr}$ and $I_e = I_{cr}$ when $M_a >> M_{cr}$, Equation 2.17 was obtained as:

$$I_e = I_{cre} + (I_g - I_{cre})^{\phi} \tag{2.17}$$

where I_e is the effective moment of inertia, I_{cre} is the cracked moment of inertia approximation, and I_g is the gross moment of inertia, and

$$\phi = -(M_a / M_{cr})(L_{cr} / L)\rho > 1\% \tag{2.17a}$$

$$\phi = -(M_a / M_{cr})(L_{cr} / L) \leq 1\% \tag{2.17b}$$

where

M_a = applied moment
M_{cr} = cracking moment

L_{cr} = cracked length
L = length of the member
ρ = reinforcement ratio

The term ϕ is empirical and was determined from the data of over 340 previously conducted laboratory tests.

The authors showed that their model produced reasonable results when used to estimate the deflection of experimental reinforced concrete members. When compared to the other available models it was not any more accurate at higher reinforcement ratios, but, in the case of reinforcement ratios near or below 1 percent, the model performed significantly better than the Branson model and the models developed by Al-Zaid et al. (1991).

2.6 Summary

The deflection a reinforced concrete member experiences due to service load is a complex subject. A subject that quickly became a concern of the reinforced concrete design community in the late 1950's when stronger concretes and steels were made available to the industry and the ultimate design philosophy began to gain popularity. The concern of service load deflection prompted many studies during those transitional periods and continues to be a topic of debate. One of those early studies produced the most notable contribution to the topic of reinforced concrete deflection, Branson's effective moment of inertia model. The model developed by Branson is given in most; if not every American design standard that addresses reinforced concrete design. Even though the research presented herein has shown the shortcomings of Branson's equation (Equation 1.1), it still remains the chosen means of calculating the effective moment of inertia for the purpose of estimating reinforced concrete member deflection.

The accuracy of Branson's equation is questionable though, especially for non-uniform load conditions. A classic example would be a reinforced concrete bridge girder subjected to a tandem-axle load configuration. Such is the scenario faced by U.S. Army field engineers when trying to determine the capacity of an in-service T-beam bridge. Therefore, the I_e models selected for study (the "modified" Branson model, the "cracked length" model, and the Fikry and Thomas model) may provide a more accurate effective moment of inertia calculation, thus giving a better estimate of bridge capacity.

Effective moment of inertia models based on moment-curvature relationships are ignored due to the difficulty of measuring curvature in the field. Graphical representations (Lutz 1973) and simplified methods (Grossman 1981) available to design engineers are based on Branson's effective moment of inertia equation and are also ignored due to discrepancies later revealed in this thesis.

3 Testing Program

3.1 Introduction

The objective of the laboratory testing program is twofold: the evaluation of a selection of effective moment of inertia models as a component of the proposed evaluation procedure, as well as the evaluation of the application of a laser level device as a deflection measurement instrument during field bridge load testing. This study will address the portion related to the evaluation of effective moment of inertia models. Personnel from the ERDC will address the evaluation of the applicability of using a laser level device for deflection measurements. The instrumentation, concrete testing, test set-up and implementation of the testing procedure described herein were primarily developed and performed by personnel from ERDC.

3.2 Test Specimens

The primary load-carrying element in a cast-in-place reinforced concrete bridge is a T-beam girder. A T-beam consists of a web, which refers to the portion of the bridge below the deck shown in Figure 1.1, and a flange, which is formed by an "effective" width of deck. A monolithic casting procedure unites the web and deck, allowing them to resist load as a single element, a T-beam. Therefore, the testing program's focus was full-scale T-beams subjected to a closely spaced, tandem-axle load configuration, which is typical of military-vehicles used during theater-of-operations scenarios.

3.2.1 T-beam Development

The basis for the design of the full-scale T-beam test specimens was a modified field design scenario as seen from one of the bridges owned by the Virginia Department of Transportation. Bridge girder elements were designed using the provisions within the load factor design section in the AASHTO Standard Specifications (AASHTO 1996), which are the design guidelines currently used by the Virginia Department of Transportation.

3.2.1.1 Specimen Geometry. The bridge design under consideration consisted of a 31-span with no skew, with two traffic lanes and two 3-ft

shoulders. To accommodate the prescribed lane and shoulder width, the bridge needed to be 29 ft 2 in. wide. Once typical parapet walls were included, that would leave a clear roadway width of 26 ft 6 in. The 29 ft 2 in. bridge width required the placement of four T-beam girders spaced transversely at 7 ft 9 in. (center-to-center). The transverse spacing of the girders controlled the effective width (b_e) (as calculated per the AASHTO Standard Specification (1996)) of an interior girder flange, making b_e = 93 in. Also, incorporated into the design was a dynamic load allowance equal to 1.33 (AASHTO 1996) and a load distribution factor of 1.29 (S/6 in AASHTO 1996). Preliminary calculations established a web thickness at 18 in., a flange thickness at 8 in., and an overall depth of 35 in. (Figure 3.1).

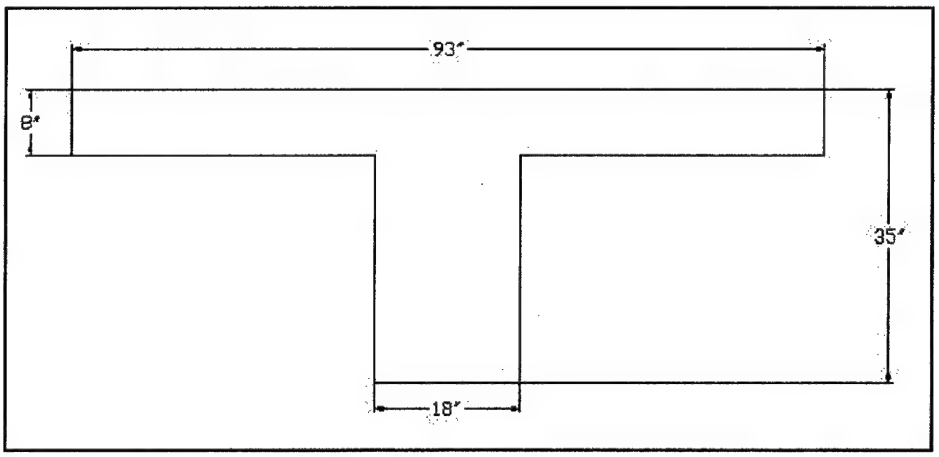

Figure 3.1. Initial T-beam Model Dimensions

The T-beam girder obtained from the aforementioned design had an estimated weight of 19.9 tons, which was significantly heavier than the 15-ton capacity of the ERDC testing laboratory crane that would be used to set the beam in place. Thus, the dimensions of the design girder were modified to achieve a test specimen that could be handled safely by the ERDC laboratory equipment (Figure 3.2).

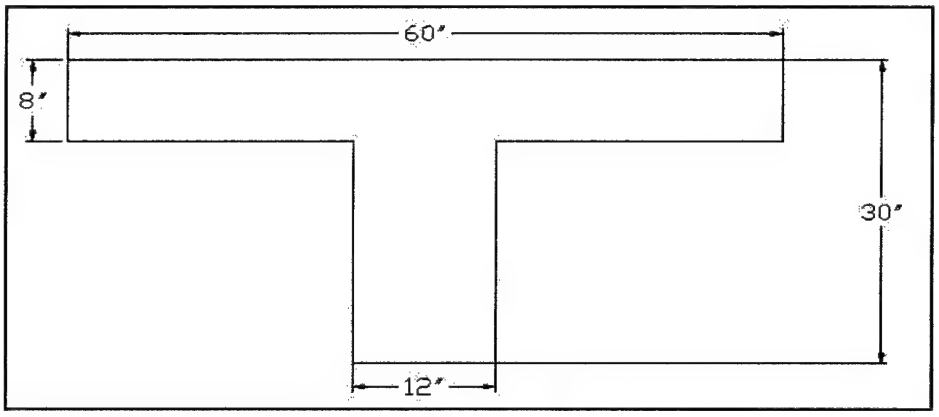

Figure 3.2. Test Specimen Dimensions

To accommodate there requirements, the overall length of the T-beam member was reduced by 2 ft to achieve a final total length of 29 ft, while still maintaining a length that reasonably represents the span of a simply supported T-beam bridge. The depth of the flange was kept at 8 in, which provides a reasonable representation of deck thickness in these type of bridges. The web thickness was reduced to 12 in. to allow the horizontal clearance for three columns of flexural reinforcement (ACI 1999) as compared to adequate clearance of four rows within the initial 18 in. web (ACI 1999). Once the geometric parameters were defined, the overall flange width was reduced to 60 in. while the overall depth was reduced to 30 in. to achieve an acceptable overall weight. These geometric reductions resulted in an estimated beam total weight of 10.9 tons, which was within the capacity limitations prescribed by the laboratory lifting crane equipment.

3.2.1.2 Specimen Reinforcement. Once the geometry of the test specimen was established, an analysis was conducted to determine the effects that different levels of reinforcement ratios would have in the load-deflection behavior of the member. The analysis theoretically subjected the test specimen to an AASHTO alternative military load configuration (AML) (AASHTO 1996). An AML, designated HS25 by AASHTO (Figure 3.3), consists of a tandem axle load configuration (spaced 4 ft center-to-center) that supplies two concentrated loads, each equaling 24 kips. The AML was utilized in lieu of a typical AASHTO design truck because the proposed analysis procedure will be used in situations where heavier, more closely spaced wheel loads, typical of military equipment, are of concern. The tandem-axle load configuration was situated symmetrically about the mid-span of the T-beam to produce the largest possible deflection due to the twin 24 kip loads.

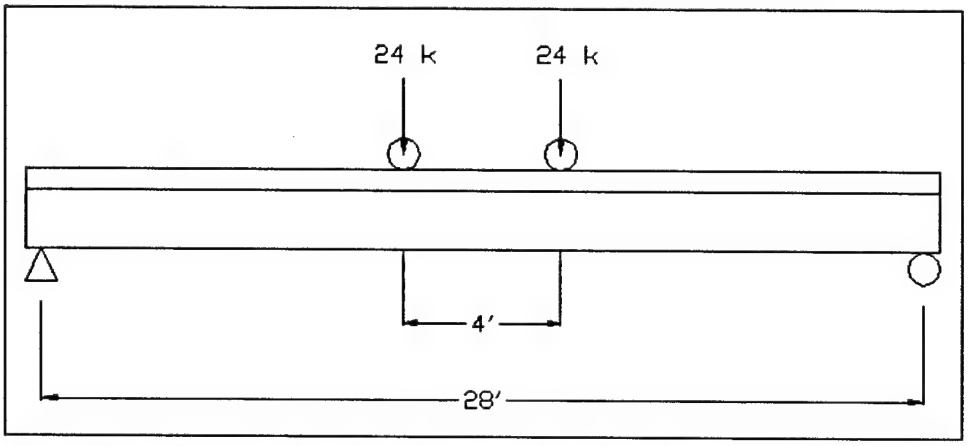

Figure 3.3. AASHTO Alternative Military Load Configuration

The analysis revealed that the test specimen would experience significant variations in deflection when reinforced with steel areas, A_s, between the minimum allowed area of steel, $A_{s\text{-}min}$ (the amount of steel required to prevent an abrupt failure at loads near the cracking moment) and approximately 50 percent of the balanced area of steel, A_{sb} (the area of steel associated with the state where there is simultaneous yielding of the steel reinforcement and crushing of the concrete's extreme fiber). The values of $A_{s\text{-}min}$ and A_{sb} corresponding to a typical

test specimen (0.88 in.^{2} and 30.5 in.^{2}, respectively) are calculated per ACI 318-99 and MacGregor (1997), respectively. A sample calculation of both values is provided in Appendix D.

This behavior is illustrated in Figure 3.4, where it can be seen that for reinforcement levels greater than 50 percent of A_{sb} there is a minimal variation in the member's deflection under loading.

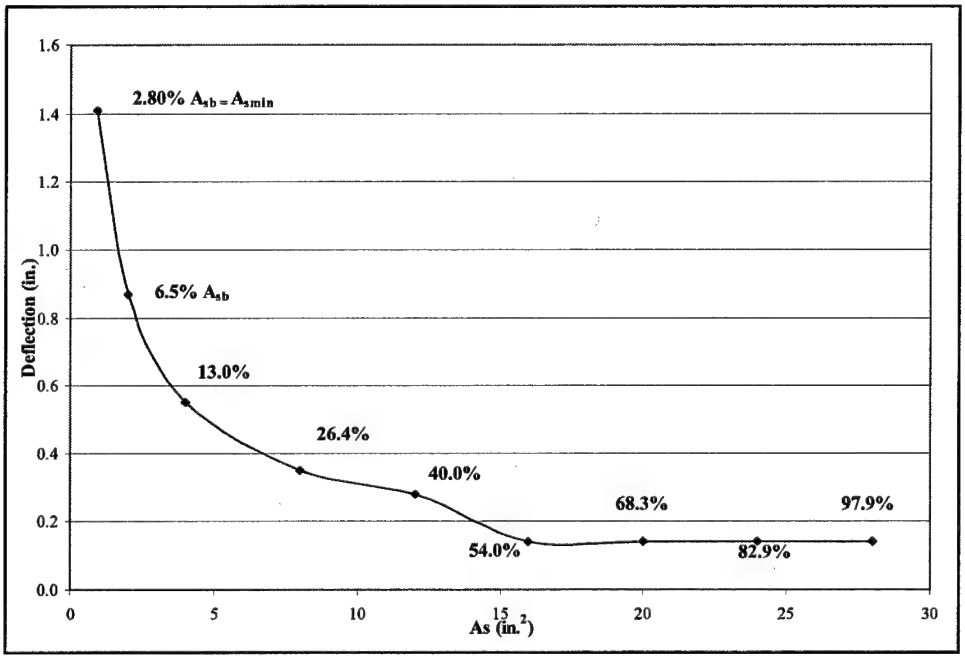

Figure 3.4. Variation of Deflection with Amount of Steel Reinforcement

Based on these observations, a decision was made to fabricate the test specimens with three different amounts of reinforcement. The reinforcement amounts selected for the testing program corresponded to $A_b = 8$ in^2, $A_b = 5$ in^2, and $A_b = 3$ in^2. For these levels of reinforcement, the calculated vertical deflections corresponded to $\Delta = 0.33$ in, $\Delta = 0.47$ in, and $\Delta = 0.70$ in, respectively. The analysis of members with various levels of reinforcement would allow researchers to evaluate the accuracy of a laser level device in capturing small variations in deformation due to its flexural stiffness variation. It would also provide a basis to evaluate which effective moment of inertia model provide the most accurate characterization of the stiffness behavior of reinforced-concrete beam members.

3.2.1.3 Basic Properties. A total of nine T-beam test specimens were fabricated. These were classified in three similar sets of beams ("Set A", "Set B", and "Set C"), with each set having one beam of each reinforcement level. The basic specimen properties for each reinforcement quantity are presented in Table 3.1. A cross-section of each reinforcement quantity is shown in Appendix D.

Table 3.1 Gross Cross-Section Properties			
A_s (in.^{2})	8	5	3
I_g (in.^{4})	51530	51530	51530
ρ (%)	2.66	1.60	0.93
d (in.)	25.1	26.1	26.9

A_s = area of steel reinforcement.
I_g = gross moment of inertia.
ρ = steel reinforcement ratio.
d = effective depth of steel reinforcement.

3.3 Materials

3.3.1 Concrete

The concrete used for the test specimens was batched at a local ready mix plant and trucked to a site on the grounds of ERDC for casting. The constituents of the concrete-mix were Type I cement, fine aggregate, river gravel (chert) as coarse aggregate, water, and an ad-mixture that was added at the site (D-19) to allow for increased workability of the uncured concrete. Quality control tests in the form of slump and air content were performed upon delivery of the uncured concrete. To provide means for testing cured concrete properties, specifically compressive and tensile strength, twelve 6-in by 12-in cylinders were cast simultaneously with each test specimen. A set of three concrete cylinders was tested to determine compressive strength on the 28th-day as well as on the day of testing to ensure the prescribed 4000 psi strength (Table 3.2).

Table 3.2 Compressive Strength					
		Compressive Strength			
Specimen	Casting Date	28 Day Test Day	28 Day Test Day	28 Day Test Day	Average
A8	18-Apr-01	4850	4780	4640	4760
		5100	4860	4800	4920
A5		4340	4360	4190	4300
		5000	4740	5000	4910
A3		4600	4670	4660	4640
		4900	5200	5300	5130
B8	17-May-01	4170	4260	4440	4290
		5230	5070	5320	5210
B5		5050	4660	4760	4820
		5870	5890	5720	5830
B3		4450	4210	4370	4340
		5260	5300	5080	5210
C8	14-Jun-01	5000	5070	4840	4970
		5700	5760	5700	5720
C5		4630	4520	4580	4580
		5300	5370	5300	5320
C3		4150	3920	4110	4060
		4610	4540	4800	4650

The value of compressive strength used in theoretical calculations has a significant effect on numerous cross-sectional properties. Listed in Tables 3.3 and 3.4, respectively, are the affected properties and their values as calculated with the 28-day compressive strength and the test day compressive strength. Sample calculations for E_c, I_{cr}, and M_{cr} are given in Appendix D.

All calculations made hereafter incorporate the values determined with the test day compressive strength. The test day strength is utilized to eliminate the error that occurs between experimental and theoretical results if the 28-day strength or the prescribed 4000 psi strength is employed the theoretical calculations.

Table 3.3 Cross-Section Properties (28 day)

28 Day Specimen Properties									
Set	A			B			C		
A_s (in.^{2})	8.0	5.0	3.0	8.0	5.0	3.0	8.0	5.0	3.0
f_c (psi)	4760	4300	4640	4290	4820	4340	4970	4580	4060
?	6.1	6.7	6.3	6.8	6.0	6.7	5.8	6.3	7.1
E_c (ksi)	3940	3740	3890	3740	3960	3760	4020	3860	3640
I_{cr} (in.^{4})	25700	20000	13100	27000	18800	13400	25400	19200	13800
M_{cr} (ft*kip)	107.9	100.9	105.6	102.0	108.1	102.6	109.8	105.4	99.2

Table 3.4 Cross-Section Properties (Test Day)

Test Day Specimen Properties									
Set	A			B			C		
A_s (in.^{2})	8.0	5.0	3.0	8.0	5.0	3.0	8.0	5.0	3.0
Age (days)	41.0	48.0	44.0	68	61	54	49	49	43
f_c (psi)	4920	4910	5130	5210	5830	5210	5720	5320	4650
?	5.9	5.9	5.7	5.6	5.0	5.6	5.1	5.5	6.2
E_c (ksi)	4000	4000	4090	4114	4352	4114	4311	4157	3887
I_{cr} (in.^{4})	25500	18700	12500	24900	17300	12400	23900	18000	13000
M_{cr} (ft*kip)	109.2	109.1	111.5	112.4	118.9	112.4	117.8	113.6	106.2

3.3.2 Reinforcement

Two sizes of deformed mild-steel bars (Grade 60) were used as various forms of reinforcement in the T-beam test specimens. In all specimens the flexural reinforcement consisted of some quantity of No. 9 deformed steel bars. The shear reinforcement (U-shaped stirrups), as well as the flange reinforcement, was No. 4 deformed steel bars.

The amount of shear reinforcement necessary to guard against a shear failure during the testing program was determined as prescribed by the provisions in Section 11.5 of the ACI Building Code (2002). The test specimen requiring the greatest amount of shear reinforcement was that with 8 in^2 of flexural reinforcement, for which it was necessary to provide No. 4 stirrups spaced at 12 in. (center-to-center). The same shear reinforcement schedule was called out for all test specimens to simplify the fabrication process.

The longitudinal reinforcement located in the flange of the test specimen is representative of flexural reinforcement present in the deck of a T-beam bridge.

This reinforcement becomes compressive reinforcement when a single-span T-beam is subjected to positive bending, but its effect is ignored herein. The reinforcing bar material utilized was frequently used in projects at the ERDC and the material properties were determined as follows: steel yield strength (f_y) equaled 60,000 psi and the modulus of elasticity (E_c) equaled 29,000 ksi. A typical reinforcement layout is illustrated in Figure 3.5 below.

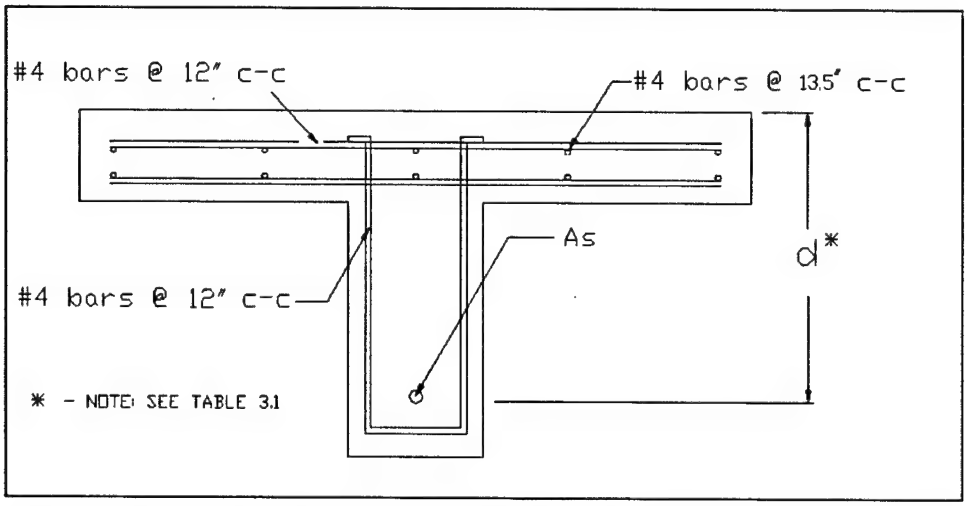

Figure 3.5. Typical Reinforcement Layout for Specimen

3.4 Casting

One set of test specimens (with T-beams corresponding to steel reinforcement areas of 8 in.^{2}, 5 in.^{2}, and 3 in.^{2}, respectively) was cast on the same day, resulting in three different days of casting for all three sets. Each test specimen required 5.55 yd^3 of concrete; therefore a single ready-mix truck was dispatched for the casting of each beam. Prior to casting, the formwork was constructed at the pour location and the reinforcement properly placed (Figure 3.6). Incorporated in the reinforcement were two steel anchors, placed near the top, at strategic locations, to allow for handling (Figure 3.6).

During casting, the concrete was carefully poured on each form and thoroughly vibrated for placement consistency. After the casting was complete, the exposed surface of the specimen was finished and the set was left to cure. Fourteen days after casting, the formwork was removed and the beams were stored until testing could take place.

3.5 Instrumentation

Various forms of instrumentation were utilized on the test specimens to monitor their behavior during testing. Before casting, three MicroMeasurements strain gages were attached to three different reinforcing bars near the centroid of the steel reinforcement on each girder. These strain gages were installed to

monitor the tensile stresses in the steel reinforcement during testing. Attached to the top surface (compression face) of each test specimen were seven MicroMeasurements strain gages that recorded the compressive strain in the concrete. To insure a good contact between each strain gage and the concrete, a hand-held circular grinder was used to smooth the concrete surface before

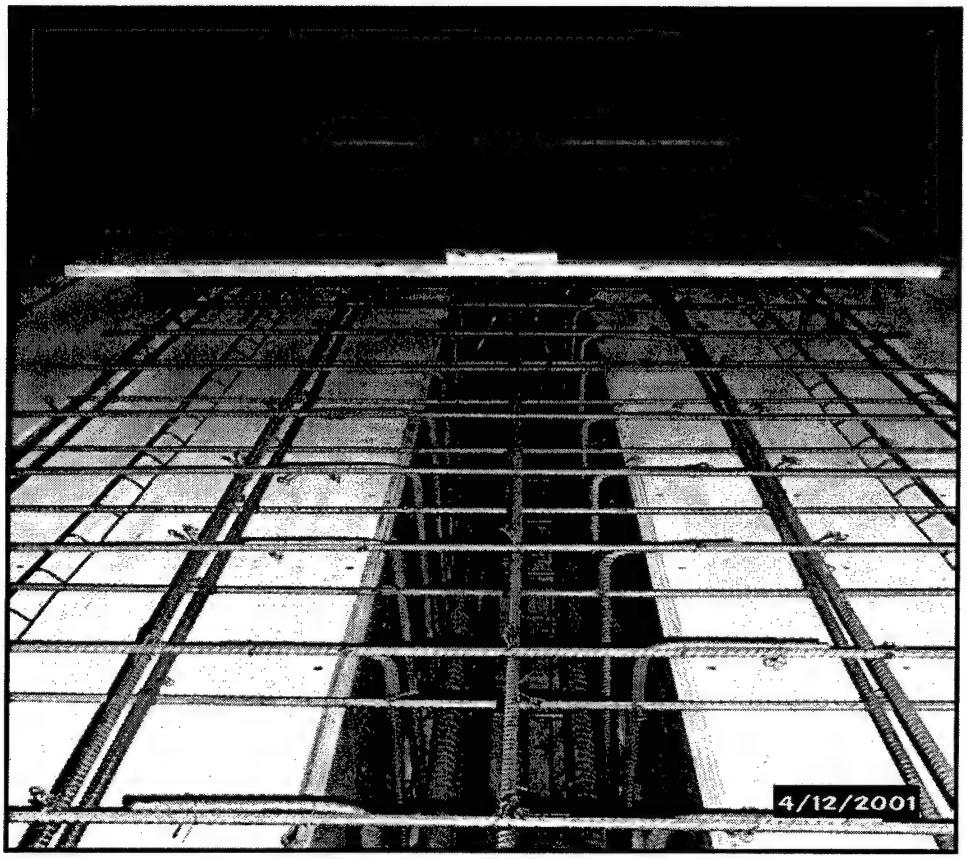

Figure 3.6. Typical Reinforcement Layout

attaching the gages. Five gages were placed directly over top of the beam web and one gage was placed out on each flange (Figure 3.7).

Once a specimen was set into place amidst the load frame, five Sensortec DLF3000 linear voltage displacement transducers (LVDTs) were placed in strategic locations to monitor vertical deflection during testing. Three LVDTs were centered under the web, one at mid-span and one under each load (Figure 3.8). An LVDT was also placed on the outer edge of each flange at mid-span to monitor rotation of the specimen during testing. The strain gages and each LVDT were wired to a MEGADAC 3415AC data acquisition system, which continuously recorded the data for later analysis.

3.6 Test Setup

A test specimen was supported on simulated, steel bridge bearings; which modeled typical end conditions of a T-beam bridge. One of the steel bearings was allowed to rotate as well as to translate horizontally (acting as a roller), while the other one was only allowed to rotate (acting as a pin).

Figure 3.7. Strain Gage Configuration

An elevation view of the test set-up is illustrated in Figure 3.9. A simulated, tandem-axle service load was supplied by two MTS hydraulic actuators spaced 5-ft apart (center-to-center) and placed symmetrically about the girder's mid-span. The spacing was limited by the center-to-center minimum spacing of the hydraulic actuator system of 5-feet. It should be noted that this spacing slightly differs from the tandem load center-to-center spacing of 4 ft prescribed by the AASHTO AML load configuration being represented on this test. Special steel braces were designed and placed near the lateral ends of the test specimen (as shown in Figure 3.10) to ensure that the specimen would not rotate and/or fall off from its steel bearings during load testing.

3.7 Testing Procedure

Each test consisted of various cycles of service load to produce a moment equal to that generated by an AASHTO AML load configuration. The service load moment was calculated as 348 ft-kip, which represents a required applied load by each actuator equal to 30 kips.

During each load cycle, the applied load, deflection, and strain values measured by the hydraulic actuators, LVDTs, and strain gages respectively were continuously recorded by the Mega-DAC 3415AC. The applied load was stabilized at 10 kip load intervals (5 kip/actuator) to allow a deflection reading to be taken using the Laica N2002 digital laser level.

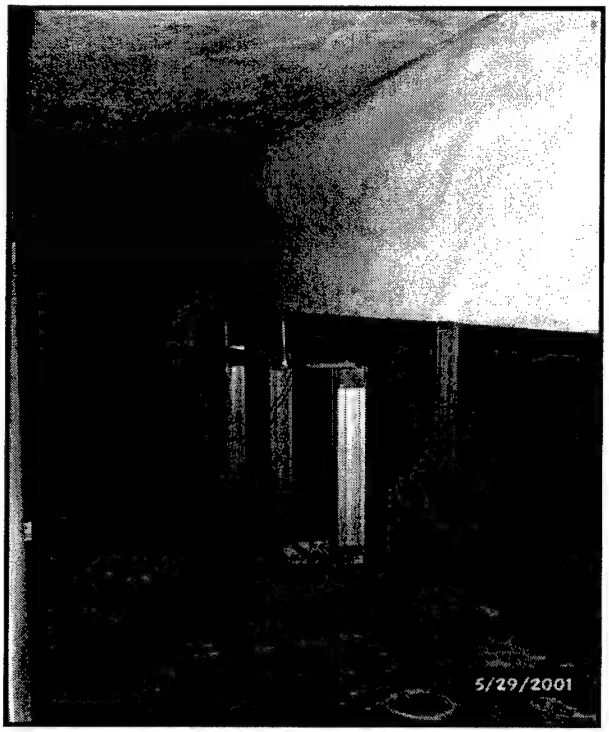

Figure 3.8. LVDTs Location on T-beam Specimen

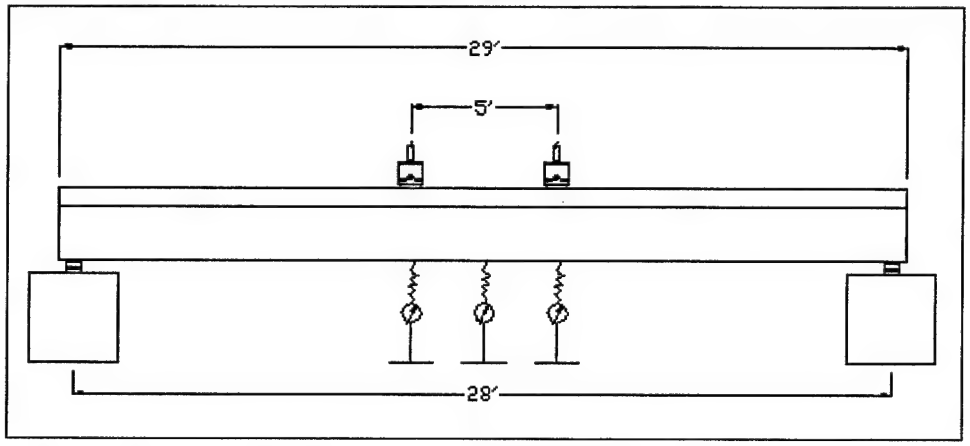

Figure 3.9. Elevation View of Test Setup

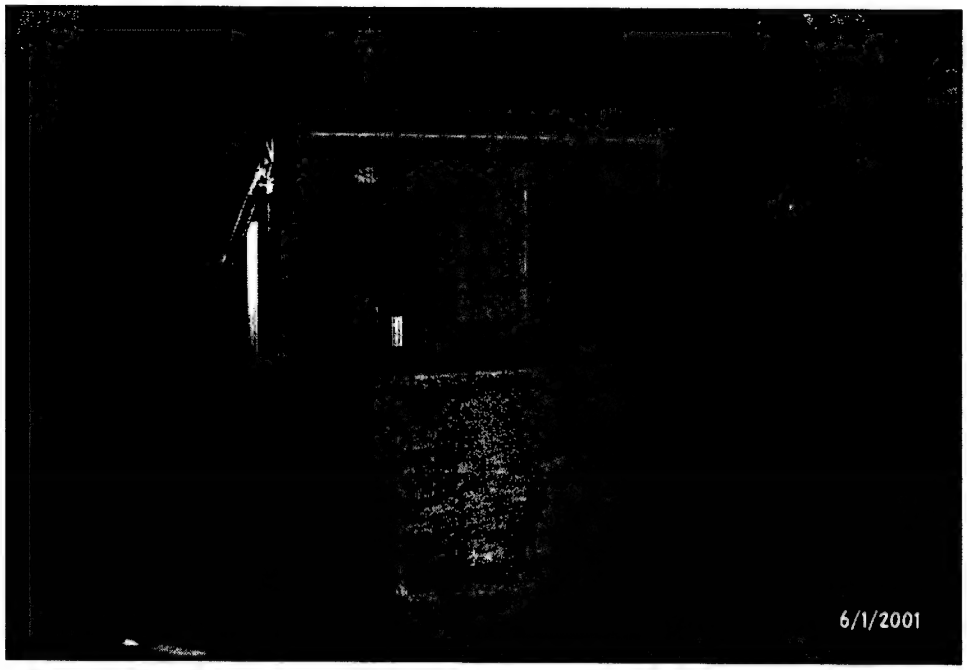

Figure 3.10. Cross Section View of Test Setup

3.8 Summary

The testing program described in Chapter 3 was aimed at recording test data needed to evaluate the accuracy of various effective moment of inertia models in characterizing the load-deflection behavior of reinforced concrete T-beam subjected to a tandem-axle load configuration. The data included the measurement of midspan deflections and corresponding load magnitudes, as well as compressive strain deformations in the member. The load versus deflection plots for all T-beam specimens are presented in Appendix A.

4 Test Specimen Behavior

4.1 General

The idealized flexural behavior of a beam cross section under increasing loading is depicted in Figure 4.1 (MacGregor 1997, Nawy 1996). In this chapter, both the idealized as well as the actual T-beam behavior are discussed, as a prelude to the comparison between the experimental data and the theoretical data presented in Chapter 5.

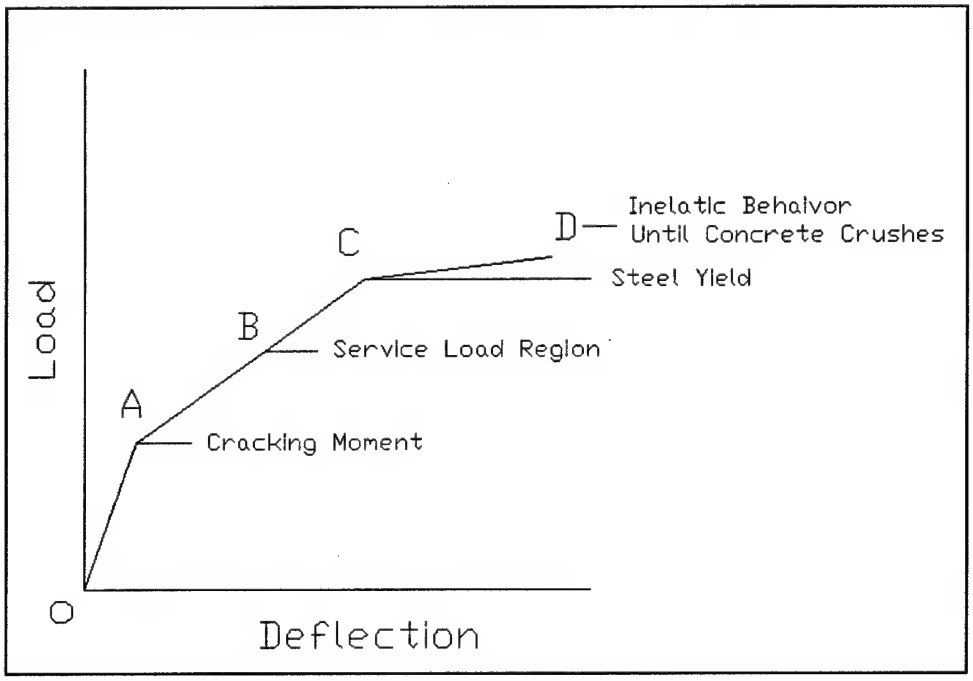

Figure 4.1. Idealized Flexural Behavior of a Beam

4.2 Idealized T-beam Behavior

A T-beam cross-section which is previously uncracked, will elastically resist the applied load (see Region OA of Figure 4.1) until the cracking moment (i.e., the moment at which the tensile stress in the bottom fiber of the concrete exceeds

the concrete's flexural tensile strength) is exceeded at some location along the length of the member. At point A depicted in Figure 4.1, the applied moment reaches the member's cracking moment at or near the section of maximum moment, which results in tensile cracking. The bending stiffness at a crack location is immediately reduced to that provided by a cracked section; which reduces the specimen's overall bending stiffness. As applied load increases, the cracking phenomenon is repeated along the length of the member resulting in a continual reduction of bending stiffness, allowing greater deflection per load increment throughout the service load region of Figure 4.1 (Region AC). In Figure 4.1, although Region AC is modeled with a linear line segment (i.e., elastic behavior), the reality is that Region AC will exhibit a non-linear behavior due to the inelastic effects of tensile cracking.

At a specific service load level the bending stiffness varies along the length of the T-beam due to alternating cracked and uncracked cross-sections. As later discussed, this variable stiffness is addressed by assuming an "effective" bending stiffness constant over the T-beam's entire length. All subsequent loads less than the largest applied load are resisted by the effective bending stiffness. Graphically, subsequent load cycles would follow a linear line segment that originates at an offset (the permanent deflection sustained by the member due to the inelastic of tensile cracking) from the origin in Figure 4.1 and extends to the terminus of the idealized load versus deflection plot (a function of applied load).

If the member is subjected to ever increasing load magnitudes, the member's overall bending stiffness will eventually be reduced to that provided by a single cracked section. This occurs when the additional stiffness provided by uncracked concrete becomes negligible. All load applied beyond that is resisted by the bending stiffness of a cracked section until the steel reinforcement yields (Point C, Figure 4.1). After the steel reinforcement yields, additional load causes the T-beam to behave in an inelastic manner until compressive stresses exceed the compressive strength of the concrete, which is considered failure.

In general, bending stiffness is a product of the constituent material's modulus of elasticity and the member's moment of inertia. In the case of a reinforced concrete T-beam, the modulus of elasticity is typically assumed to be constant, thus the bending stiffness is directly proportional to the cross-sectional moment of inertia. Therefore, to better understand bending stiffness behavior, the ratio of actual moment of inertia (I_{act}) to a member's gross moment of inertia (I_g) is plotted versus the ratio of applied moment (M_a) to cracking moment (M_{cr}) (Figure 4.2).

The curve in Figure 4.2 illustrates that the actual moment of inertia is equal to the gross moment of inertia until the applied moment reaches the cracking moment (Region OA of Figure 4.2). As the magnitude of applied moment increases (Region B of Figure 4.2), the rate at which the actual moment of inertia

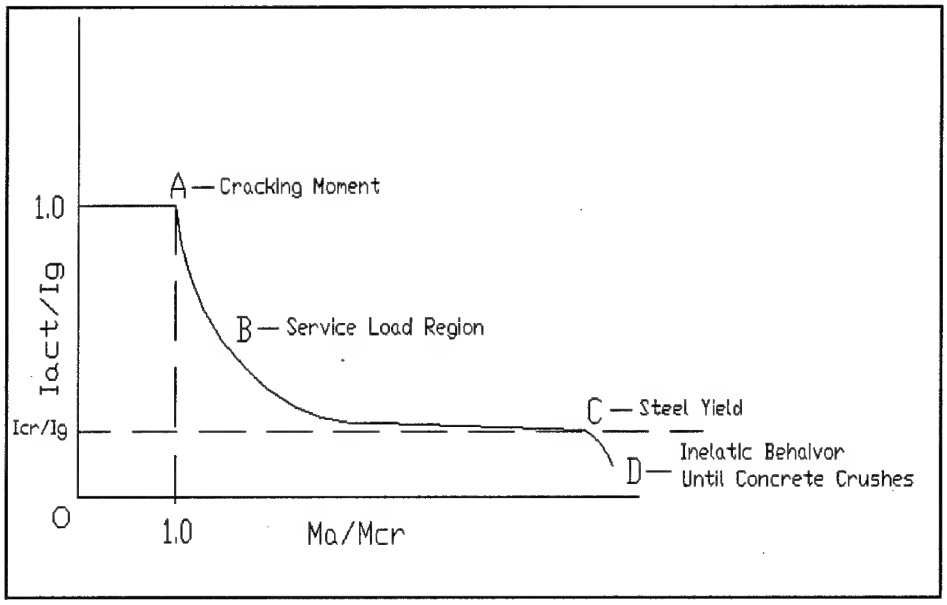

Figure 4.2. Idealized Moment of Inertia versus Applied Load

decreases is sharp at first, but the behavior of I_{act} becomes asymptotic to I_{cr} for larger values of M_a. If loading is continued, the actual moment of inertia continues to decay until it reaches the cracked moment of inertia. After that, the cracked moment of inertia will resist the applied load until the steel reinforcement achieves yielding (Point C, Figure 4.2).

4.2.1 Variable moment of inertia

The moment of inertia of a reinforced concrete T-beam just before its cracking moment is exceeded corresponds to the gross moment of inertia of the cross-section. After cracking takes place, the moment of inertia at the crack location corresponds to the cracking moment, while other sections continue to behave as uncracked. The alternating cracked and uncracked cross-sections along the length of the member are commonly addressed by calculating an effective moment of inertia value and assuming that value constant over the member's length. Assuming a constant moment of inertia value simplifies the flexural analysis of the T-beam to that of most prismatic members, even though its cross-sectional properties vary along its length due to cracking.

The sketches in Figure 4.3 illustrate the variation of moment of inertia over the length of a reinforced concrete T-beam. Section a-a shows an uncracked section and section b-b shows a cracked section Figure 4.3). A sample calculation for both the gross moment of inertia and the cracked moment of inertia are presented in Appendix D.

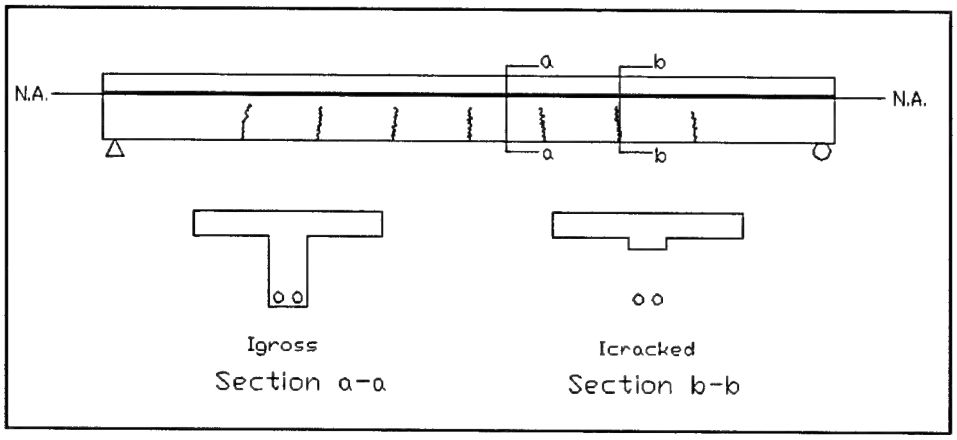

Figure 4.3. Variation of I_{act} along a Reinforced Concrete Member

4.3 Typical Experimental Behavior

The typical behavior of the T-beam test specimens was similar to the idealized behavior explained in the previous section. To show the typical test specimen behavior a representative load versus deflection plot is presented Figure 4.4.

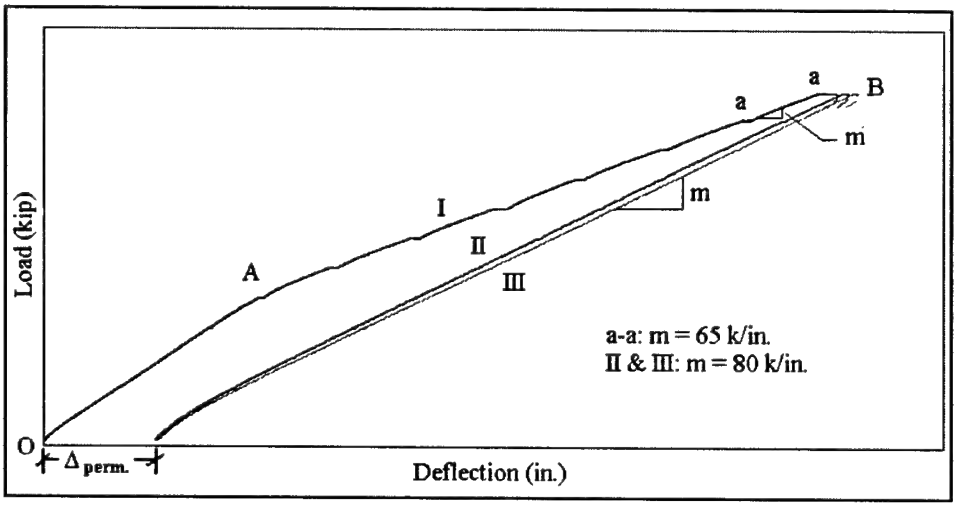

Figure 4.4. Actual Load versus Deflection Plot (Specimen A8)

Figure 4.4 exhibits three load versus deflection curves, one for each cycle of service load applied to specimen A8. Note that these load versus deflection curves are up to service load, which is represented by region B in Figure 4.1.

4.3.1 Initial Load Cycle

The first load cycle was applied to an uncracked test specimen. Figure 4.4 shows Curve I of the form of the idealized load versus deflection plot previously illustrated in Figure 4.1. In this figure, segment a-a is defined as the upper portion of Curve I, which will be discussed further in detail in the upcoming paragraphs.

The portion of Curve I leading up to segment a-a exhibits a less steeper slope than the one corresponding to Curves II and III. Since a concrete member is most rigid during the first applied load cycle --when the member is uncracked--, Curve I should have presented a steeper slope than Curves II and III.

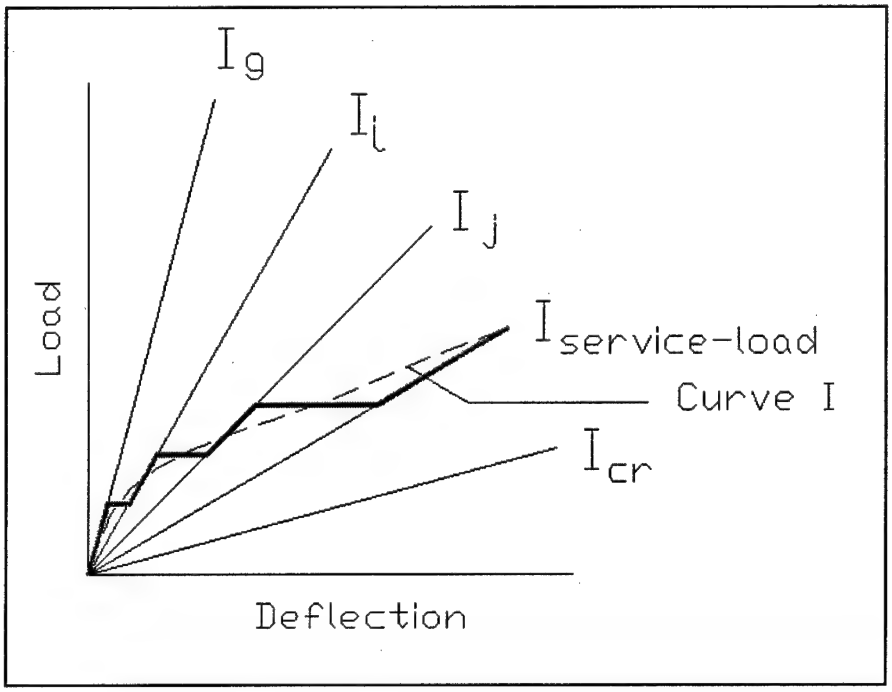

Figure 4.5. Initial Load Cycle Behavior

The arrays propagating outward from the origin in the plot shown in Figure 4.5 represent different moment of inertia values that a reinforced concrete member is capable of exhibiting under increasing amounts of applied load. The array closest to the vertical axis represents the gross moment of inertia, I_g, for the member while the array closest to the horizontal axis represents its cracked moment of inertia, I_{cr}. These are the upper and lower bound values of the member's actual moment of inertia, I_{act}. The intermediate arrays represent values of I_{act} bounded between I_g and I_{cr} that are achievable as the member is subjected to larger applied loads.

As an uncracked member is loaded for the first time, the stiffness behavior of the member initially follows a pattern closed to that of I_g. The behavior of the member follows this array until the first crack occurs, when its moment of inertia "jumps" to a lower moment of inertia level (I_i, I_j, etc.). This phenomenon

continues as more cracks form at regular intervals along the length of the member (i.e., for each crack formed another "jump" occurs on the plot). In reality, these "jumps" are not distinguishable because an actual load versus deflection plot is smoothed by the average moment of inertia of the member. Hence the behavior illustrated by Curve I in Figure 4.4. This study is concerned with measuring and modeling the actual moment of inertia of an in-service (previously cracked) T-beam bridge girder. Therefore, the values obtained from the first load cycle are not discussed any further.

4.3.2 Subsequent Load Cycles

Figure 4.2 clearly illustrates that the actual moment of inertia of a reinforced concrete member is a function of the applied load. In theory, the behavior exhibited in the second (Curve II) and third (Curve III) load cycles of Figure 4.4 should exhibit approximately similar slope as the final segment (Section a-a) in Curve I. Displayed in Figure 4.6 are the approximate slopes corresponding to segment a-a and Curves II and III. A comparison of the values reveals the slope (i.e., the stiffness) of Curves II and III (80 kip/in.) is greater than the one corresponding to segment a-a (65 kip/in.).

In the case of an in-service T-beam, generally there is little knowledge of load history, although, it is reasonable to assume that the member has experienced significant cracks due to applied loads that exceeded the cracking moment. The in-service T-beam possesses some amount of permanent deflection due to the inelastic effects of tensile cracking, which is unknown in an in-field situation. Consequently, the loads versus deflection curves generated during an in-field load test are analogous to the curves in Figure 4.6, which correspond to Curves II and III shown in Figure 4.4 with the permanent deflection subtracted from them.

4.4 Test Specimen Behavior Conclusions

A member's actual moment of inertia (I_{act}) is a function of applied load. The behavior of an in-service T-beam in terms of its moment of inertia is greatly influenced by the largest applied load the member has resisted during its service life. Due to that load, a given T-beam exhibits an actual moment of inertia that is some value less than its gross moment of inertia and greater than or equal to its cracked moment of inertia.

The actual moment of inertia of a reinforced concrete T-beam member can be obtained by conducting a field load test. Due to the fact that actual moment of inertia is a function of applied load the magnitude of the test load will affect the results of the analysis. To better explain this, a load versus deflection plot (Figure 4.7) illustrating the behavior of a generic T-beam bridge girder, over its service life, is given. The service load cycle behavior can be assumed linear, which

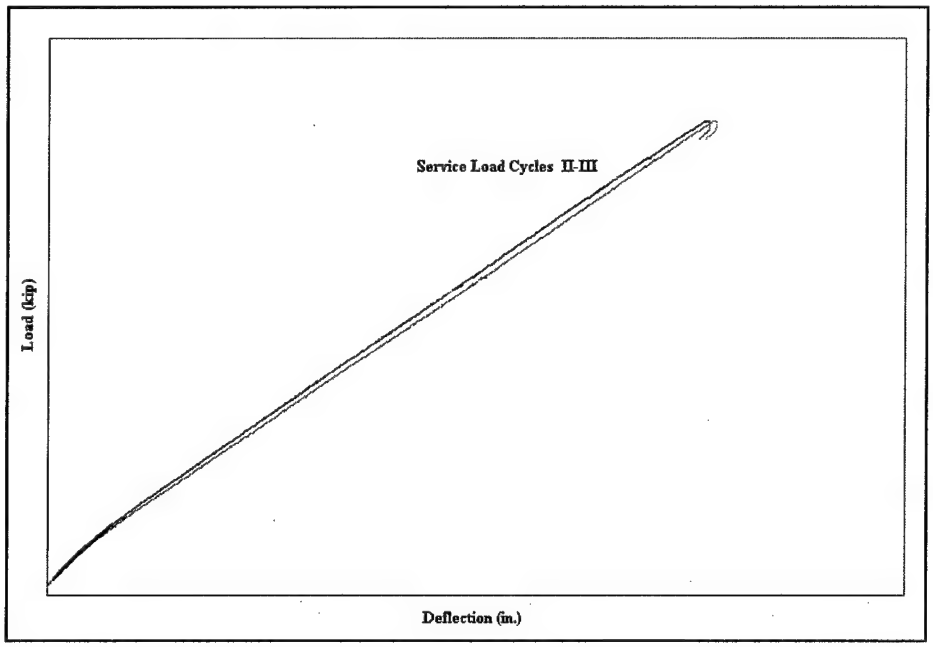

Figure 4.6. Specimen Load versus Deflection Curves (specimen A8)

represents a reasonable assumption for load levels greater than approximately 1.5 M_{cr}. Also note that the permanent deflection is ignored in Figure 4.7 as to model the load versus deflection curves obtained from an in-field load test.

For simplicity, assume that the initial load cycle curve in Figure 4.7 is the largest load in the girder's load history. If the in-field test load is some fraction less than the initial load the resulting curve follows the service load cycle curve on the left in Figure 4.7. In this situation, the load and deflection values at service load produce approximately the same conservative I_{act} value. Conservative because the service load versus deflection behavior of a reinforced concrete member is approximately linear and the test load is less than the largest sustained load.

If a field test load is larger than the initial service load, the load versus deflection curve follows the service load curve on the left, then, the overload cycle curve in Figure 4.7. The resulting load versus deflection will produce an inaccurate actual moment of inertia value due to additional cracking when the member is subjected to the larger load for the first time. For this reason, it is recommended that during a field load test a subject bridge be pre-loaded before any measurements are recorded. In the event an overload occurs, the subsequent test load cycle will follow the service load curve to the right in Figure 4.7. In this situation a conservative estimate of I_{act} is obtained as long as the overload did not exceed the capacity of the member. To avoid approaching a bridge's ultimate load capacity during a field test, safe-loading criteria needs to be established. It is the goal that such criteria can be established from the findings of this research and previous projects that focused on the behavior of reinforced concrete T-beams.

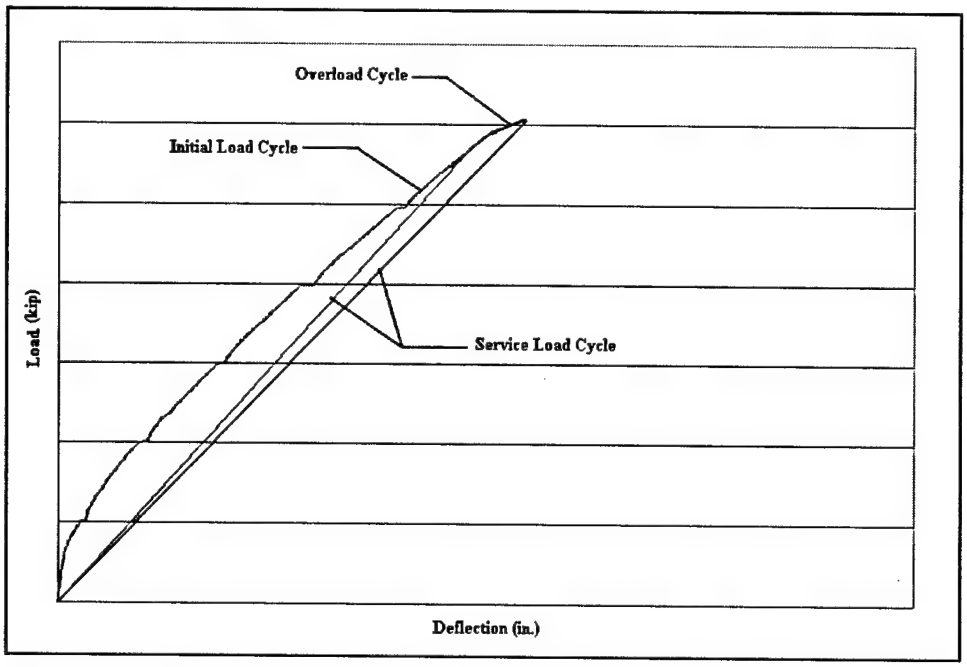

Figure 4.7. Life-cycle Behavior of T-beam Bridge Girder

5 Analysis of Results

5.1 General

The LVDT measured mid-span deflections and corresponding applied load values generated during the testing program outlined in Chapter 3 are used herein to determine which effective moment of inertia model (selected for study as a component of the proposed analysis procedure) most accurately models the service load behavior of a reinforced concrete T-beam subjected to a tandem-axle load configuration, typical of military equipment (AASHTO 1996). The models selected for study are:

a. The ACI Code Equation (Branson's model) (ACI 2002, Branson 1963), as given by Equation 1.1.

b. A generalized version of Branson's model (Al-Zaid et al. 1991), as given by Equation 2.8.

c. A cracked length form of Branson's model (Al-Zaid et al. 1991), as given by Equation 2.10.

d. The Fikry and Thomas model (Fikry and Thomas 1998), as given by Equation 2.17.

As a component of the proposed analysis procedure, the models listed above yield a value for the cracked moment of inertia (I_{cr}) when a field-measured moment of inertia (I_{act}) is substituted for I_e. For example, Equation 5.1 is Branson's model rearranged to solve for I_{cr} when I_e is replaced with I_{act}.

$$I_{cr} = [I_{act} - (M_{cr} / M_a)^3 \cdot I_g] / [1 - (M_{cr} / M_a)^3] \tag{5.1}$$

where

I_{cr} = cracked moment of inertia of the section
I_{act} = actual moment of inertia of the section
I_g = gross moment of inertia of the section
M_a = applied moment
M_{cr} = cracked moment of inertia of the section

The I_{act} term in Equation 5.1 is obtained by solving an elastic deflection relationship for the moment of inertia, given a deflection and corresponding load generated during a field load test.

As mentioned before, the primary function of the proposed analysis procedure is to estimate the amount of flexural reinforcement (A_s) contained in an in-service T-beam bridge girder. An estimate of A_s can be made by solving the higher order polynomial that results from substituting the value of I_{cr}, obtained from Equation 5.1 or a similar model, into the equation below (Equation 5.2), which is obtained from a transformed section analysis.

$$I_{cr} = (1/3)bc^3 + \eta As(d-c)^2 \tag{5.2}$$

where

I_{cr} = cracked moment of inertia
b = width of section
c = depth to neutral axis
η = modular ratio (E_s/E_c)
d = effective depth of reinforcement

The focus of this discussion is to compare experimental moment of inertia values to theoretical moment of inertia values obtained from the selected effective moment of inertia models. First, the discussion focuses on the well-known Branson model then progresses to two "enhanced" forms of Branson's model whose forms compensate for the shortcomings of the Branson model discussed in Chapter 2. A fourth model is also discussed which was derived with the purpose of eliminating the same Branson model shortcomings. In conclusion, the model that most accurately models the behavior of a cracked, reinforced concrete T-beam subjected to a load configuration typical of military equipment will be recommended for use in the proposed analysis procedure.

5.2 The Branson Model

A discussion regarding effective moment of inertia models begins with the model developed by Branson in the early 1960s (Branson 1963). Since its conception, it has been the chosen method for calculating the moment of inertia of a reinforced concrete member for the purpose of estimating deflection. This model is recommended by the ACI Building Code (ACI 2002), as well as, most other design building codes that address reinforced concrete design.

Branson's model yields an effective moment of inertia value that corresponds to the total deflection a reinforced concrete member experiences due to a given service load (PCA 1999). Total deflection is that measured from a datum, set when the member is cast, therefore including the deflection a reinforced concrete member cannot elastically recover from due to cracking (i.e., permanent deflection).

In the proposed analysis procedure a deflection and corresponding load from an in-field load test will be used to calculate a member's actual moment of inertia (I_{act}). If the resulting I_{act} value is substituted into Equation 5.1 (Branson's model rearranged to solve for I_{cr}) an erroneous I_{cr} value will be generated since the permanent deflection of the member has not been measured. The magnitude of the error is determined in the following discussion, which compares moment of inertia values calculated by Branson's model to moment of inertia values obtained from experimental data.

5.2.1 Branson Model Versus Experimental Values

The data generated during the aforementioned testing program, which included load-testing nine T-beam test specimens, is evaluated to understand the discrepancy that occurs when substituting an I_{act} value, obtained during a field load test, into Branson's model to determine I_{cr}. Representative data for each flexural reinforcement quantity (8 in.^{2}, 5 in.^{2}, and 3 in.^{2}) is presented both graphically and numerically in this discussion.

The data is presented in the form of load versus deflection graphs and in table format, both provide a comparison between theoretical and experimental data. Note that all data presented in section 5.2.1 is void of permanent deflection, which is typical of data obtained during an in-field load test.

5.2.1.1 T-beam Specimens with A_s = 8 in^2. The three test specimens having an area equal to 8 in.^{2} of flexural reinforcement (specimens A8, B8, and C8) all exhibited similar behavior when subjected to the service-loading testing program. Specimens B8 and C8 were subjected to a total of five load cycles, while specimen A8 was subjected to three load cycles. After the final service load cycle was applied to beam A8, it was loaded to failure to create a control for future testing that is not germane to the objective of this thesis. The test data for specimen B8 is presented herein as representative of the specimens containing 8 in.^{2} of flexural reinforcement. The curves in Figure 5.1 show that Branson's model overestimates the testing program deflection by approximately 20 percent. They illustrate that the calculated stiffness per Branson's model (Equation 1.1) is less than the stiffness resisting the applied service load.

To validate this, the effective moment of inertia values obtained from Branson's model ($I_{e\text{-BRANSON}}$) are compared to actual moment of inertia values (I_{act}) (obtained experimentally) over a range of applied load values (M_a/M_{cr}), as presented in Table 5.1. At service load, Branson's model produces a moment of inertia value that is approximately 17.5 percent less than the measured I_{act}. The difference is most likely due to the inclusion of inelastic effects, due to tensile cracking, by Branson's model.

Table 5.2 shows the cracked moment of inertia values obtained from Branson's model (defined as $I_{cr\text{-}BRANSON}$, where I_{act} is substituted for I_e) and compared to $I_{cr\text{-}TR}$, which is the moment of inertia obtained from a transformed section analysis (as given by Equation 5.2). This comparison reveals that if Branson's model is

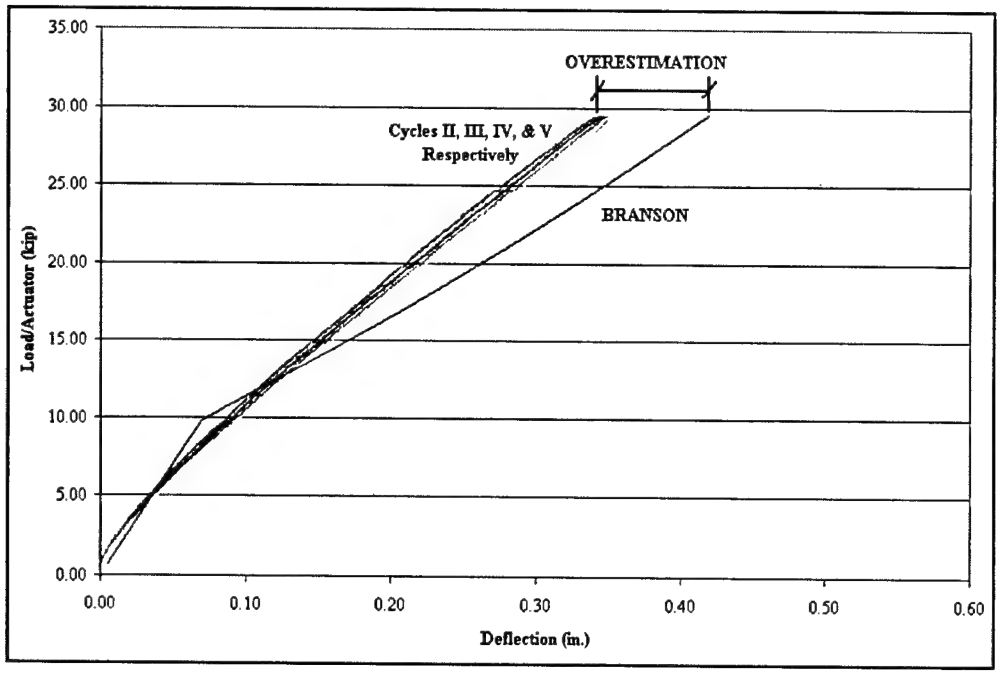

Figure 5.1. Typical Load versus Deflection A_s = 8 in.^{2} (Specimen B8)

Table 5.1
Moment of Inertia Values A_s = 8 in.^{2} (B8)

M_a/M_{cr}	I_{act} (in.^{4})	$I_{e\text{-BRANSON}}$ (in.^{4})	% Difference
0.51	50700	51600	-1.8
1.02	39700	49800	-25.4
1.36	37100	35500	4.3
1.53	35800	32300	9.8
1.70	35000	30300	13.4
1.87	34400	29000	15.7
2.05	33800	28100	16.9
2.21	33300	27400	17.7
2.38	32800	26900	18.0
2.56	32300	26500	18.0
2.73	32000	26300	17.8
2.90	31600	26000	17.7
3.05	31400	25900	17.5

used to determine I_{cr} (using the values of I_{act} from Table 5.1), I_{cr} is overestimated with respect to $I_{cr\text{-}TR}$. If a measured I_{act} from an in-service bridge test is substituted into Equation 5.1, a non-conservative estimate of I_{cr} will be obtained since permanent deflection can not be measured during a field load test. Therefore, the measured I_{act} is greater than the moment of inertia required to obtain the I_{cr} value calculated with Equation 5.2 for the T-beam in question.

Table 5.2 Comparison of I_{cr} Values A_s = 8 in.^{2} (B8)			
M_a/M_{cr}	$I_{cr\text{-}BRANSON}$ (in.^{4})	$I_{cr\text{-}TR}$ (in.^{4})	% Difference
0.51	51700	24900	51.8
1.02	*	24900	*
1.36	27700	24900	10.1
1.53	29800	24900	16.4
1.70	30900	24900	19.4
1.87	31400	24900	20.7
2.05	31500	24900	21.0
2.21	31500	24900	21.0
2.38	31400	24900	20.7
2.56	31100	24900	19.9
2.73	31000	24900	19.7
2.90	30800	24900	19.2
3.05	30700	24900	18.9
Note: (*) Model gives large, unrealistic results at loads close to M_{cr}.			

5.2.1.2 T-beam Specimens with A_s = 5 in^2. The test specimens containing an area equal to 5 in.^{2} of flexural reinforcement (specimens A5, B5, and C5) also exhibited similar behavior, as a group, when subjected to service load. Test specimens A5 and C5 exhibited almost identical behavior, while specimen B5 experienced deflections approximately 8 percent higher at all load levels. A possible cause for the discrepancy is a computer malfunction that prevented the deflection and load from being recorded until approximately 30 percent of the service load was applied to the member. Specimens B5 and C5 were subjected to five load cycles, while specimen A5 was subjected to three load cycles and then loaded to failure to create a control for future testing that is not germane to this thesis. The test data for specimen C5 is presented herein as representative of the specimens containing 5 in.^{2} of flexural reinforcement.

Similar to the specimens containing an area equal to 8 in.^{2} of flexural reinforcement, the curves in Figure 5.2 illustrate that the use of Branson's model overestimates the measured deflections by approximately 11 percent for specimens possessing 5 in.^{2} of flexural reinforcement.

Once again, the calculated stiffness per Branson's model (Equation 1.1) is less than the stiffness resisting the applied service load. To better understand, effective moment of inertia values obtained from Branson's model ($I_{e\text{-BRANSON}}$) are compared to actual moment of inertia values (I_{act}) (obtained experimentally) over a range of applied load values (M_a/M_{cr}) (Table 5.3). The values in Table 5.3 reveal an approximate 12.5 percent difference between experimental and theoretical moments of inertia. This is due, in part, to the model's inclusion of the inelastic effects of tensile cracking. Table 5.4 compares the cracked moment of inertia values obtained from Branson's model, $I_{cr\text{-}BRANSON}$, (as when I_{act} is substituted for I_e) to cracked moment of inertia values obtained from a transformed section analysis ($I_{cr\text{-}TR}$).

The values in Table 5.4 reveal that I_{cr} is overestimated if I_{act} is substituted into Equation 5.1 as compared to the I_{cr} values obtained from a transformed section analysis. Once again it can be observed that if Branson's model is used

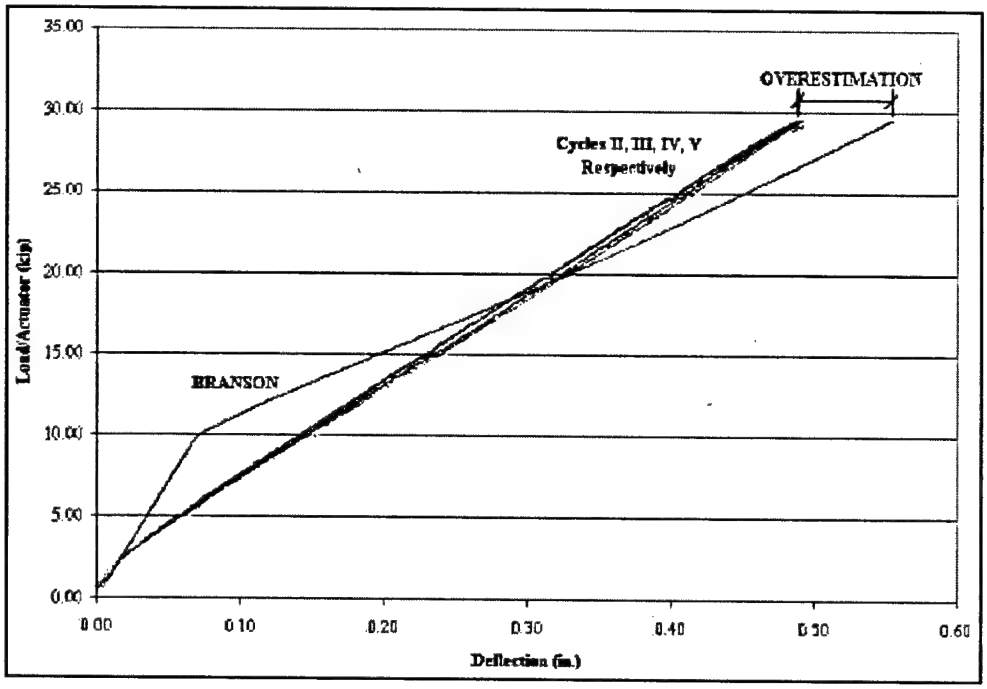

Figure 5.2. Typical Load versus Deflection A_s = 5 in.^{2} (Specimen C5)

Table 5.3
Moment of Inertia Values A_s = 5 in.^{2} (C5)

M_a/M_{cr}	I_{act} (in.^{4})	$I_{e\text{-BRANSON}}$ (in.^{4})	% Difference
0.51	30000	51600	-72.0
1.01	24600	50400	-104.9
1.35	23600	31800	-34.7
1.52	23000	27600	-20.0
1.69	22800	25100	-10.1
1.85	22700	23300	-2.6
2.02	22400	22100	1.3
2.19	22300	21200	4.9
2.36	22200	20600	7.2
2.53	22100	20100	9.0
2.70	22000	19800	10.0
2.87	22000	19500	11.4
3.02	22000	19300	12.3

to determine I_{cr} given an I_{act} from an in-service bridge load test, I_{cr} will be overestimated for the reasons discussed previously in section 5.2.1.1.

5.2.1.3 T-beam Specimens with A_s = 3 in.^{2} The test specimens containing 3 in.^{2} of flexural reinforcement (specimens A3, B3, and C3) possessed the lightest reinforcement ratio of the T-beam test specimens. Due to the small amount of reinforcement, the service load moment was reduced by approximately 30 percent to avoid failure of the member. Experimental deflection and corresponding load data were collected for specimens B3 and C3 only, both of which were subjected

Table 5.4
Comparison of I_{cr} Values A_s = 5 in.^{2} (C5)

M_{cr}/M_a	$I_{cr\text{-}BRANSON}$ (in.^{4})	$I_{cr\text{-}TR}$ (in.^{4})	% Difference
0.51	54800	18000	67.2
1.01	*	18000	*
1.35	4300	18000	-319
1.52	11600	18000	-55.2
1.69	15300	18000	-17.6
1.85	17400	18000	-3.4
2.02	18500	18000	2.7
2.19	19300	18000	6.7
2.36	19800	18000	9.1
2.53	20200	18000	10.9
2.70	20500	18000	12.2
2.87	20700	18000	13.0
3.02	20900	18000	13.9

Note: (*) Model gives large, unrealistic results at loads close to M_{cr}.

to five cycles of service load. No usable data was obtained for specimen A3 due to an attempt to conduct the test procedure in deflection control, which did not allow the actuators to apply equal magnitude loads. The test data for specimen C3 is presented herein as representative of the specimens containing 3 in.^{2} of flexural reinforcement.

The curves in Figure 5.3 illustrate that Branson's model underestimates the testing program deflection by approximately 10 percent with respect to specimens containing 3 in.^{2} of flexural reinforcement. In contrast to the specimens containing 8 in.^{2} and 5 in.^{2} of flexural reinforcement, the stiffness calculated per Branson's model is greater than the stiffness resisting the applied service load. This is validated by the comparison of effective moment of inertia values obtained from Branson's model ($I_{e\text{-}BRANSON}$) to actual moment of inertia values (I_{act}) (obtained experimentally) over a range of applied load values (M_a/M_{cr}) (Table 5.5).

The values in Table 5.5 reveal that Branson's model overestimates moment of inertia by approximately 8 percent at service load. The inability of Branson's model to accurately model lightly reinforced concrete members was also observed by Fikry and Thomas (1998). Therefore, the performance of Branson's model with respect to its intended purpose (estimating effective moment of inertia for the purpose of calculating reinforced concrete member deflection that includes permanent deflection) is presented in section 5.2.3.

In Table 5.6 cracked moment of inertia values, obtained from Branson's model (when I_{act} is substituted for I_e) ($I_{cr\text{-}BRANSON}$), are compared to cracked moment of inertia values obtained from a transformed section analysis ($I_{cr\text{-}TR}$). The values shown reveal an approximate 11 percent underestimation of I_{cr} if the underestimated I_{act} value is substituted for I_e in Equation 5.1. In this case, if Branson's model is used to determine I_{cr} from a field measured I_{act}, I_{cr} will be conservatively underestimated.

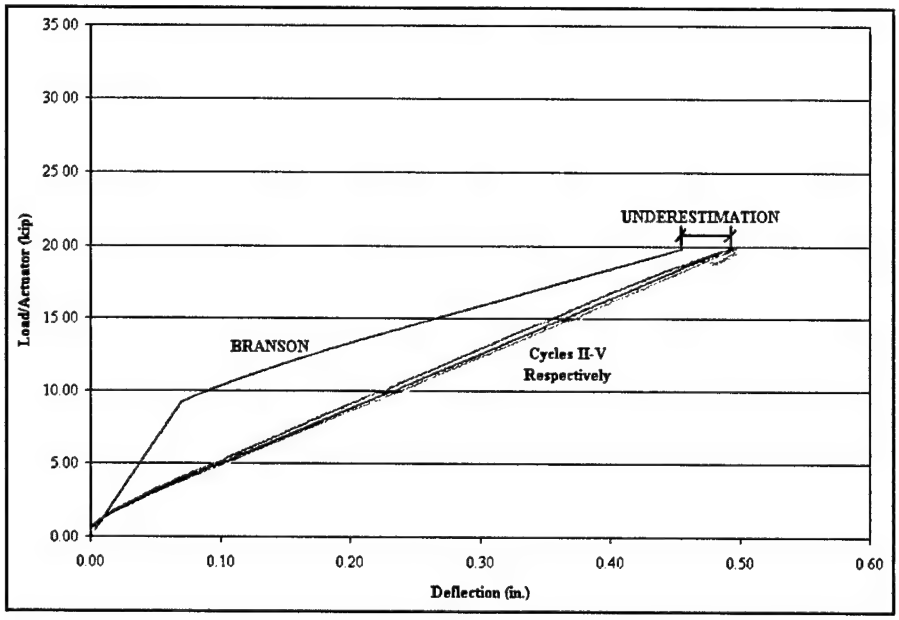

Figure 5.3 - Typical Load versus Deflection A_s = 3 in.^{2} (Specimen C3)

Table 5.5
Moment of Inertia Values A_s = 3 in.^{2} (C3)

M_a/M_{cr}	I_{act} (in.^{4})	$I_{e\text{-BRANSON}}$ (in.^{4})	% Difference
0.54	19300	51600	-167.4
1.08	16500	43400	-163.0
1.35	16300	28600	-75.5
1.43	16200	26100	-61.1
1.52	16100	24100	-49.7
1.60	16000	22500	-40.6
1.68	16000	21200	-32.5
1.76	15900	20100	-26.4
1.84	15900	19200	-20.8
1.92	15800	18500	-17.1
2.00	15800	17800	-12.7
2.08	15700	17300	-10.2
2.17	15600	16800	-7.7

5.2.2 Branson Model Conclusions

The comparison of measured deflections to deflections obtained using the Branson model revealed that an inaccurate I_{cr} value is obtained when I_{act} (obtained experimentally) is substituted into Branson's model. In the instance of members containing 8 in.^{2} and 5 in.^{2} of flexural reinforcement, this is most likely

Table 5.6
Comparison of I_{cr} Values A_s = 3 in.^{2} (C3)

M_a/M_{cr}	$I_{cr\text{-}BRANSON}$ (in.^{4})	$I_{cr\text{-}TR}$ (in.^{4})	% Difference
0.54	57700	13000	77.5
1.08	*	13000	*
1.35	*	13000	*
1.43	*	13000	*
1.52	1900	13000	-584.2
1.60	4500	13000	-188.9
1.68	6500	13000	-100.0
1.76	7900	13000	-64.6
1.84	9100	13000	-42.9
1.92	10000	13000	-30.0
2.00	10800	13000	-20.4
2.08	11300	13000	-15.0
2.17	11700	13000	-11.1

Note: (*) Model gives large, unrealistic results at loads close to M_{cr}.

due to the fact that permanent deflections are included in the Branson model but were not measured. In the case of 3 in.^{2} of flexural reinforcement the error is more likely due to the inherent inability of the Branson model to accurately model lightly reinforced cross-sections. The sign and magnitude of the error is relative to the amount of reinforcement in the member's cross-section. In the instance of 8 in^2 and 5 in^2 of flexural reinforcement, I_{cr} is unconservatively overestimated and in the instance of 3 in^2 of flexural reinforcement I_{cr} is conservatively underestimated.

The data presented in Tables 5.1 through 5.6 also reveals that the in-field test load must be significantly larger than the cracking moment to avoid the large, unrealistic behavior exhibited at low load levels, close to the cracking moment.

5.2.3 Total Deflection

As detailed in Chapter 2, numerous researchers have shown that Branson's model has inherent shortcomings (e.g., Fikry and Thomas 1998 and Al-Zaid et al. 1991). Therefore, the performance of the model, with respect to its intended purpose (estimating effective moment of inertia for the purpose of calculating total deflection) is presented. Typical load versus deflection plots are presented below for each reinforcement ratio (Figures 5.4, 5.5, and 5.6). These plots are similar to Figures 5.1, 5.2, and 5.3; the difference being, the permanent deflection experienced by the member is shown in Figures 5.4, 5.5, and 5.6. The permanent deflection is the deflection recorded after each load cycle was complete.

These plots (Figures 5.4, 5.5, & 5.6) show that Branson's model provides a reasonable estimate of service load deflection with respect to a reinforced concrete specimen containing 8 in.^{2} of flexural reinforcement, but as reinforcement ratio decreases Branson's model increasingly underestimates the deflection (overestimates effective moment of inertia) of the member. As mentioned earlier, this discrepancy at low levels of reinforcement was also observed by Fikry and Thomas (1998).

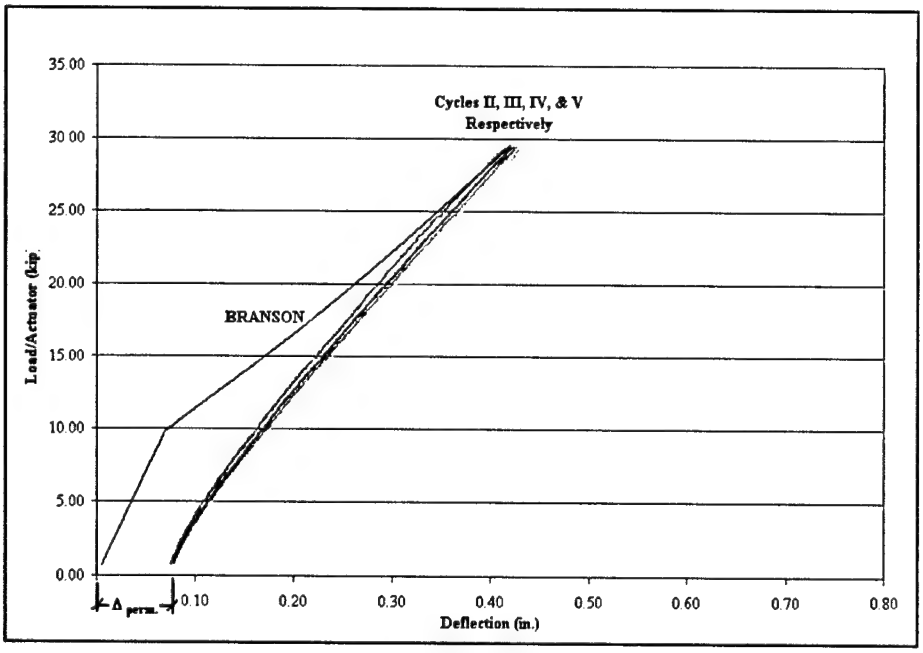

Figure 5.4.Typical Load versus Deflection (including $\Delta_{perm.}$) A_s= 8 in.^{2} (Specimen B8)

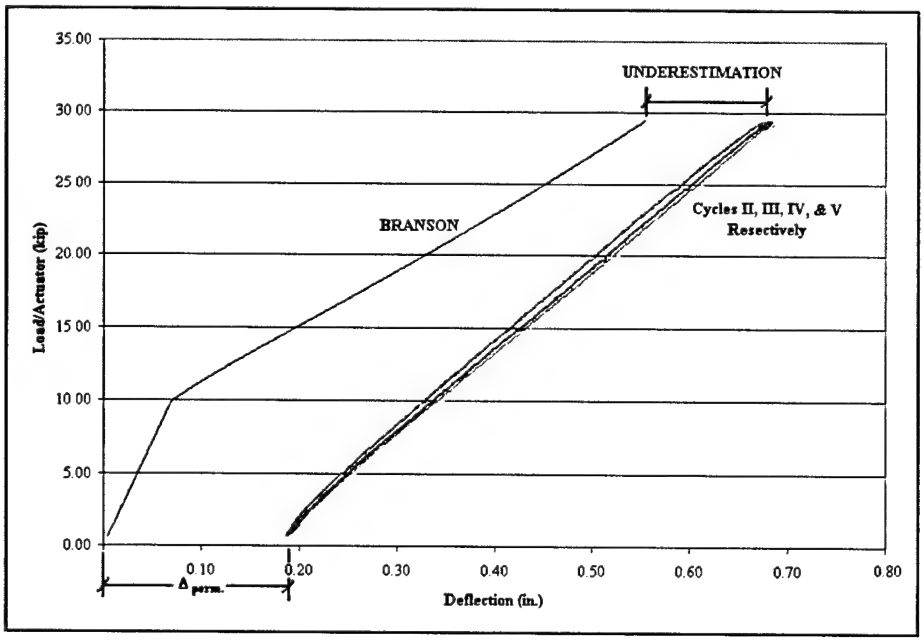

Figure 5.5.Typical load versus Deflection (including $\Delta_{perm.}$) A_s= 5 in.^{2} (Specimen C5)

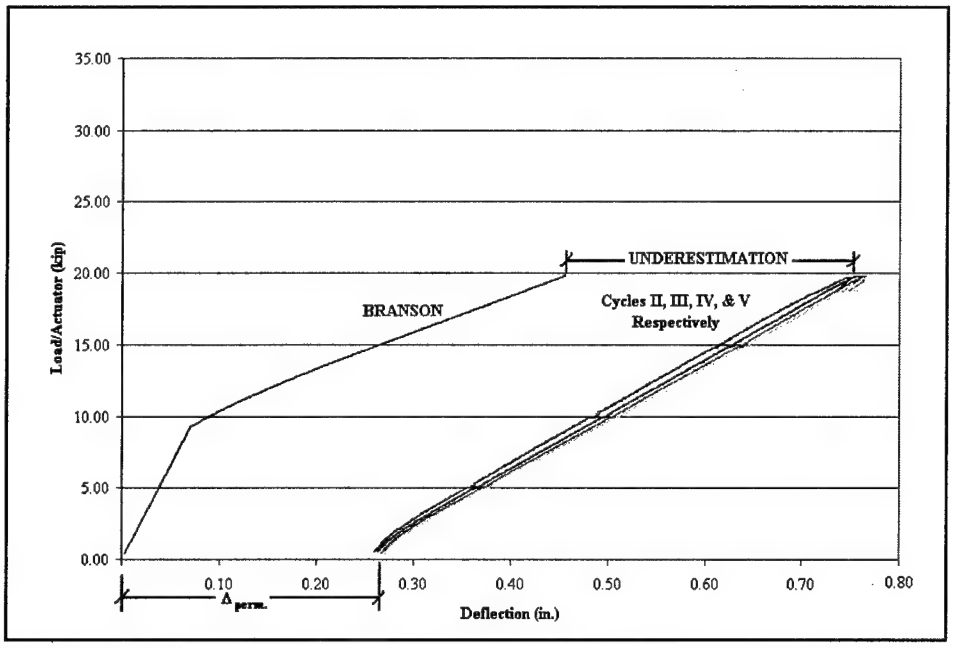

Figure 5.6. Typical load versus Deflection (including $?_{perm.}$) A_s= 3 in.^{2} (Specimen C3)

The underestimation of member deflection is approximately 21 percent for members containing 5 in.^{2} of flexural reinforcement and 60 percent for members possessing 3 in.^{2}

The discrepancy between measured deflection (total deflection) at service load and theoretical deflection obtained from Branson's model for specimens containing 5 in.^{2} and 3 in.^{2} of flexural reinforcement (Figures 5.5 and 5.6) reveals that the discrepancy observed in sections 5.2.1.2 and 5.2.1.3 (Figures 5.2 and 5.3), when permanent deflection was not measured, is in-part caused by the inherent shortcomings associated with Branson's model. Possible reasons for the discrepancies observed in Figures 5.5 and 5.6 are discussed in the technical writings referenced in Chapter 2 (Al-Zaid et al. 1991, Al-Shaikh and Al-Zaid 1993, Fikry and Thomas 1998, Grossman 1981).

5.3 Alternative Effective Moment of Inertia Models

Since it first appeared in the ACI Building Code (1971), the accuracy of Branson's model has been a source of debate in both the design and academic communities. As discussed in Chapter 2, numerous researchers have successfully shown the inherent shortcomings of Branson's model, and a few took the next step and somehow improved or modified Branson's model. In all cases, the respective researchers were interested in the agreement between theoretical deflection and experimental deflection (total deflection). Even though, the resulting models were created to serve that purpose, their form allows them to be "calibrated," making them suitable as a component of the proposed analysis procedure.

Particularly of interest are three studies, two of which were conducted by Al-Zaid et al. (1991) and Al-Shaikh and Al-Zaid (1993) and bore two improved forms of Branson's model (Equation 1.1); and a third study that developed a new, effective moment of inertia model from proven, concrete response theory (Fikry and Thomas 1998).

5.3.1 Modified Branson Model

Al-Zaid et al. (1991), and Al-Shaikh and Al-Zaid (1993) initially addressed the discrepancy between experimental moment of inertia (that corresponding to total deflection) and theoretical moment of inertia (obtained from Branson's model) by changing the cubic exponent in Branson's model to a variable (m), and solving for it experimentally. During the course of their research they observed that the exponent (m) was a function of both reinforcement ratio and load configuration (i.e., cracked length - the length over which a member's cracking moment is exceeded by applied moment).

The curves in Figures 5.1 through 5.3, which illustrate inconsistent flexural behavior between T-beams differing only in the amount of flexural reinforcement in their cross-sections, confirm that one exponent (m) cannot produce precise results for all reinforcement ratios. The fact that the exponent (m) is a function of the quantity of flexural reinforcement (Al-Shaikh and Al-Zaid, 1993) presents a drawback in an in-field situation when the amount of flexural reinforcement is unknown. In contrast to the findings drawn by Al-Zaid et al. (1991), data obtained during this testing program reveals that load configuration (i.e., cracked length) has an insignificant affect on the actual moment of inertia of a T-beam bridge girder. The curves in Figure 5.7 illustrate the difference in moment magnitude along the length of a generic T-beam test specimen when loaded to the same service load moment by two different load configurations. One load configuration is that implemented in the aforementioned testing program and described in Chapter 3. The other is a uniform load configuration, which is the load configuration considered by Branson during the development of Equation 1.1.

Labeled on Figure 5.7 is the difference in cracked length, dL_{cr}, at each end of the member (one-half L_{cr} in this case), a combined difference of approximately 3 ft over the entire 28 ft span. In contrast to the relatively short (8.21 ft), rectangular (9.5 in. by 8 in.) cross-sections tested by Al-Zaid et al. (1991), load configuration has an insignificant effect on the longer, larger T-beam test specimens. Therefore, in a situation involving an in-service T-beam, the primary parameter affecting the exponent m is the quantity of flexural reinforcement contained in the member.

5.3.1.1 Procedure. A portion of the research conducted by Al-Zaid et al. (1991), and Al-Shaikh and Al-Zaid (1993) focused on determining an exponent m for a specific load configuration and/or reinforcement ratio. A similar operation is performed with the T-beam test data to obtain an exponent m that replaces the

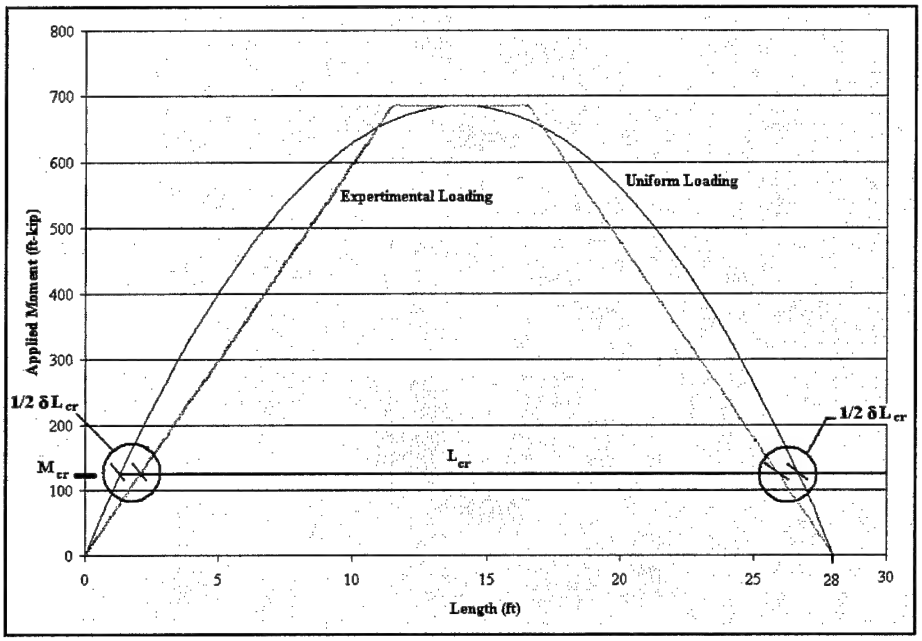

Figure 5.7. Variation of Moment over Member's Length

cubic exponent in Branson's model, allowing it to more accurately model the cracked T-beam behavior observed during the testing program. First, the experimental deflection and corresponding load data were substituted into the proper elastic deflection relationship (Equation 5.3) (PCI 1999).

$$\Delta = [kM_a/(E_c I_e)](3l^2 - 4a^2) \tag{5.3}$$

where

Δ = mid-span deflection
k = load configuration/end restraint constant (1/24 for test configuration)
M_a = applied load
E_c = elastic modulus of concrete
I_e = effective moment of inertia
l = member length
a = moment arm (which is equal to 1/2 [l – center-to-center load spacing])

An equation for the T-beam's actual moment of inertia (I_{act}) was then obtained by rearranging Equation 5.3 to the form of Equation 5.4 where I_e is replaced with I_{act}.

$$I_{act} = [kM_a/(E_c \Delta_{exp})](3l^2 - 4a^2) \tag{5.4}$$

where I_{act} is the experimental moment of inertia of the member and Δ_{exp} is the experimental mid-span deflection during testing. The actual moment of inertia was then substituted for the I_e term in Equation 2.8 to obtain Equation 5.5.

$$I_{act} = (M_{cr} / M_a)^m * I_g + [1 - (M_{cr} / M_a)^m] * I_{cr} \quad (5.5)$$

where

m = experimentally determined exponent
I_{act} = actual moment of inertia
I_{cr} = cracked moment of inertia
I_g = gross moment of inertia
M_a = applied moment
M_{cr} = cracking moment

Upon arrangement of the terms in Equation 5.5, the expression of the exponent m can then be determined for a specific load configuration and/or reinforcement ratio as follows:

$$m = \log [(I_{act} - I_{cr})/(I_g - I_{cr})] / \log(M_{cr} / M_a) \quad (5.6)$$

5.3.1.2 Exponent *m* behavior. The behavior of the exponent m, with respect to applied load, is evaluated by applying the procedure outlined in section 5.3.1.1 to the test data. First, the behavior of m is evaluated over a complete (zero-to-failure) load cycle, and then the focus turns to the behavior of m over a typical service load cycle. This was accomplished by using the data generated from testing specimen A5 up to failure. Figure 5.8 shows a plot of m versus the ratio of M_a/M_{cr} for specimen A5. Note that this specimen was tested to failure. In general, the behavior illustrated in Figure 5.8 is typical of the exponent m behavior observed during the testing of all reinforced concrete members by Al-Zaid et al. (1991) and Al-Shaikh and Al-Zaid (1993) and those tested to failure herein. No values for m are given in Figure 5.8 to avoid later confusion regarding the value of m, which is a function of reinforcement ratio.

In this figure, the curve reveals that the value of m is very sensitive at low and high ratios of M_a/M_{cr}, but tends to be constant otherwise. The low point of the curve is around $M_a/M_{cr} = 3.5$. The service load moment used during the testing program was approximately 3.1 times the cracking moment, therefore allowing the constant, experimental value of m to be determined for each test specimen. In the case of specimens containing $A_s = 3$ in.^{2}, the M_a/M_{cr} ratio was approximately 2.2, which is at the beginning of the constant region of m values. The smaller M_a/M_{cr} was agreed upon during testing as to not approach the failure strength of the $A_s = 3$ in.^{2} test specimens.

The typical form of an exponent (m) versus M_a/M_{cr} plot generated by applying four service load cycles to a cracked, T-beam test specimen (specimen B8), as presented in Figure 5.9. The sensitive portion of the curve ($M_a/M_{cr} < 1.5$) is ignored leaving a curve that illustrates the approximately constant value of m referred to in Figure 5.8.

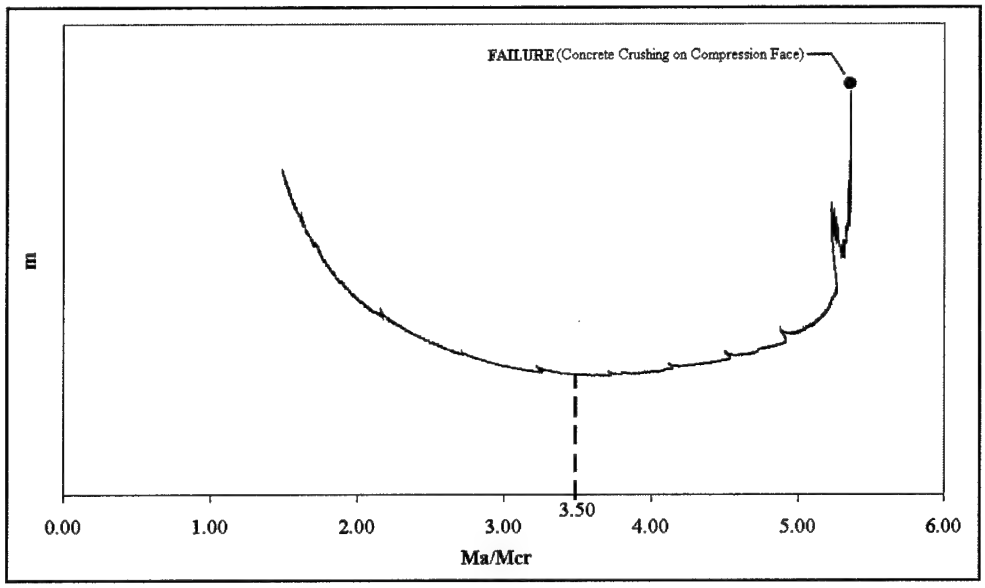

Figure 5.8. Exponent *m* versus Applied Load over a Complete Load Cycle (Specimen A5)

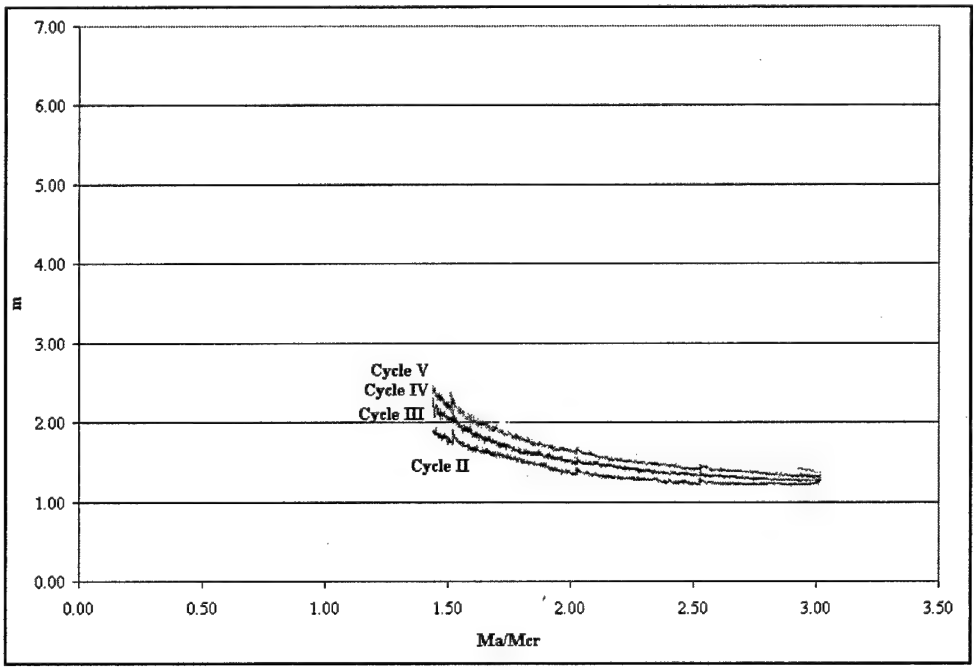

Figure 5.9. Typical *m* versus applied load (Specimen B8)

5.3.1.3 Determination of the Exponent *m*. A means of determining the constant value of m, mentioned above, is developed with the aid of the m versus applied load plots for each reinforcement ratio, thus presenting the exponent m as a function of applied load. This is done by using curve fitting of the individual (Cycle II, Cycle III, etc.) m versus M_a/M_{cr} curves with trend lines (as shown in Appendix B). The individual trend lines were then averaged, to obtain one M_a/M_{cr} curve for each test specimen. The "best-fit" curves corresponding to each test specimen are then combined with its peers (i.e., A8, B8, and C8) and averaged to generate a M_a/M_{cr} curve for each reinforcement ratio. The three resulting equations are:

For $A_s = 8$ in^2:

$$m = -0.675(M_a / M_{cr})^3 + 5.27(M_a / M_{cr})^2 - 14.0(M_a / M_{cr}) + 14.1 \quad (5.7)$$

For $A_s = 5$ in^2:

$$m = -1.06(M_a / M_{cr})^3 + 8.50(M_a / M_{cr})^2 - 23.3(M_a / M_{cr}) + 24.0 \quad (5.8)$$

For $A_s = 3$ in^2:

$$m = -3.96(M_a / M_{cr})^3 + 27.9(M_a / M_{cr})^2 - 66.5(M_a / M_{cr}) + 57.4 \quad (5.9)$$

Note that the test data corresponding to specimen B5 is ignored due to reasons previously explained.

To obtain a value for the exponent m for use in the modified Branson model a load ratio (corresponding to the testing program service load) is substituted into Equations 5.7, 5.8, and 5.9. The resulting exponent (m) values are presented in Table 5.7.

Table 5.7
Experimental Exponent *m* Values

A_s (in.^{2})	M_a/M_{cr}	m
8	3.1	1.2
5	3.1	1.9
3	2.2	4.0

5.3.1.4 Branson and Modified Models Compared. The accuracy of a "modified" Branson model that incorporates these experimentally determined exponents is shown in Tables 5.8 through 5.10. The tables present values of I_e determined with the original form of Branson's model ($I_{e\text{-}BRANSON}$) (Equation 1.1) and values of I_e determined with the Al-Zaid et al. (1991) modified form of the model ($I_{e\text{-}"modified"}$) (Equation 2.8). The accuracy of the models is represented by the ratio of actual moment of inertia (I_{act}) (experimentally obtained) to each theoretical moment of inertia. The table values are average values associated with the same representative test specimen used to previously illustrate the accuracy of Branson's model. In each case, application of the experimentally determined

exponent m forces the "modified" model to produce an effective moment of inertia approximately equal to I_{act} at service load. Therefore, data from only the representative test specimen for each reinforcement quantity is reported to show the improvement and to observe the model's accuracy over the range of testing program M_a/M_{cr} ratios.

Table 5.8
Theoretical Moment of Inertia Comparison A_s = 8 in.^{2} (specimen B8)

M_a/M_{cr}	I_{act} (in.^{4})	$I_{e\text{-BRANSON}}$ (in.^{4})	$I_{act}/I_{e\text{-BRANSON}}$	$I_{e\text{-"modified"}}$ (in.^{4})	$I_{exp}/I_{e\text{-"modified"}}$
0.51	50700	51600	0.98	51600	0.98
1.02	39700	49800	0.80	50900	0.78
1.36	37100	35500	1.04	43400	0.86
1.53	35800	32300	1.11	40900	0.88
1.70	35000	30300	1.16	39000	0.90
1.87	34400	29000	1.19	37500	0.92
2.05	33800	28100	1.20	36200	0.93
2.21	33300	27400	1.22	35200	0.95
2.38	32800	26900	1.22	34300	0.96
2.56	32300	26500	1.22	33600	0.96
2.73	32000	26300	1.22	32900	0.97
2.90	31600	26000	1.22	32400	0.98
3.05	31400	25900	1.21	31900	0.98

Table 5.9
Theoretical Moment of Inertia Comparison A_s = 5 in.^{2} (specimen C5)

M_a/M_{cr}	I_{act} (in.^{4})	$I_{e\text{-BRANSON}}$ (in.^{4})	$I_{act}/I_{e\text{-BRANSON}}$	$I_{e\text{-"modified"}}$ (in.^{4})	$I_{exp}/I_{e\text{-"modified"}}$
0.51	30000	51600	0.58	51600	0.58
1.01	24600	50400	0.49	50800	0.48
1.35	23600	31800	0.74	37100	0.63
1.52	23000	27600	0.83	33200	0.69
1.69	22800	25100	0.91	30500	0.75
1.85	22700	23300	0.97	28400	0.80
2.02	22400	22100	1.01	26800	0.83
2.19	22300	21200	1.05	25600	0.87
2.36	22200	20600	1.08	24600	0.90
2.53	22100	20100	1.10	23800	0.93
2.70	22000	19800	1.11	23100	0.95
2.86	22000	19500	1.13	22600	0.97
3.02	22000	19300	1.14	22200	0.99

Table 5.10
Theoretical Moment of Inertia Comparison A_s = 3 in.^{2} (specimen C3)

M_a/M_{cr}	I_{act} (in.^{4})	$I_{e\text{-BRANSON}}$ (in.^{4})	$I_{act}/I_{e\text{-BRANSON}}$	$I_{e\text{-"modified"}}$ (in.^{4})	$I_{exp}/I_{e\text{-"modified"}}$
0.54	19300	51600	0.37	51600	0.37
1.08	16500	43400	0.38	41100	0.40
1.35	16300	28600	0.57	24500	0.66
1.43	16200	26100	0.62	22100	0.73
1.52	16100	24100	0.67	20300	0.79
1.60	16000	22500	0.71	19000	0.84
1.68	16000	21200	0.75	17900	0.89
1.76	15900	20100	0.79	17100	0.93
1.84	15900	19200	0.82	16400	0.97
1.92	15800	18500	0.86	15900	1.00
2.00	15800	17800	0.88	15400	1.02
2.08	15700	17300	0.91	15100	1.04
2.17	15600	16800	0.93	14800	1.06

The values in Tables 5.8 through 5.10 reveal that using an appropriate experimentally determined exponent m allows Al-Zaid et al. (1991) and Al-Shaikh and Al-Zaid's (1993) "modified" form of Branson's model to more accurately model the behavior of the cracked T-beam test specimens that contain 8 in.^{2} and 5 in.^{2} of flexural reinforcement. Conversely, in the case of specimens containing 3 in.^{2} of flexural reinforcement the modified model provides no significant improvement. The magnitude of the discrepancy remains the same, only a change of sign occurs. This is partly due to the consideration of only two specimens containing 3 in.^{2} of flexural reinforcement, which did not behave similarly, thus resulting in a poor average for the exponent (m); and partly due to the model's form, which is inherently unable to accurately model reinforced concrete members with low quantities of reinforcement (Fikry and Thomas 1998).

The I_{act} values obtained from the experimental data were substituted into the modified Branson model (Equation 5.5), utilizing the respective exponent m, to obtain I_{cr}. The subsequent I_{cr} values ($I_{cr\text{-}"modified"}$) are compared to I_{cr} values obtained per a transformed section analysis ($I_{cr\text{-}TR}$) in Tables 5.11 through 5.13. The values in Tables 5.11 through 5.13 reveal that the modified Branson model along with its respective exponent (m) produce reasonable estimates for I_{cr} in the case of specimens containing 8 in.^{2} and 5 in.^{2} of flexural reinforcement. The same is not true for specimens containing 3 in.^{2} of flexural reinforcement for reasons previously discussed.

Table 5.11
Cracked Moment of Inertia Comparison A_s = 8 in.^{2} (specimen B8)

M_a/M_{cr}	$I_{cr\text{-}"modified"}$ (in.^{4})	$I_{cr\text{-}TR}$ (in.^{4})	% Difference
0.51	52300	24900	52.4
1.02	*	24900	*
1.36	4900	24900	-408.2
1.53	12400	24900	-100.8
1.70	16600	24900	-50.0
1.87	19200	24900	-29.7
2.05	20800	24900	-19.7
2.21	21900	24900	-13.7
2.38	22600	24900	-10.2
2.56	23100	24900	-7.8
2.73	23700	24900	-5.1
2.90	23900	24900	-4.2
3.05	24300	24900	-2.5

Note: (*) Model gives large, unrealistic results at loads close to M_{cr}.

5.3.1.5 Modified Branson Model Conclusions. It was shown that the Al-Zaid et al. (1991) form of Branson's model accurately models the behavior of a cracked, reinforced concreter member whenever the proper exponent is utilized. The exponent (m) is dependent on the reinforcement quantity though, an unknown parameter. For the modified form of Branson's model to be considered as a component of the proposed analysis procedure, a value for m that can be used in all field situations must be available.

A survey of some in-service T-beam bridges, spanning approximately 30 to 50 ft, in the Virginia Department of Highways Salem District revealed it is

Table 5.12
Cracked Moment of Inertia Comparison A_s = 5 in.^{2} (specimen C5)

M_a/M_{cr}	$I_{cr\text{-}"modified"}$ (in.^{4})	$I_{cr\text{-}TR}$ (in.^{4})	% Difference
0.51	59700	18000	69.8
1.01	*	18000	*
1.35	*	18000	*
1.52	*	18000	*
1.69	5900	18000	-205.1
1.85	9800	18000	-83.7
2.02	12100	18000	-48.8
2.19	13900	18000	-29.5
2.36	15100	18000	-19.2
2.53	16100	18000	-11.8
2.70	16800	18000	-7.1
2.86	17400	18000	-3.4
3.02	17900	18000	-0.6

Note: (*) Model gives large, unrealistic results at loads close to M_{cr}.

Table 5.13
Cracked Moment of Inertia Comparison A_s = 3 in.^{2} (specimen C3)

M_a/M_{cr}	$I_{cr\text{-}"modified"}$ (in.^{4})	$I_{cr\text{-}ACI}$ (in.^{4})	% Difference
0.54	57700	13000	77.5
1.08	∞	13000	∞
1.35	∞	13000	∞
1.43	∞	13000	∞
1.52	1900	13000	-584.2
1.60	4500	13000	-188.9
1.68	6500	13000	-100.0
1.76	7900	13000	-64.6
1.84	9100	13000	-42.9
1.92	10000	13000	-30.0
2.00	10800	13000	-20.4
2.08	11300	13000	-15.0
2.17	11700	13000	-11.1

Note: (*) Model gives large, unrealistic results at loads close to M_{cr}.

reasonable to assume that a typical T-beam bridge girder contains more than 3 in.^{2} of flexural reinforcement (better referred to in terms of reinforcement ratio here, $\rho = 0.93$). Therefore, the values associated with the specimens having a reinforcement ratio of $\rho = 0.93$ can be ignored because it is unlikely a member with such a low reinforcement ratio will be encountered in a real situation. The low-end reinforcement ratio was chosen at the on-set of the testing program to evaluate if selected effective moment of inertia models could distinguish between the different reinforcement quantities over the range of A_s that allowed the most member deflection (Figure 3.4) and return the proper value of I_{cr}. As shown, this is not the case unless the proper value for m is utilized.

Elimination of Equation 5.9 leaves the relationships for A_s = 5 in.^{2} (Equation 5.8) and A_s = 8 in.^{2} (Equation 5.7). A conservative approach is to determine which exponent produces a conservative estimation of I_{cr} for the other situation.

Considering the initial value of m (3), the conservative value is the exponent that is produced by the 8 $in.^2$ relationship. This raises the question, does the exponent m continue to decrease with higher reinforcement ratios or is the behavior asymptotic to some value, a question that cannot be answered with the testing program data. Therefore, based on the findings of this research and conservative assumptions, it is recommended that a value of $m = 1.2$ be utilized in lieu of the cubic exponent incorporated into Branson's model when the modified Branson model is utilized in the proposed analysis procedure.

5.3.2 Cracked Length Model

Al-Zaid et al. (1991) also developed an effective moment of inertia model that inherently accounts for the observed affect that loading configuration has on effective moment of inertia. The model (Equation 2.10) accounts for the effect by using a form of Branson's model written in terms of the cracked length and the overall length of the member. The form of the model leaves the exponent (m') solely dependent on the reinforcement ratio.

5.3.2.1 Procedure. Generally, the values for m' were calculated in the same manner as the exponent (m) was previously calculated, but instead of substituting I_{act} into Equation 2.8, I_{act} replaced the I_e term in Equation 2.10 to obtain Equation 5.10.

$$I_{act} = (L_{cr}/L)^{m'} * I_{cr} + [1-(L_{cr}/L)^{m'}] * I_g \tag{5.10}$$

where

I_{act} = the actual moment of inertia
I_{cr} = cracked moment of inertia
I_g = gross moment of inertia
m' = experimentally determined exponent
L_{cr} = cracked length of the member
L = length of the member

Equation 5.10 can be rearranged to solve for the unknown exponent (m') as follows,

$$m' = \log[(I_g - I_{act})/(I_g - I_{cr})]/\log(L_{cr}L) \tag{5.11}$$

The exponent (m') can then be determined for each reinforcement ratio.

5.3.2.2 Exponent *m'* Behavior. The behavior of the exponent m', with respect to applied load, is evaluated by applying the procedure outlined in section 5.3.2.1, along with the changes of section 5.3.2.1, to the test data. First, the behavior of m' is evaluated over a complete (zero-to-failure) load cycle, and then the focus turns to the behavior of m' over a typical service load cycle. This was accomplished using the data generated from testing specimen A5. Figure 5.10 shows a plot of m' versus the ratio of M_a/M_{cr} for specimen A5. Note that this

specimen was tested to failure and that no values for *m'* are given in Figure 5.10 to avoid later confusion regarding the value of *m'*, which is a function reinforcement ratio.

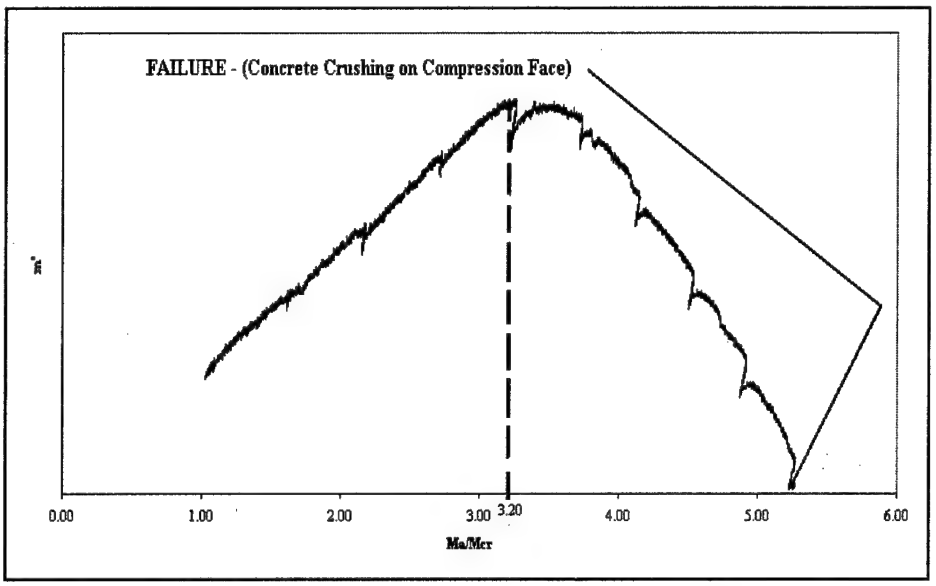

Figure 5.10. Exponent *m'* versus Applied Load over a Complete Load Cycle (Specimen A5)

The curve exhibits an apex at approximately $M_a/M_{cr} = 3.2$ and reveals that m' is sensitive at low and high ratios of M_a/M_{cr}, characteristics similar to the behavior of exponent (*m*). Conversely, the m' versus M_a/M_{cr} curve is concave down and exhibits parabolic, rather than cubic behavior. The region of constant exponent values observed with the exponent m data is less pronounced in this case due to the parabolic behavior of the m' data.

The typical form of an exponent *m'* versus M_a/M_{cr} plot produced by the application of four service load cycles to a T-beam test specimen (B8) is presented in Figure 5.11 (Appendix C – *m'* versus M_a/M_{cr} for all specimens). The sensitive portion of the curve ($M_a/M_{cr} < 1.0$) is ignored leaving a curve that illustrates the values of *m'* between the cracking moment and the service load moment.

5.3.2.3 Determination of Exponent *m'*. The curve fitting procedure that was applied to the exponent m data is similarly applied to the exponent *m'* versus M_a/M_{cr} plots to obtain a relationship for *m'* that is a function of M_a/M_{cr} for each reinforcement ratio. The three resulting relationships are:

For $A_s = 8$ in^2:

$$m' = -0.052\,(M_a/M_{cr})^2 + 0.420\,(M_a/M_{cr}) + 0.021 \qquad (5.12)$$

For $A_s = 5$ in^2:

$$m' = -0.014\,(M_a/M_{cr})^2 + 0.182\,(M_a/M_{cr}) + 0.03 \qquad (5.13)$$

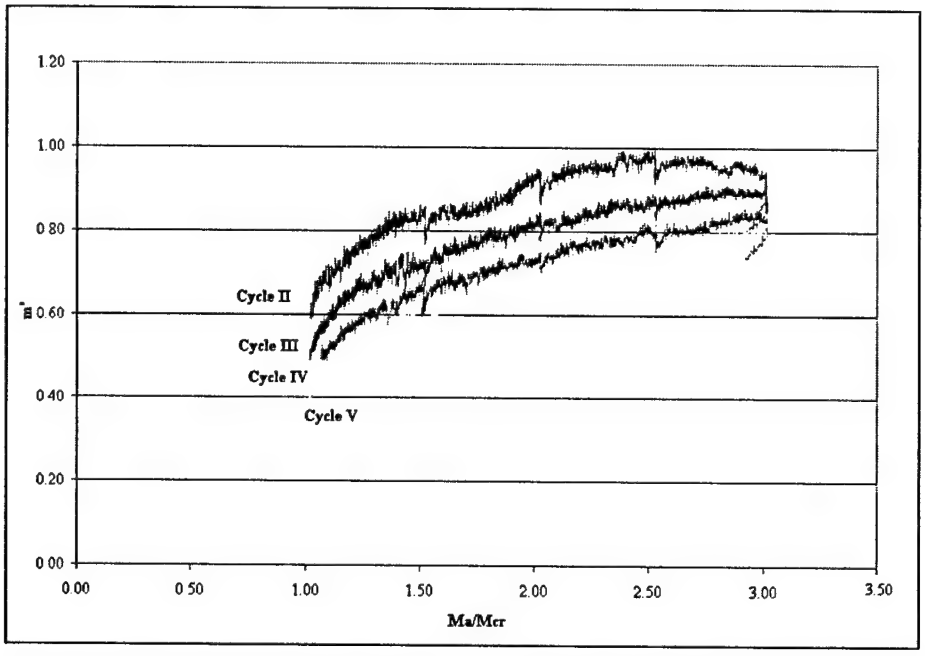

Figure 5.11. Typical *m'* versus Applied Load (Specimen B8)

For $A_s = 3$ in.^{2}:

$$m' = -0.012\,(M_a / M_{cr})^2 + 0.095\,(M_a / M_{cr}) + 0.037 \qquad (5.14)$$

Note that the data associated with specimen B5 is ignored once again due to the malfunction of the data acquisition system. To obtain a value for the exponent *m'* for use in the "cracked" model, the appropriate load ratio (ratio corresponding to testing program service load) is substituted into Equations 5.12, 5.13, and 5.14. The respective M_a/M_{cr} ratios and the resulting exponent (*m'*) values are presented in Table 5.14.

Table 5.14
Experimental *m'* Values

A_s (in.^{2})	M_a/M_{cr}	m'
8	3.1	0.82
5	3.1	0.46
3	2.2	0.11

5.3.2.4 Branson and Cracked Models Compared. The accuracy of the cracked length form of Branson's model that incorporates these experimentally determined exponents is revealed in the values of Tables 5.15 through 5.17. The tables list the values of I_e obtained from the original form of Branson's model

Table 5.15
Theoretical Moment of Inertia Comparison A_s = 8 in.^{2} (specimen B8)

M_a/M_{cr}	I_{act} (in.^{4})	$I_{e\text{-BRANSON}}$ (in.^{4})	$I_{act}/I_{e\text{-BRANSON}}$	$I_{e\text{-"cracked"}}$(in.^{4})	$I_{exp}/I_{e\text{-"cracked"}}$
0.51	50700	51600	0.98	25800	1.96
1.02	39700	49800	0.80	45200	0.88
1.36	37100	35500	1.04	39800	0.93
1.53	35800	32300	1.11	38000	0.94
1.70	35000	30300	1.16	36700	0.96
1.87	34400	29000	1.19	35600	0.97
2.05	33800	28100	1.20	34600	0.97
2.21	33300	27400	1.22	33900	0.98
2.38	32800	26900	1.22	33200	0.99
2.56	32300	26500	1.22	32600	0.99
2.73	32000	26300	1.22	32200	1.00
2.90	31600	26000	1.22	31700	1.00
3.05	31400	25900	1.21	31400	1.00

Table 5.16
Theoretical Moment of Inertia Comparison A_s = 5 in.^{2} (specimen C5)

M_a/M_{cr}	I_{act} (in.^{4})	$I_{e\text{-BRANSON}}$ (in.^{4})	$I_{act}/I_{e\text{-BRANSON}}$	$I_{e\text{-"cracked"}}$(in.^{4})	$I_{exp}/I_{e\text{-"cracked"}}$
0.51	30000	51600	0.58	18300	1.64
1.01	24600	50400	0.49	34900	0.70
1.35	23600	31800	0.74	29000	0.81
1.52	23000	27600	0.83	27400	0.84
1.69	22800	25100	0.91	26300	0.87
1.85	22700	23300	0.97	25400	0.89
2.02	22400	22100	1.01	24600	0.91
2.19	22300	21200	1.05	24100	0.93
2.36	22200	20600	1.08	23600	0.94
2.53	22100	20100	1.10	23100	0.95
2.70	22000	19800	1.11	22800	0.97
2.86	22000	19500	1.13	22500	0.98
3.02	22000	19300	1.14	22200	0.99

Table 5.17
Theoretical Moment of Inertia Comparison A_s = 3 in.^{2} (specimen C3)

M_a/M_{cr}	I_{act} (in.^{4})	$I_{e\text{-BRANSON}}$ (in.^{4})	$I_{act}/I_{e\text{-BRANSON}}$	$I_{e\text{-"cracked"}}$(in.^{4})	$I_{exp}/I_{e\text{-"cracked"}}$
0.54	19300	51600	0.37	13700	1.41
1.08	16500	43400	0.38	19500	0.85
1.35	16300	28600	0.57	17500	0.93
1.43	16200	26100	0.62	17100	0.95
1.52	16100	24100	0.67	16800	0.96
1.60	16000	22500	0.71	16500	0.97
1.68	16000	21200	0.75	16300	0.98
1.76	15900	20100	0.79	16100	0.99
1.84	15900	19200	0.82	15900	1.00
1.92	15800	18500	0.86	15700	1.00
2.00	15800	17800	0.88	15600	1.01
2.08	15700	17300	0.91	15500	1.01
2.17	15600	16800	0.93	15400	1.02

($I_{e\text{-}BRANSON}$) (Equation 1.1) and values of I_e determined with the cracked length form of the model ($I_{e\text{-}"cracked"}$) (Equation 2.10). The accuracy of the models is represented by the ratio of actual moment of inertia to each theoretical moment of inertia. The table values are average values associated with the same representative test data used previously to evaluate the accuracy of both the Branson model and the "modified" Branson model. As in the case of the "modified" Branson model, the application of the experimentally determined exponent m' forces the cracked model to produce an effective moment of inertia approximately equal to I_{act} at service load. Therefore, the data from only the representative test specimen for each quantity of flexural reinforcement is reported to show the improvement and to observe the model's accuracy over the range of testing program M_a/M_{cr} ratios.

The values of Tables 5.15 through 5.17 reveal that use of an appropriate m' value allows the cracked length form of Branson's model to accurately model the behavior of the cracked, T-beam test specimens. Comparison of Tables 5.15 through 5.17 to their counterpart in the exponent m discussion (Tables 5.8 through 5.10) reveals that the cracked length model is consistently more accurate over a larger range of M_a/M_{cr} values. This behavior may be attributed to the parabolic behavior of the exponent m'. Over the range of M_a/M_{cr} values approaching service load, the rate of change is less in the case of the m' data due to its parabolic rather than cubic behavior, for this reason the cracked length model is more accurate over a larger range of applied load values.

The I_{act} values obtained during the experimental program are now substituted into the cracked length model, utilizing the respective exponent m', to obtain I_{cr}. The subsequent I_{cr} values ($I_{cr\text{-}"cracked"}$) are compared to I_{cr} values obtained per a transformed section analysis ($I_{cr\text{-}TR}$) in Tables 5.18 through 5.20. The values in Tables 5.18 through 5.20 reveal that the cracked length model along with its respective exponent (m') produce reasonable estimates for I_{cr} in the case of all three reinforcement quantities.

Table 5.18
Cracked Moment of Inertia Comparison A_s = 8 in.^{2} (specimen B8)

M_a/M_{cr}	$I_{cr\text{-}"cracked"}$ (In.^{4})	$I_{cr\text{-}TR}$ (In.^{4})	% Difference
0.51	50700	24900	50.9
1.02	*	24900	*
1.36	19000	24900	-31.1
1.53	20700	24900	-20.3
1.70	22100	24900	-12.7
1.87	23100	24900	-7.8
2.05	23700	24900	-5.1
2.21	24200	24900	-2.9
2.38	24400	24900	-2.0
2.56	24500	24900	-1.6
2.73	24800	24900	-0.4
2.90	24800	24900	-0.4
3.05	25000	24900	0.4

Note: (*) Model gives large, unrealistic results at loads close to M_{cr}.

Table 5.19
Cracked Moment of Inertia Comparison A_s = 5 in.^{2} (specimen C5)

M_a/M_{cr}	$I_{cr\text{-}"cracked"}$ (in.^{4})	$I_{cr\text{-}TR}$ (in.^{4})	% Difference
0.51	29900	18000	39.8
1.01	*	18000	*
1.35	10100	18000	-78
1.52	12000	18000	-50.0
1.69	13500	18000	-33.3
1.85	14700	18000	-22.4
2.02	15300	18000	-17.6
2.19	16000	18000	-12.5
2.36	16500	18000	-9.1
2.53	16900	18000	-6.5
2.70	17200	18000	-4.7
2.86	17500	18000	-2.9
3.02	17800	18000	-1.1

Note: (*) Model gives large, unrealistic results at loads close to M_{cr}.

Table 5.20
Cracked Moment of Inertia Comparison A_s = 3 in.^{2} (specimen C3)

M_a/M_{cr}	$I_{cr\text{-}"cracked"}$ (in.^{4})	$I_{cr\text{-}TR}$ (in.^{4})	% Difference
0.54	18800	13000	30.9
1.08	*	13000	*
1.35	11800	13000	-10.2
1.43	12100	13000	-7.4
1.52	12400	13000	-4.8
1.60	12600	13000	-3.2
1.68	12800	13000	-1.6
1.76	12900	13000	-0.8
1.84	13100	13000	0.8
1.92	13200	13000	1.5
2.00	13300	13000	2.3
2.08	13300	13000	2.3
2.17	13400	13000	3.0

Note: (*) Model gives large, unrealistic results at loads close to M_{cr}.

5.3.2.5 Cracked Length Model Conclusions. The values in Tables 5.18 through 5.20 reveal that the cracked length form of the Branson model accurately models the behavior of the cracked, T-beam test specimens given that the appropriate *m'* value is used. Unfortunately, the exponent *m'* (just like the exponent *m*) is dependent on the member's reinforcement ratio.

The same conclusions drawn in the case of the exponent *m* discussion apply in this situation. The best option is to ignore the A_s = 3 in.^{2} relationship, (Equation 5.14) for the reasons previously discussed, and determine between the A_s = 5 in.^{2} (Equation 5.13) and A_s = 8 in.^{2} (Equation 5.12) which relationship produces a conservative estimation of I_{cr} for the other scenario. Once again, the conservative value for *m'* is produced by the A_s = 8 in.^{2} relationship (Equation 5.12). Therefore, based on the findings of this research and conservative assumptions, it is recommended that a value *m'* = 0.88 be assumed when the cracked model is utilized as a component of the proposed analysis procedure.

5.3.3 Fikry and Thomas Model

5.3.3.1 General. Another effective moment of inertia model examined for its accuracy in the modeling the behavior of a reinforced concrete T-beam was the model developed by Fikry and Thomas (Fikry and Thomas 1998). Their approximation was developed with the goal of providing a more accurately account for non-uniform load configurations and variations in reinforcement, which represent stumbling blocks for existing models (Fikry and Thomas 1998). Another goal of the model was to eliminate the cumbersome I_{cr} calculation associated with Branson's model and its spin-offs.

Similar to the previously discussed models, the Fikry and Thomas model was derived to calculate the effective moment of inertia associated with total deflection (the deflection that includes permanent deflection) experienced by a reinforced concrete member. Theoretical deflection values calculated with Fikry and Thomas's model were compared to the deflection values obtained during the testing program detailed in Chapter 3. An effort was made to determine if a pattern existed between the theoretical values and the experimental values (void of permanent deflection) that could be calibrated to create a model that estimated the effective moment of inertia of a cracked T-beam girder subjected to a simulated tandem axle load configuration.

5.3.3.2 Analysis. The model's performance was compared to experimental data in the form of load versus deflection plots. The load versus deflection curve obtained with the aid of the Fikry and Thomas model was added to the experimental load versus deflection plots that were previously presented (Figures 5.1 through 5.3). Each plot represents the typical load versus deflection behavior of the stated reinforcement quantity (Figures 5.12 through 5.14).

These curves reveal that the Fikry and Thomas model yields similar results as the Branson model for all three reinforcement ratios. The desired result is for the model to accurately model the behavior of a previously cracked reinforced concrete T-beam subjected to a tandem axle truck load. It is obvious that the model does not achieve the desired result, mostly due to the model's allowance for the inelastic effects of tensile cracking of the concrete. A breakdown of the mechanics of the Fikry and Thomas model reveals that allowance for permanent deflection lies in the exponent ϕ. The value of ϕ is determined from either Equation 5.15 or 5.16.

$$\phi = -(M_a / M_{cr})(L_{cr} / L)\rho > 1\% \tag{5.15}$$

$$\phi = -(M_a / M_{cr})(L_{cr} / L) \leq 1\% \tag{5.16}$$

where

M_a = applied moment
M_{cr} = cracking moment
L_{cr} = cracked length

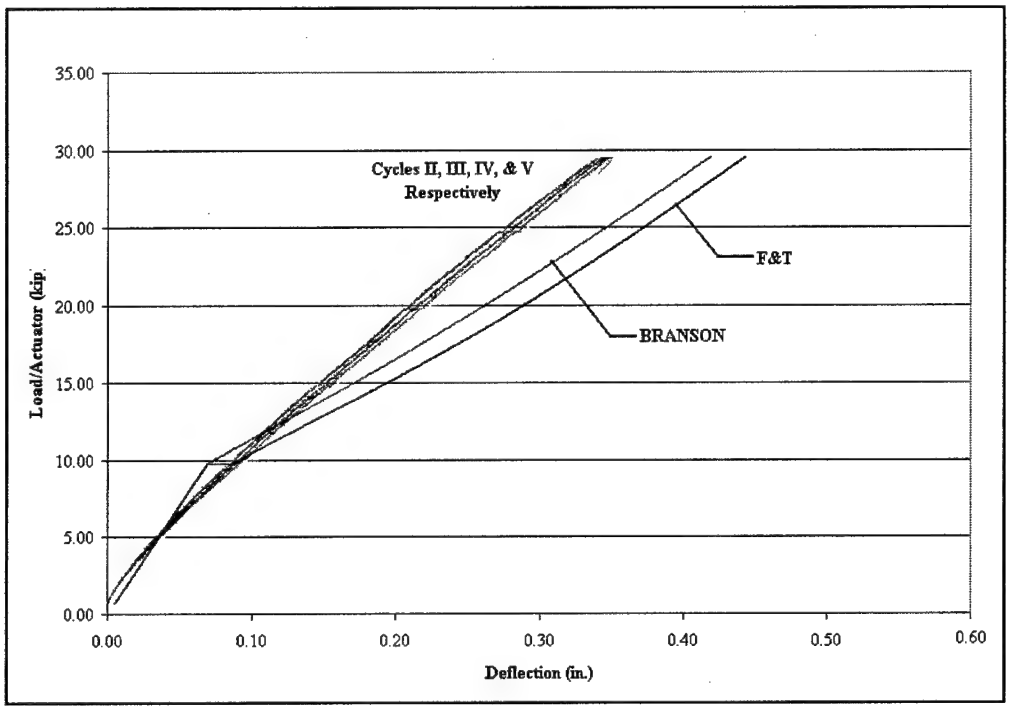

Figure 5.12. Typical Load versus Live-load Deflection A_s=8 in.^{2} (Specimen B8)

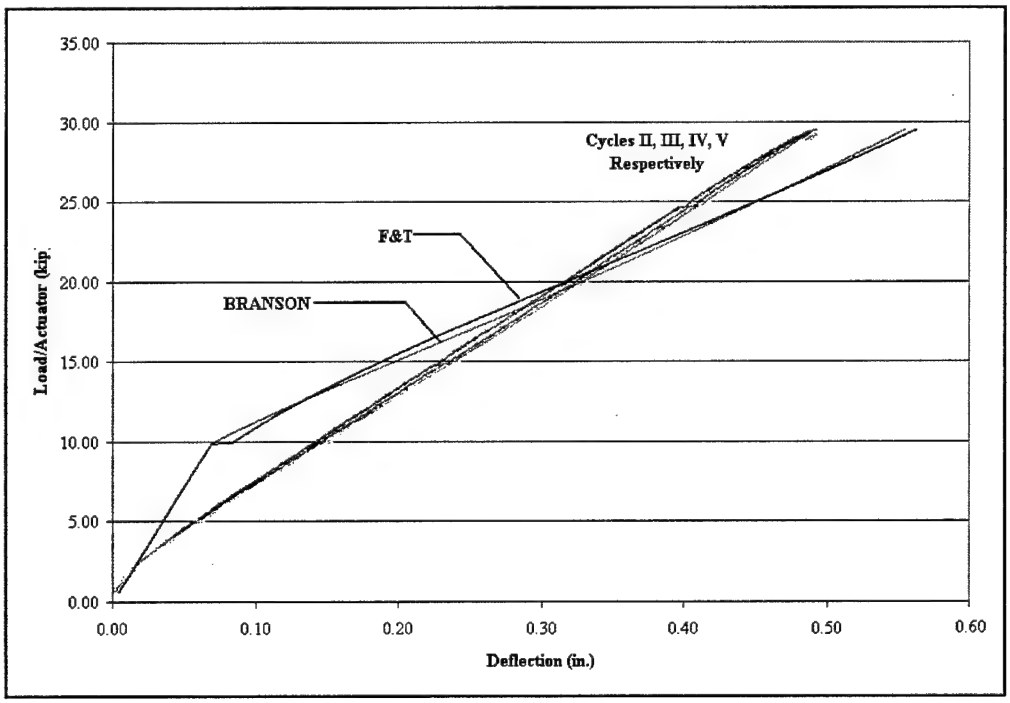

Figure 5.13. Typical Load versus Live-load Deflection A_s=5 in.^{2} (Specimen C5)

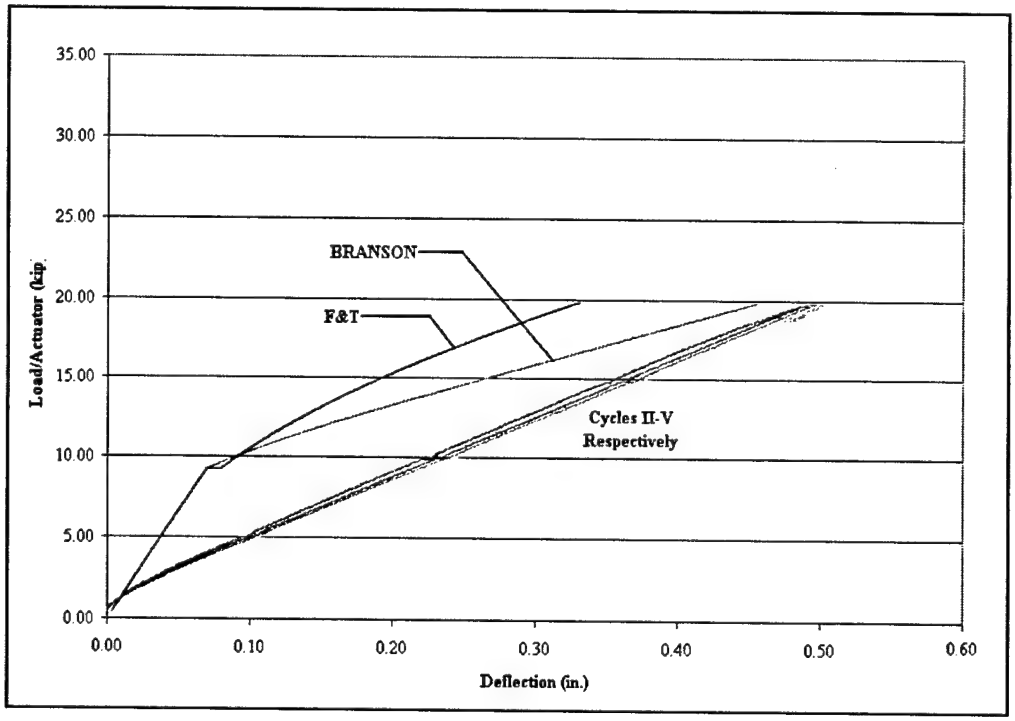

Figure 5.14. Typical Load versus Live-load Deflection A_s=3 in.^{2} (Specimen C3)

L = corresponds to the member length
ρ = reinforcement ratio

These relationships were determined empirically from over 340 laboratory tests (Fikry and Thomas 1998). A similar empirical procedure as that used to calculate the exponents of Equation 2.8 and Equation 2.10 was applied to obtain the experimental value of ϕ, and the expression can be stated as:

$$\phi_{\exp} = \ln (I_{\exp} - I_{cre}) / \ln (I_g - I_{cre}) \tag{5.17}$$

where

I_{exp} = experimental moment of inertia
I_{cre} = cracked moment of inertia approximation
I_g = gross moment of inertia

Similar to the behavior of the exponent m calculated by Equation 2.9, the behavior of ϕ_{exp} when plotted versus M_a/M_{cr} produces a curve best modeled by a cubic relationship.

An examination of the relationship for ϕ when ρ>1 (Equation 5.16), typical for a T-beam bridge girder, reveals the reinforcement ratio parameter which is unknown during the analysis of an in-service bridge enables the model to be of service in the proposed analysis procedure. The only helpful information is the cubic curve in terms of M_a/M_{cr} that was produced by plotting ϕ versus applied load. The cubic relationship could be used to calculate a ϕ so that the model could be utilized as part of the proposed analysis procedure, but that is no better

than the options produced from the analysis of the first two models. Beyond that, determining the quantity of steel from the I_{cre} model (Equation 2.14) is made difficult by the constants α and β that are functions of the unknown reinforcement ratio. For these reasons the Fikry and Thomas model is discussed no further.

6 Conclusions and Recommendations

6.1 General

The U.S. Army's maneuverability is limited during missions in foreign lands because the load capacity of in-service bridges is unknown and in some instances difficult to estimate. The bridge type that poses the greatest difficulty to field engineers is the cast-in-place, reinforced concrete bridge, more commonly known as the T-beam bridge. The products of this report represent an effort to develop a more accurate capacity analysis procedure than the currently available for this type of bridges. Specifically, the goal of this report was to determine an effective moment of inertia model to accurately predict the behavior of an in-service, reinforced concrete T-beam member subjected to a tandem axle load configuration.

Personnel from the U.S. Army Engineer Research and Development Center (ERDC) and Virginia Tech collaborated in the development of a laboratory-testing program that subjected full-scale, T-beam test specimens to a simulated tandem-axle load configuration. The mid-span deflection and corresponding load values obtained from this testing program were used to evaluate the performance of selected, effective moment of inertia models obtained during a literature review, conducted as part of this research study. The models were evaluated on their ability to return an accurate, cracked moment of inertia value given the actual moment of inertia of an in-service, T-beam bridge girder.

An effective moment of inertia model to accurately predict the behavior of a cracked, reinforced concrete T-beam is a key component in the accuracy of any rapid load-capacity evaluation procedure. A methodology for this purpose is currently under development at the ERDC for the rapid estimation of a T-beam bridge load capacity. The evaluation of various effective moment of inertia models revealed that, in general, existing models are derived to calculate an effective moment of inertia that corresponds to the service load deflection a member experiences plus the permanent deflection a member sustains due to the inelastic effects of cracking. This poses a problem since an in-service bridge possesses an unknown amount of permanent deflection. The model that is utilized in the proposed capacity analysis procedure must be able to return a cracked moment of inertia value that corresponds to the service load deflection only.

Two effective moment of inertia models, the first one developed by Al-Zaid et al., 1991 (as given by Equation 2.8), and the second one by Al-Shaikh and Al-Zaid, 1993 (as given by Equation 2.10), were found to reasonable model the behavior of a cracked reinforced concrete T-beam. The accuracy of both models depends on the exponents (m and m' respectively) incorporated into the models. The testing program data confirms the behavior observed by Al-Zaid et al. (1991) and Al-Shaikh and Al-Zaid (1993) that both exponents are a function of the quantity of flexural reinforcement in the member's cross-section, which most typically represents the unknown parameter in an in-service T-beam bridge girder.

The testing program data provided an expression for both exponents in terms of applied load (M_a/M_{cr}) for each reinforcement quantity, a total of six expressions. The two expressions representing members with a reinforcement ratio of $\rho = 0.93$ were eliminated, due to reasons explained, leaving four expressions; two expressions representing members with 5 $in.^2$ of flexural reinforcement (or a reinforcement ratio of $\rho = 1.60$) and two expressions representing members with 8 $in.^2$ of flexural reinforcement (or a reinforcement ratio of $\rho = 2.66$). The expressions that yielded a conservative estimate of I_{cr} were found to be those corresponding to a reinforcement ratio of $\rho = 2.66$, which yields the exponents values of $m = 1.2$ and $m' = 0.82$ under service loading. The quantity of flexural reinforcement is estimated (As-ESTIMATE) for each T-beam test specimen in Tables 6.1 and 6.2 by using either the "modified" model (Equation 2.8) or the "cracked" model (Equation 2.10) along with their respective exponent.

Table 6.1
Modified Model Reinforcement Estimate

Specimen	$A_{s\text{-DESIGN}}$ ($in.^2$)	M_a	$\Delta_{EXPERIMENTAL}$(in.)	I_{act} ($in.^4$)	$I_{c\text{-MODIFIED}}$ ($in.^4$)	$A_{s\text{-ESTIMATE}}$ ($in.^2$)
A8	8.0	4112	0.4072	27614	19491	6.9
B8	8.0	4112	0.3529	30980	23666	9.4
C8	8.0	4112	0.3540	29472	20993	8.9
A5	5.0	4112	0.4985	22556	12730	3.8
B5	5.0	4112	0.5327	19401	6857	1.8
C5	5.0	4112	0.4964	21796	11030	3.4
A3	3.0	No Data	No Data	No Data	No Data	No Data
B3	3.0	2760	0.5249	13980	-13604	-5.3
C3	3.0	2760	0.5056	15361	-8314	-3.1

Table 6.2
Cracked Model Reinforcement Estimate

Specimen	$A_{s\text{-DESIGN}}$ ($in.^2$)	M_a	$\Delta_{EXPERIMENTAL}$(in.)	I_{act} ($in.^4$)	$I_{c\text{-CRACKED}}$ ($in.^4$)	$A_{s\text{-ESTIMATE}}$ ($in.^2$)
A8	8.0	4112	0.4072	27614	20853	7.6
B8	8.0	4112	0.3529	30980	24948	10.1
C8	8.0	4112	0.3540	29472	22576	9.7
A5	5.0	4112	0.4985	22556	14377	4.5
B5	5.0	4112	0.5327	19401	10569	3.5
C5	5.0	4112	0.4964	21796	12944	4.2
A3	3.0	No Data	No Data	No Data	No Data	No Data
B3	3.0	2760	0.5249	13980	-3676	-1.8
C3	3.0	2760	0.5056	15361	-1946	-1.1

The values presented in Table 6.1 and 6.2 show that for specimens with 8 in.^{2} of flexural reinforcement (or $\rho = 2.66$) both models give a reasonable estimate, but is more frequently not conservative rather than conservative. As expected, both models consistently provide a conservative estimate of flexural reinforcement for members with a $\rho = 1.60$. And in the case of members with a $\rho = 0.93$ the chosen exponents cause the models to predict a negative reinforcement for the lightly reinforced members.

The aforementioned testing program was not conducive in determining, which of the effective moment of inertia models is more accurate as a component of the proposed T-beam bridge capacity analysis. Therefore, it is recommended that both models be evaluated for their accuracy during actual full-scale field-testing of these types of bridges.

6.2 Field Test Recommendations

The following recommendations are made regarding full-scale T-beam bridge testing or any field implementation of the proposed capacity analysis procedure. First, a thorough visual evaluation of the structure is recommended to note any excessive deterioration or other material abnormalities. The findings of the visual evaluation in conjunction with intelligence, regarding local materials, and sound engineering judgment allows the field engineer to make an initial assessment of the bridge's structural integrity. It is also recommended that the structure be evaluated with a sonar device to determine the approximate location of the reinforcement in the member's cross-section. Knowledge of the flexural reinforcement's location eliminates assuming an effective depth. After a satisfactory condition assessment, it is recommended that the structure in question be pre-loaded before data acquisition commences to eliminate any errors due to tensile cracking of the concrete. The structure should be loaded to a service load moment approximately three times the member's cracking moment. The testing program data reveals that for specimens with reinforcement ratios of $\rho = 2.66$ and $\rho = 1.60$ this load magnitude is significantly less than the member's ultimate capacity, however, $3*M_{cr}$ approaches the capacity of the members with a reinforcement ratio of $\rho = 0.93$. As mentioned in Chapter 5 it is reasonable to assume that T-beam bridge girders have a reinforcement ratio greater than $\rho = 0.93$.

Finally, it is assumed that an accurate method of measurement is utilized to obtain member deflection and that an accurate wheel-load distribution theory is employed. These two factors are critical to the accuracy of the proposed analysis procedure.

6.3 Recommendations for Future Testing

If, in future, any controlled testing is conducted as an extension or supplement to the testing program described herein consider the following

recommendations. During the testing procedure that applies a prescribed service load to a test specimen, overload the member and then re-apply the service load again to determine the effect that overloading has on the flexural behavior of the member. It is also recommended that specimens with larger amounts of reinforcement than those tested herein be incorporated to evaluate the behavior of the exponents corresponding to effective moment of inertia models developed by Al-Zaid et al. (1991) and Al-Shaikh and Al-Zaid (1993). Specifically, to determine if the exponent values become asymptotic to some value as the reinforcement quantity increases. Also, a larger number of test specimens and a broader range of reinforcement quantities are needed to aid in the development of relationships that facilitate the determination of the exponent values.

References

ACI Committee 307, "Deflection of Reinforced Concrete Members," ACI Journal, *Proceedings* V.27, 1931, p.351.

ACI Committee 318, "Building Code Requirements for Structural Concrete and Commentary (ACI-318-56)," American Concrete Institute, Detroit, 1956.

ACI Committee 318, "Building Code Requirements for Structural Concrete and Commentary (ACI-318-71)," American Concrete Institute, Detroit, 1971, 78 pp.

ACI Committee 318, "Building Code Requirements for Structural Concrete and Commentary (ACI-318-02)," American Concrete Institute, Detroit, 2002, 443 pp.

ACI Committee 435, "Deflection of Reinforced Concrete Flexural Members," ACI Journal, *Proceedings* V. 63, No. 6, Part 1, June 1966, pp. 637-674.

AASHTO, "Standard Specification for the Design of Highway Bridges," 16th ed., American Association of State Highway and Transportation Officials, Washington, D.C., 1996.

Al-Shaikh, A. H. and Al-Zaid, R. Z., "Effect of Reinforcement Ratio on the Effective Moment of Inertia of Reinforced Concrete Beams," *ACI Structural Journal*, V. 90, No. 2, Mar.-Apr. 1993, pp. 144-148.

Al-Zaid, R. Z. and Al-Shaikh, A. H. and Abu-Hussein, M., "Effect of Loading Type on the Effective Moment of Inertia of Reinforced Concrete Beams," *ACI Structural Journal*, V. 88, No. 2, March-April 1991, pp. 184-190.

Branson, D. E., "Instantaneous and Time-Dependent Deflections of Simple and Continuous Reinforced Concrete Beams," HPR Report No. 7 Part 1, Alabama Highway Department/U.S. Bureau of Public Roads, Aug. 1963/1965, 78 pp.

CEB-FIP, "Model Code for Concrete Structures (CEP-FIP MC 90)," Comite Euro-International Du Beton, Lausanne, 1990, 437 pp.

Fikry, A. M. and Thomas, C., "Development of a Model for the Effective Moment of Inertia of One-Way Reinforced Concrete Elements," *ACI Structural Journal*, V. 95, No. 4, July-August 1998, pp. 444-455.

Ghali, A., "Deflection of Reinforced Concrete Members: A Critical Review," *ACI Structural Journal*, V. 90, No. 4, July-August 1993, pp. 364-373.

Grossman, J. S., "Simplified Computations for Effective Moment of Inertia and Minimum Thickness to Avoid Deflection Computations," *ACI Journal*, V. 78, No. 6, November-December 1981, pp. 423-434.

Kassimali, A., Structural Analysis, PWS Publishing, Boston, MA, 1995.

Lutz, L. A., "Graphical Evaluation of the Effective Moment of Inertia for Deflection," ACI Journal, *Proceedings* V. 70, March 1973, pp. 207-213.

MacGregor, J. G., Reinforced Concrete Design, 4th ed., Prentice-Hall, Englewood Cliffs, NJ, 1999.

Nawy, Reinforced Concrete, 3rd ed., Prentice-Hall, Englewood Cliffs, NJ, 1999.

PCA, "Notes on ACI 318-99 Building Code Requirements for Structural Concrete," Portland Concrete Association, Shokie, IL, 1999.

PCI, Precast and Prestressed Design Handbook, 5th ed., Precast Concrete Institute, Chicago, IL, 1999.

Sherif, A. G., and Dilger, W. H., "Critical Review of CSA A23.3-94 Deflection Prediction for Normal and High Strength Concrete Beams," *Canadian Journal of Civil Engineering*, V. 25 1998, pp. 474-489.

Yu, W., and Winter, G., "Instantaneous and Long-Time Deflections of Reinforced Concrete Beams under Working Loads," *ACI Journal, Proceedings* V. 57, No. 1, July 1960, pp. 29-50.

Appendix A
Load versus Deflection Graphs (Not Including Permanent Deflections)

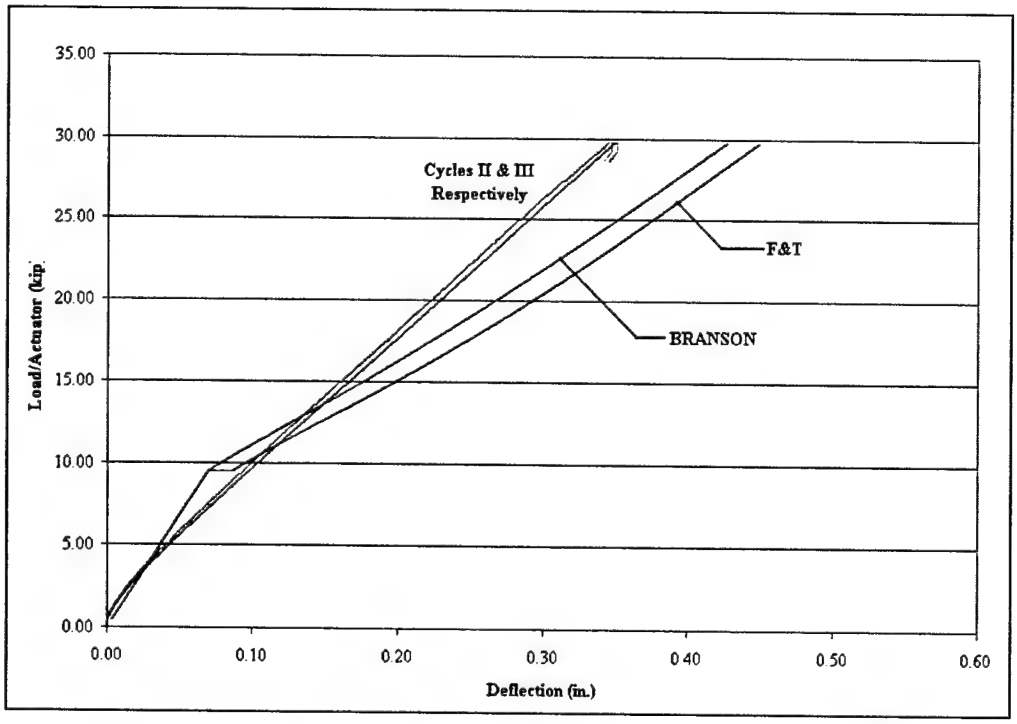

Figure A.1 - Load versus Deflection (Specimen A8)

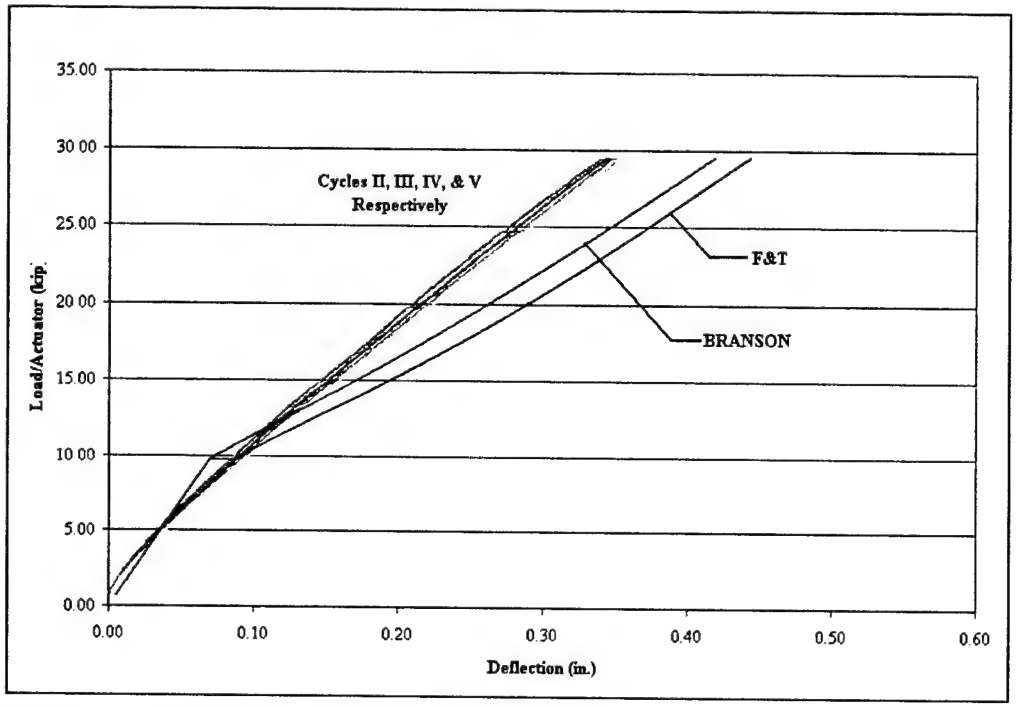

Figure A.2 - Load versus Deflection (Specimen B8)

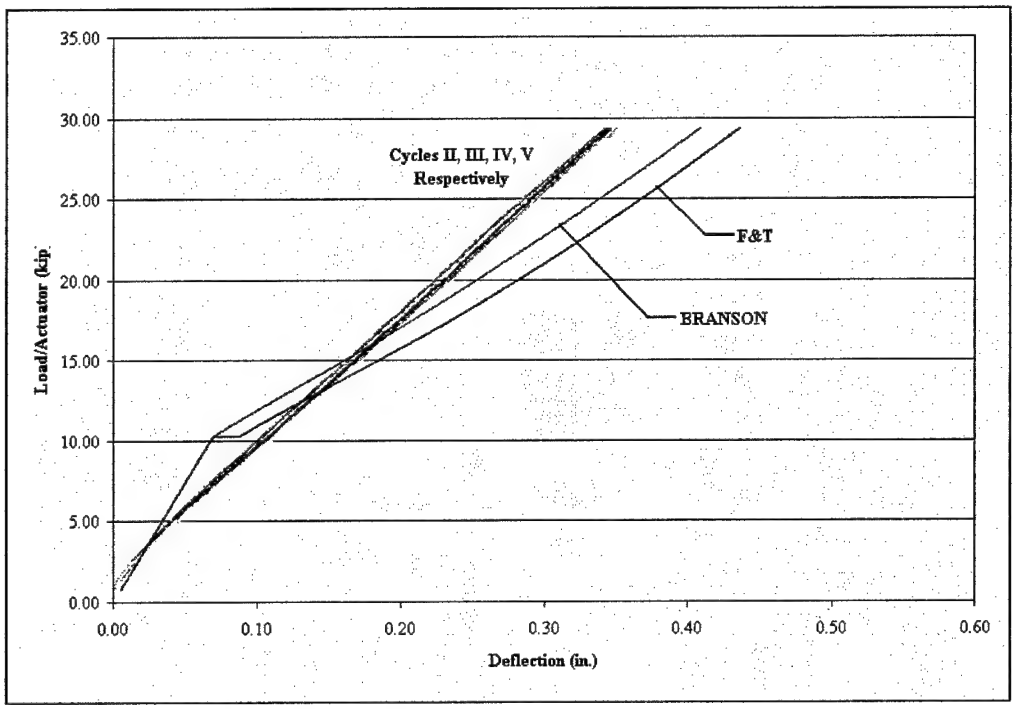

Figure A.3 - Load versus Deflection (Specimen C8)

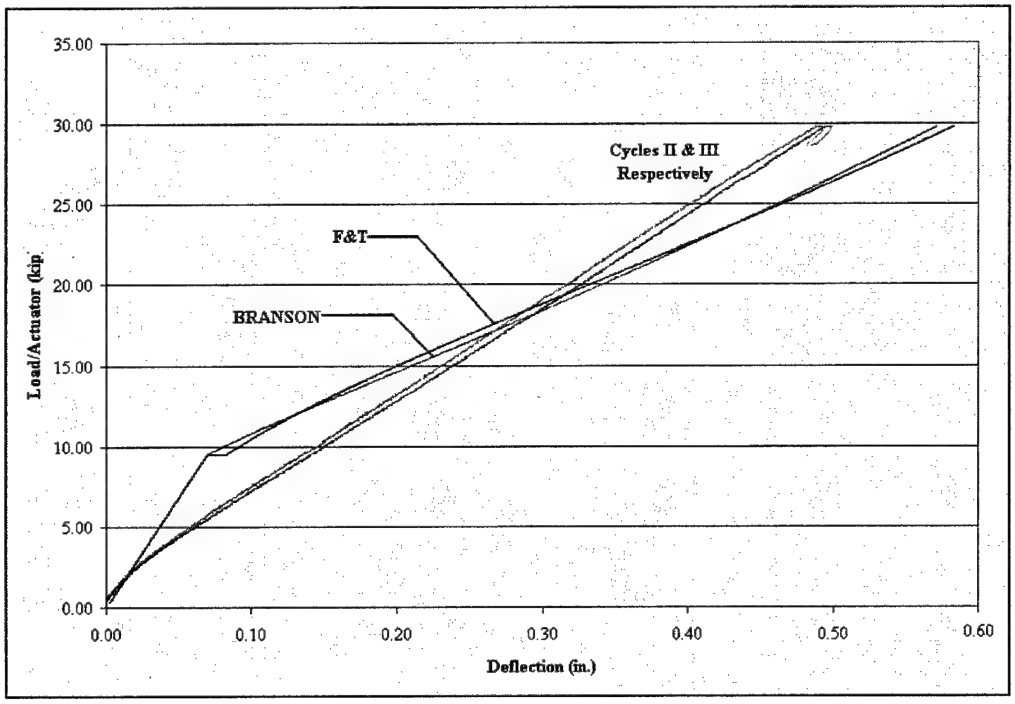

Figure A.4 - Load versus Deflection (Specimen A5)

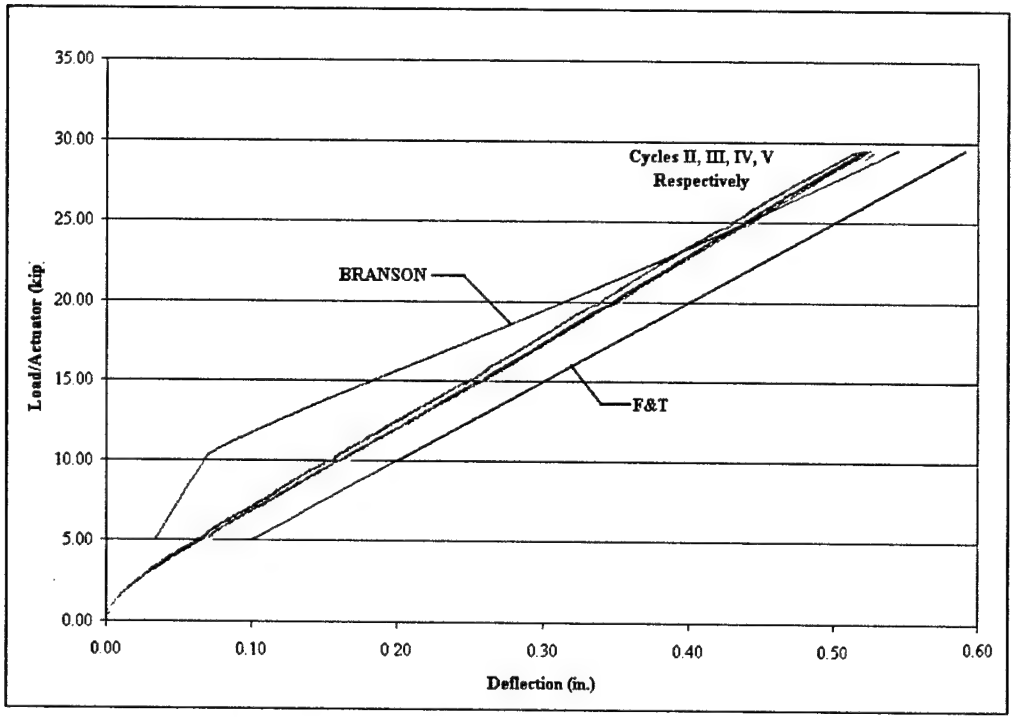

Figure A.5 - Load versus Deflection (Specimen B5)

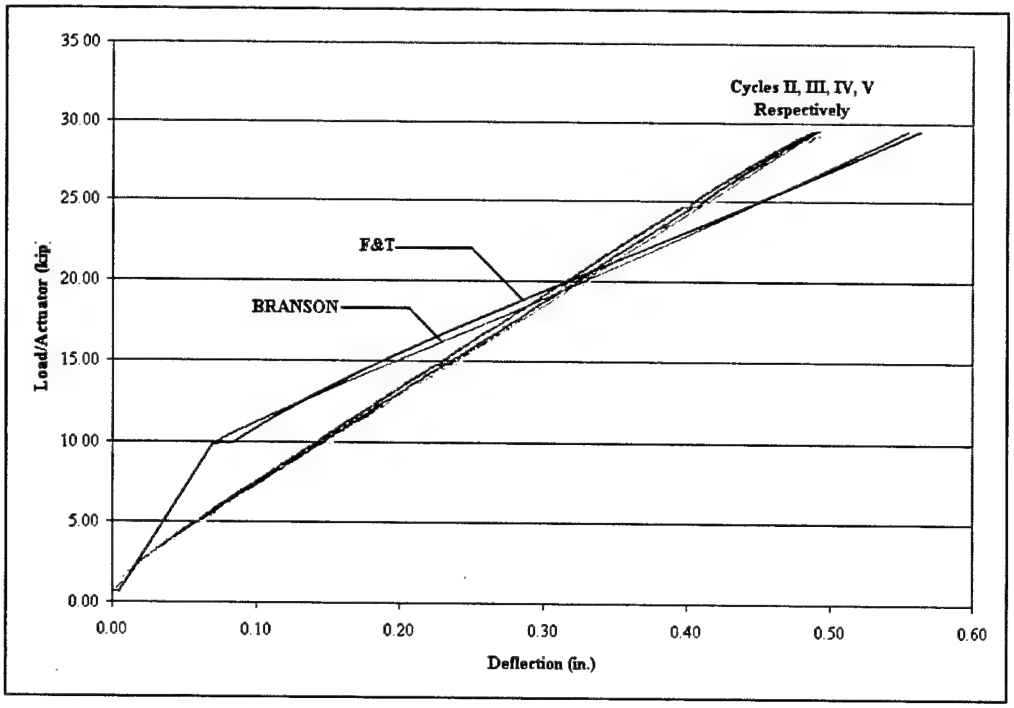

Figure A. 5 - Load versus Deflection (Specimen C5)

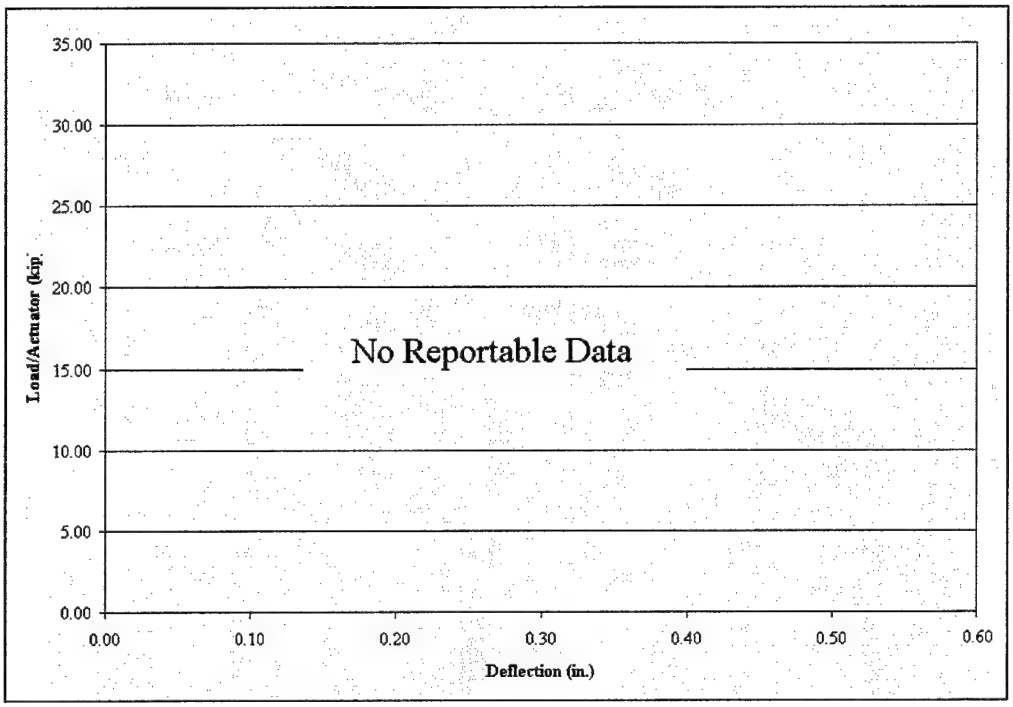

Figure A.6 - Load versus Deflection (Specimen A3)

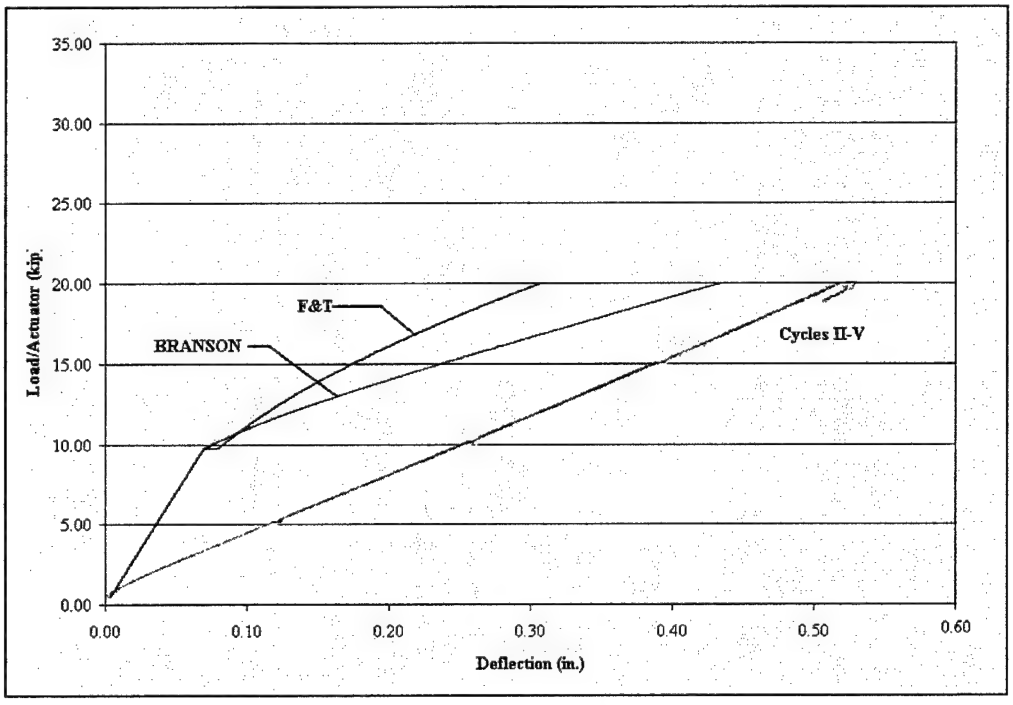

Figure A.7 - Load versus Deflection (Specimen B3)

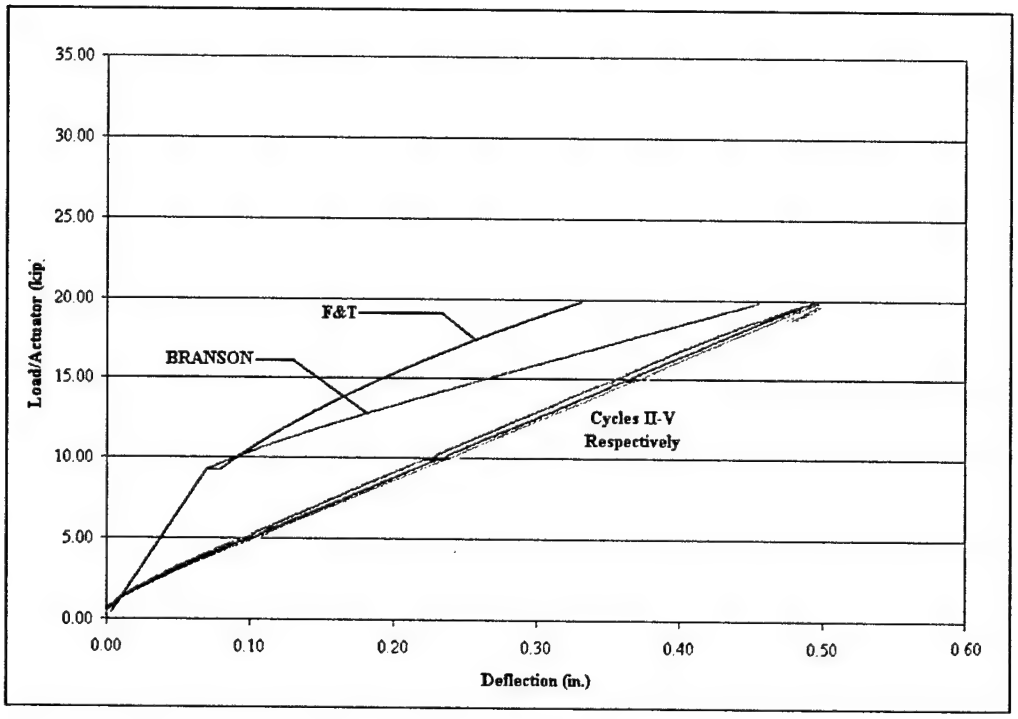

Figure A.8 - Load versus Deflection (Specimen C3)

Appendix B
Exponent *m* versus Applied Load Graphs

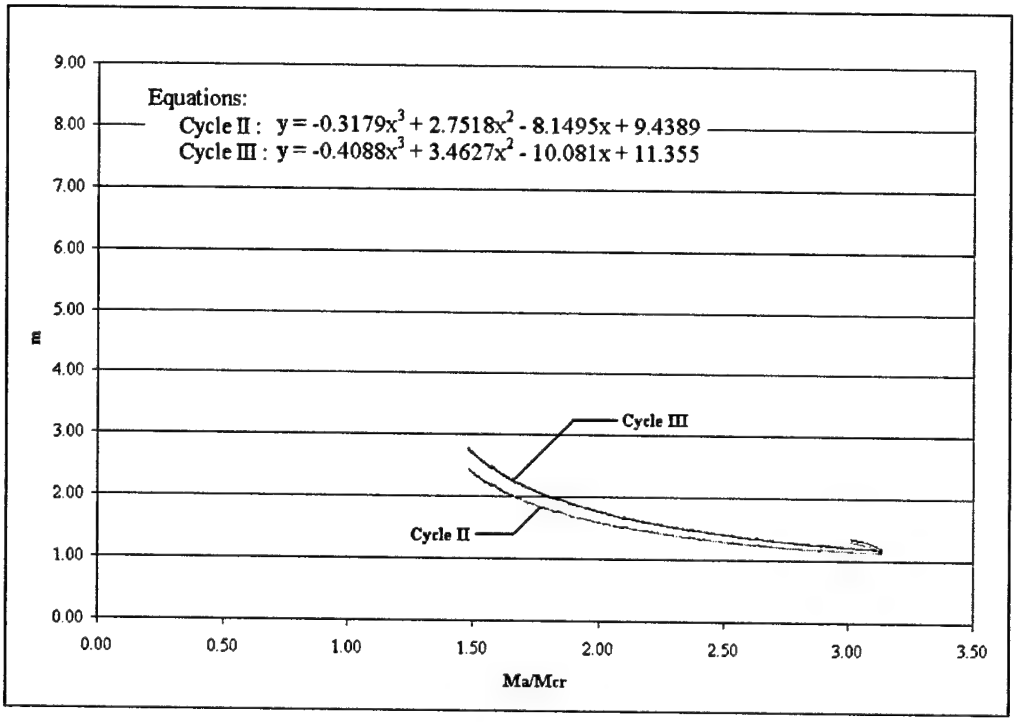

Figure B.1 – Exponent *m* versus Applied Load (Specimen A8)

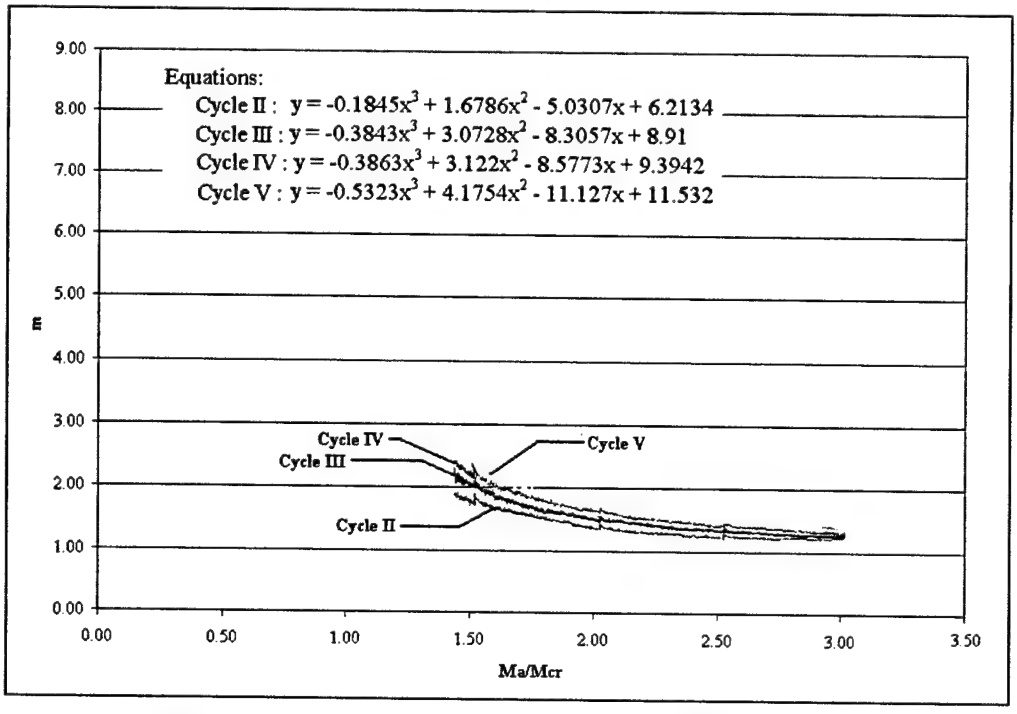

Figure B.2 - Exponent *m* versus Applied Load (Specimen B8)

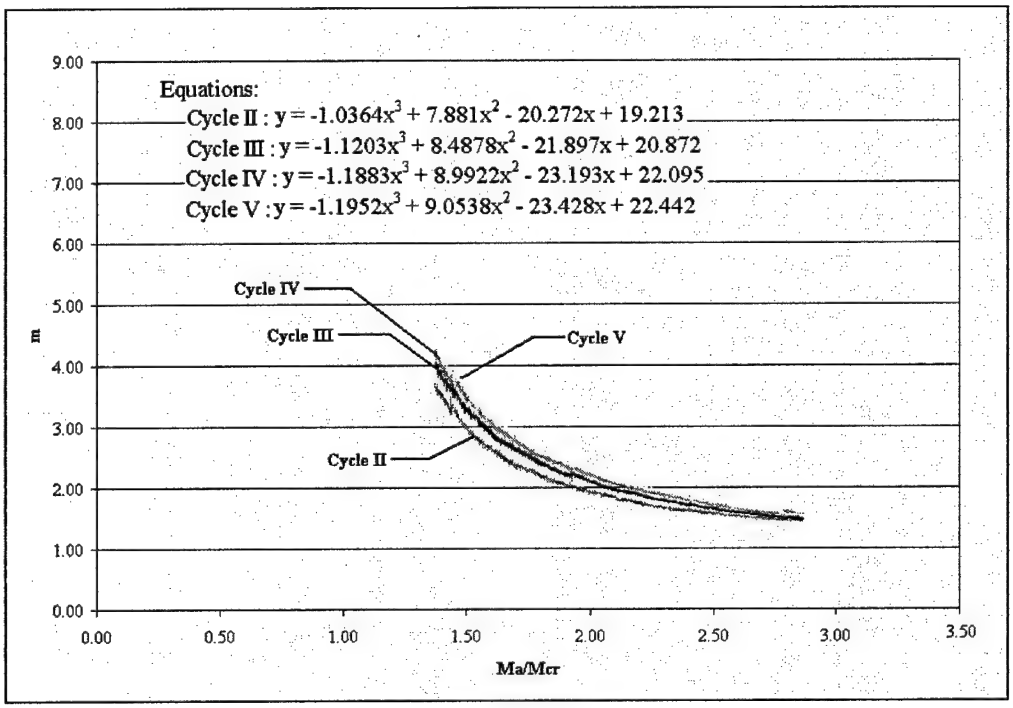

Figure B.3 - Exponent *m* versus Applied Load (Specimen C8)

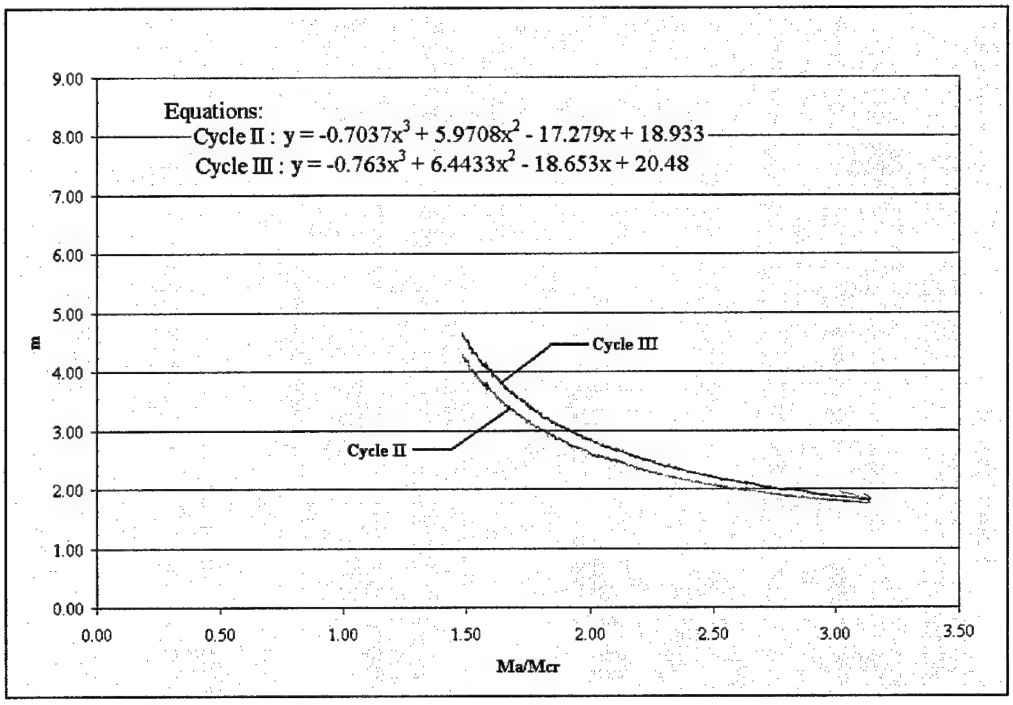

Figure B.4 - Exponent *m* versus Applied Load (Specimen A5)

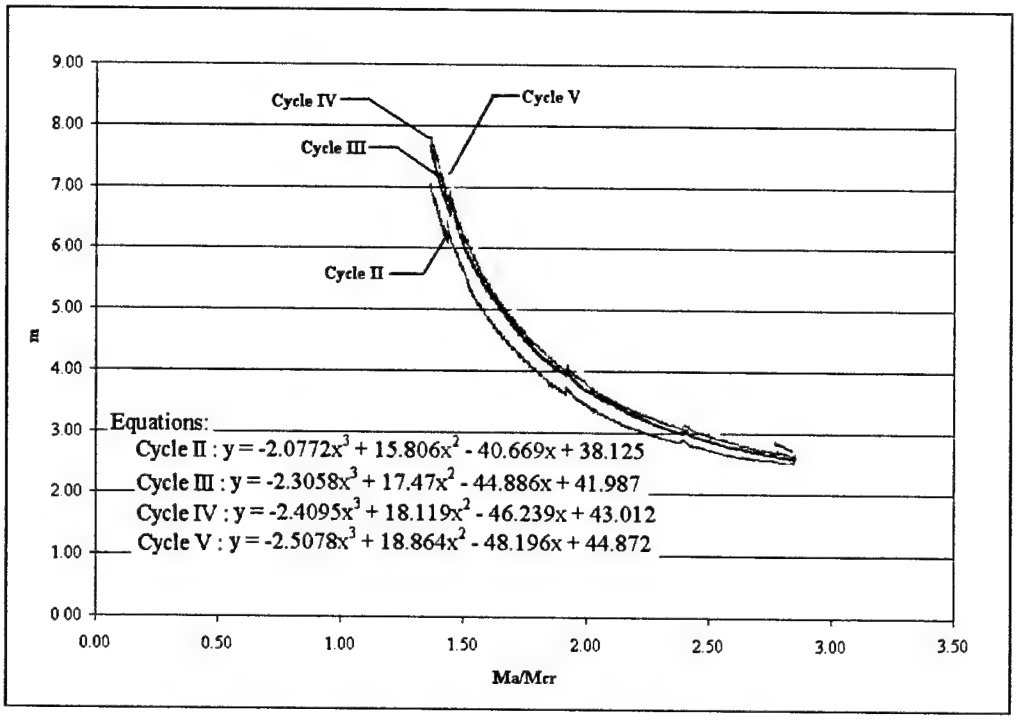

Figure B.5 - Exponent *m* versus Applied Load (Specimen B5)

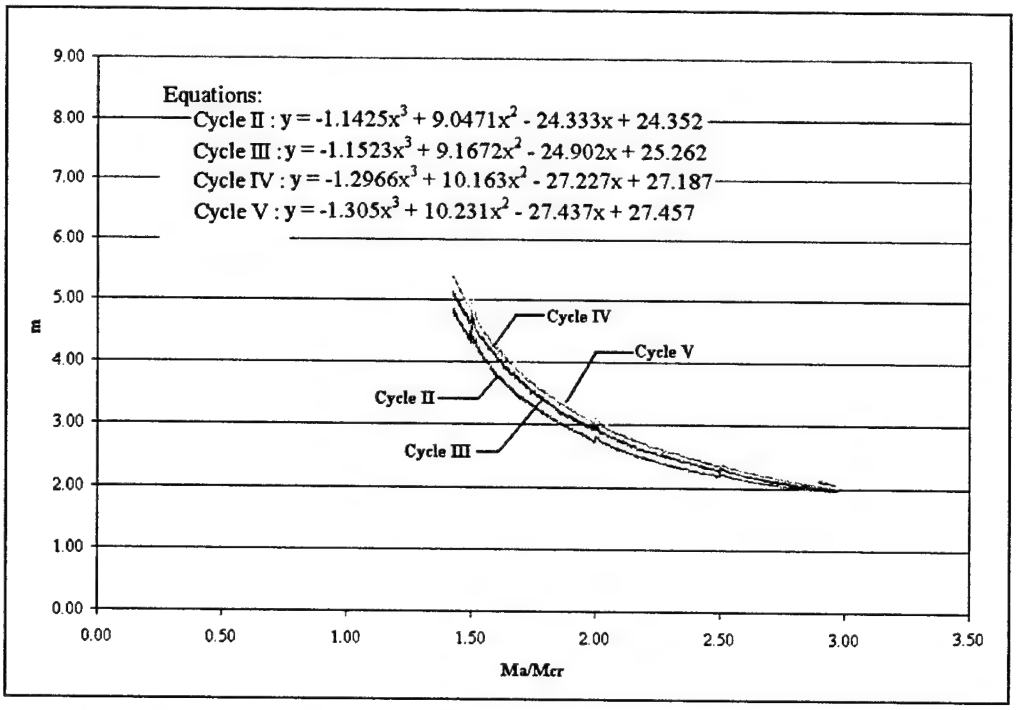

Figure B.6 - Exponent *m* versus Applied Load (Specimen C5)

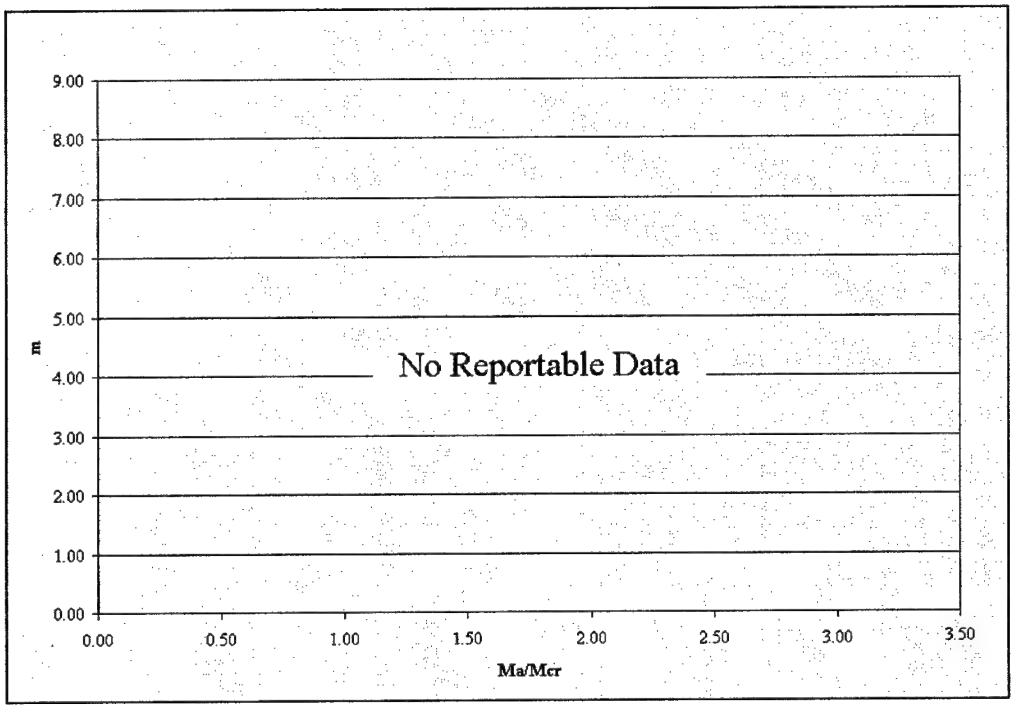

Figure B.7 - Exponent *m* versus Applied Load (Specimen A3)

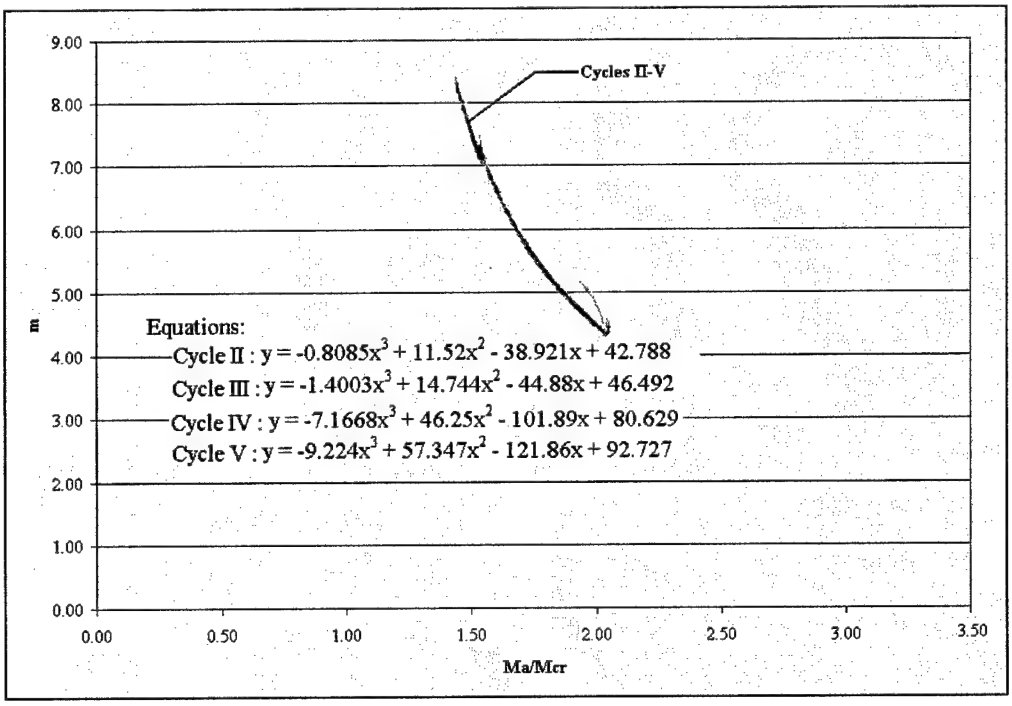

Figure B.8 - Exponent *m* versus Applied Load (Specimen B3)

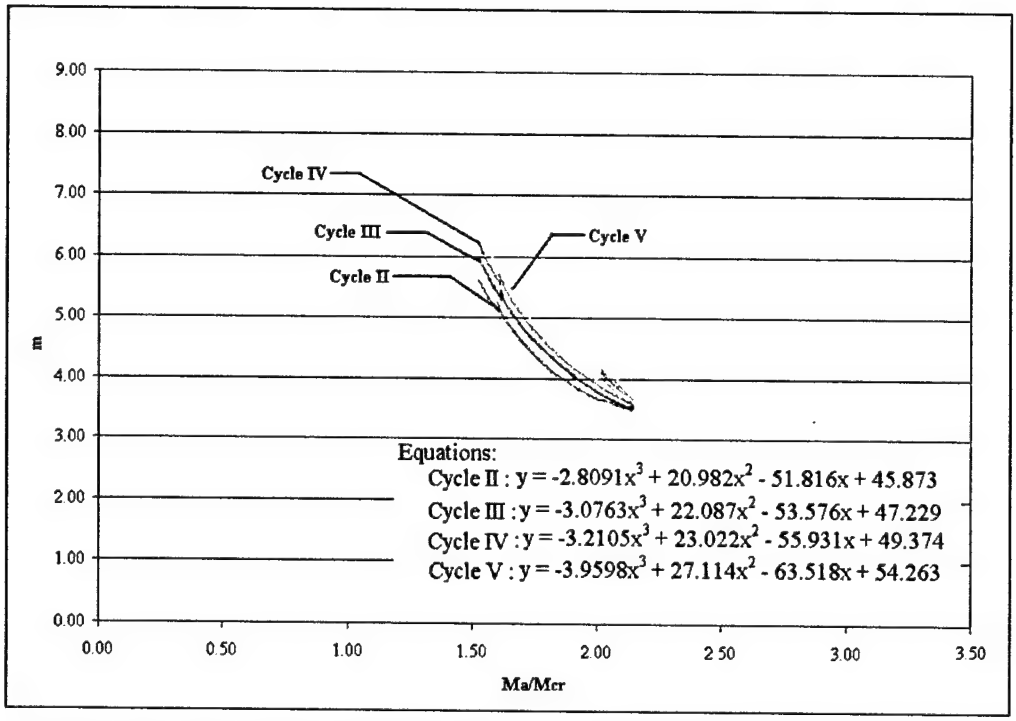

Figure B.9 - Exponent *m* versus Applied Load (Specimen C3)

Appendix C
Exponent *m'* versus Applied Load Graphs

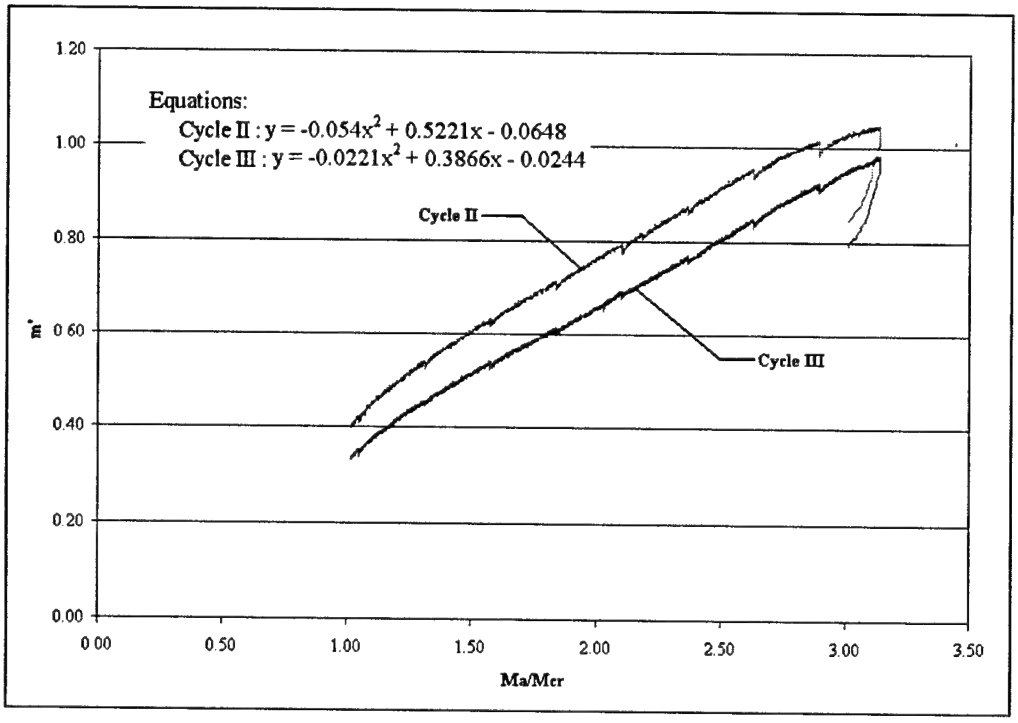

Figure C.1 – Exponent *m'* versus Applied Load (Specimen A8)

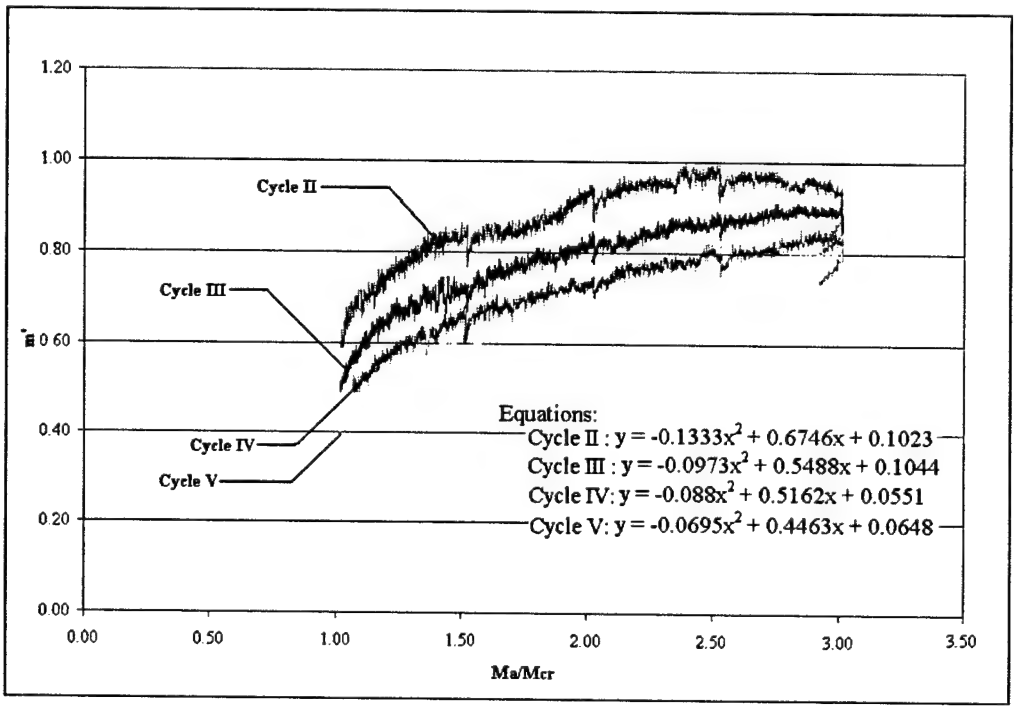

Figure C.2 - Exponent *m'* versus Applied Load (Specimen B8)

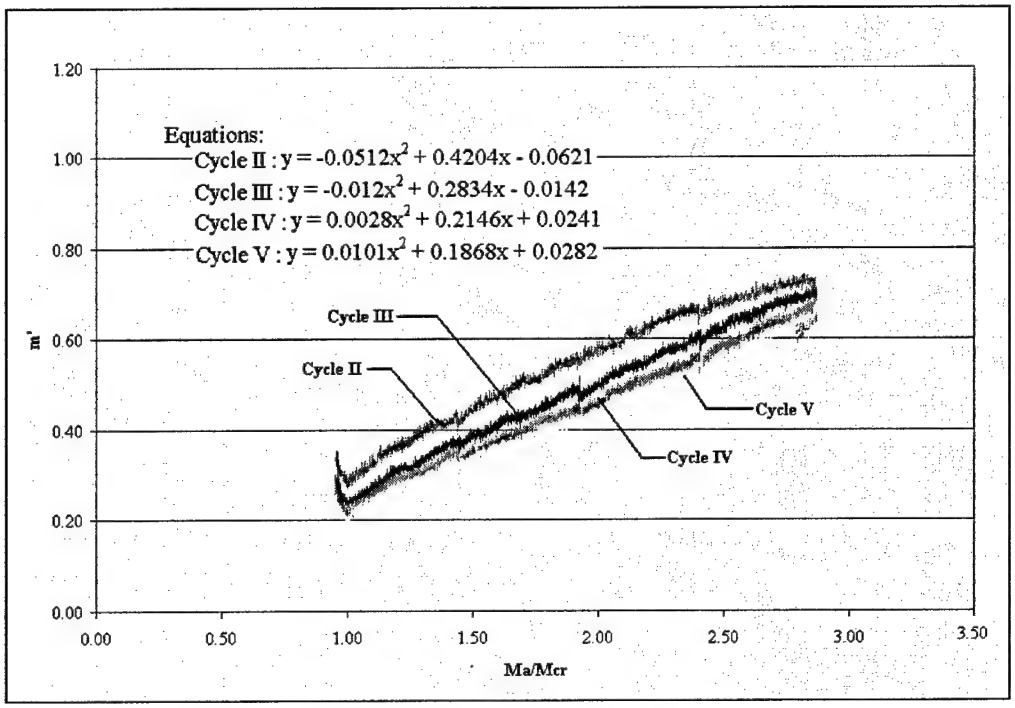

Figure C.3 - Exponent *m'* versus Applied Load (Specimen C8)

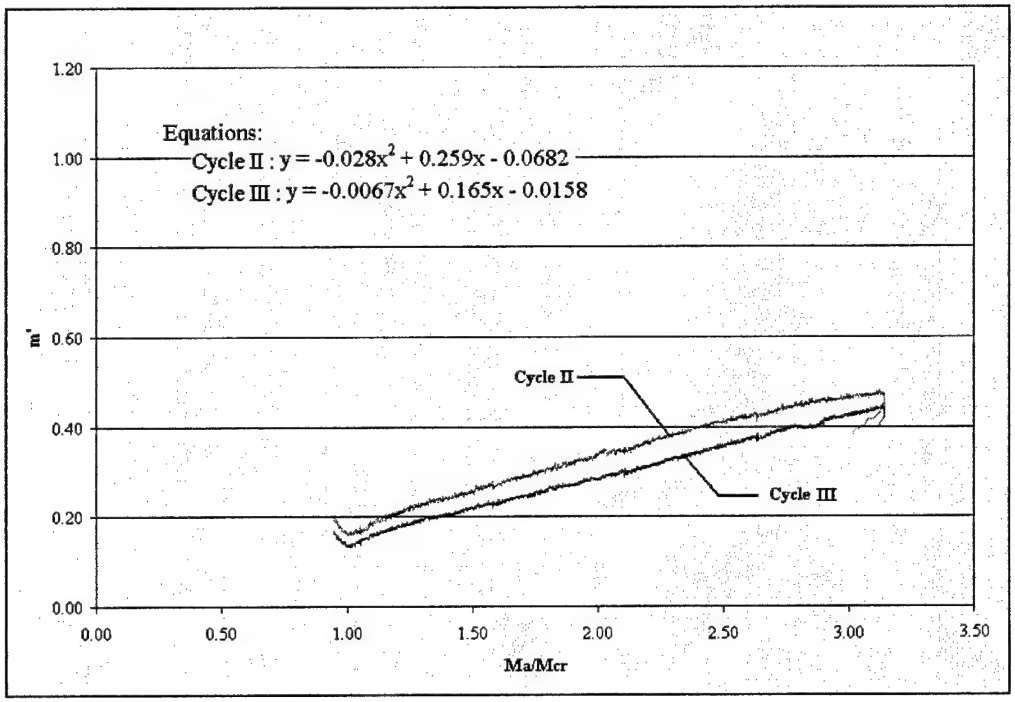

Figure C.4 - Exponent *m'* versus Applied Load (Specimen A5)

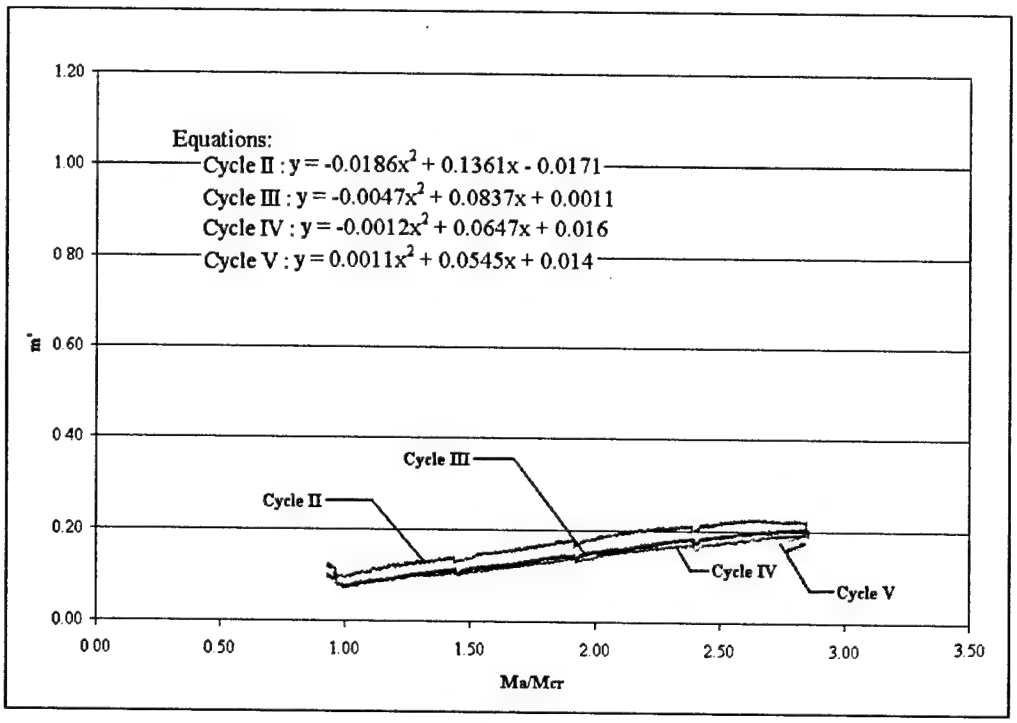

Figure C.5 - Exponent *m'* versus Applied Load (Specimen B5)

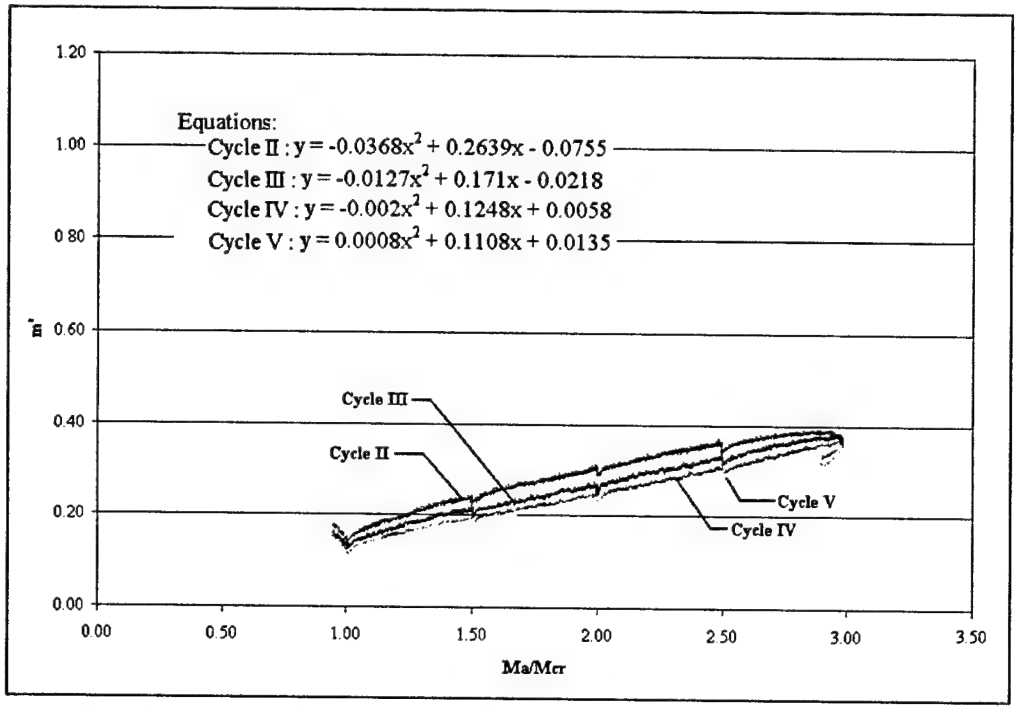

Figure C.6 - Exponent *m'* versus Applied Load (Specimen C5)

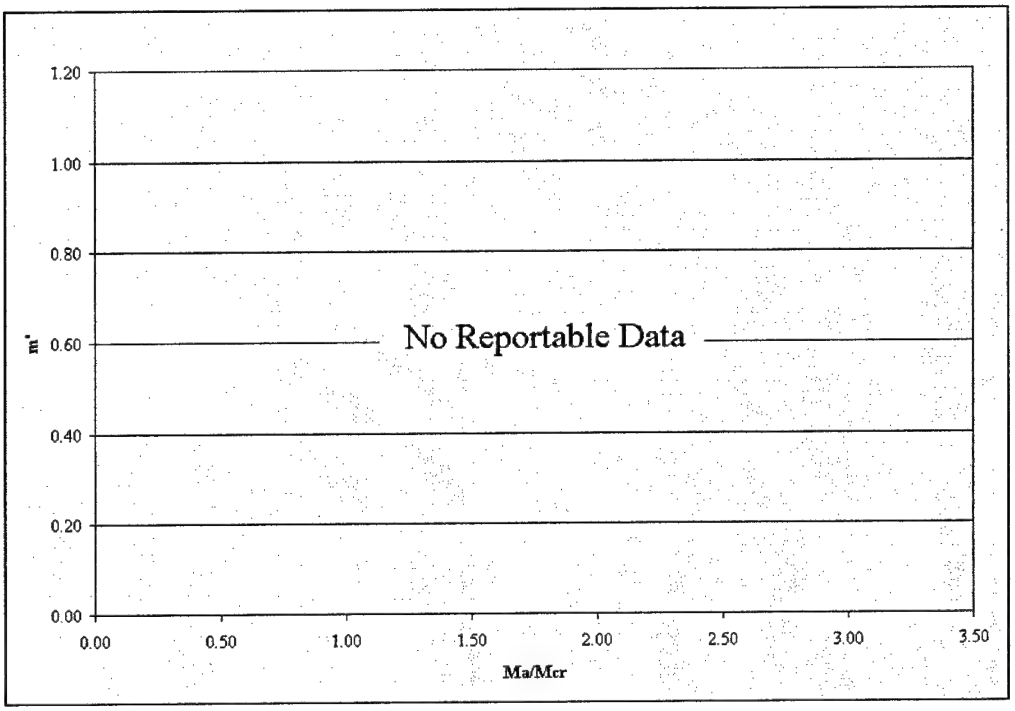

Figure C.7 - Exponent *m'* versus Applied Load (Specimen A3)

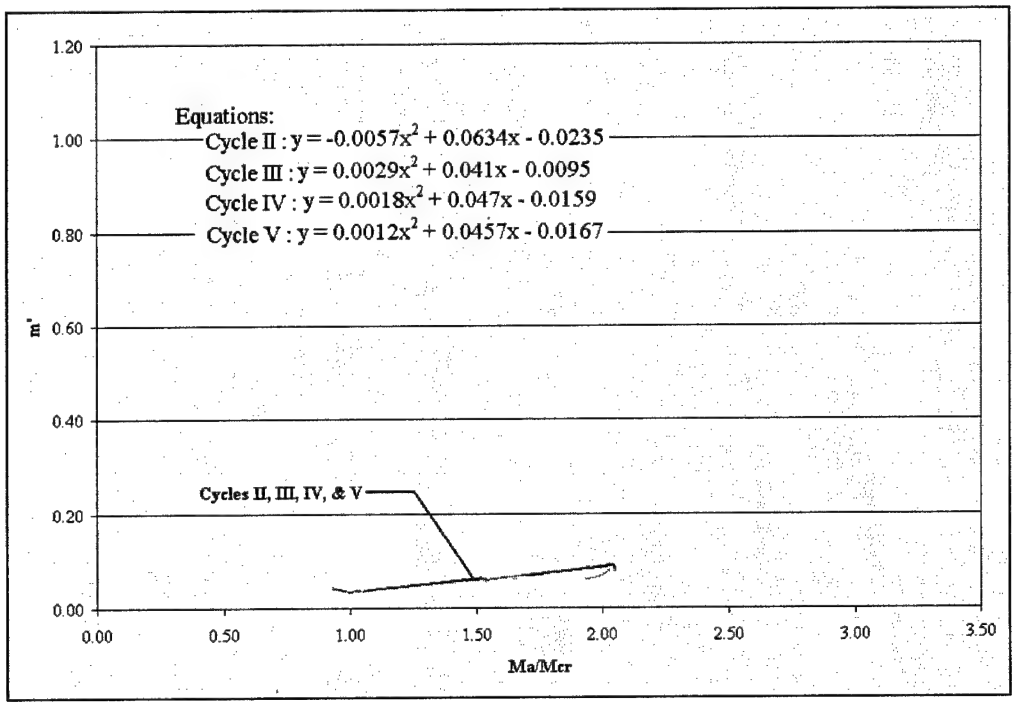

Figure C.8 - Exponent *m'* versus Applied Load (Specimen B3)

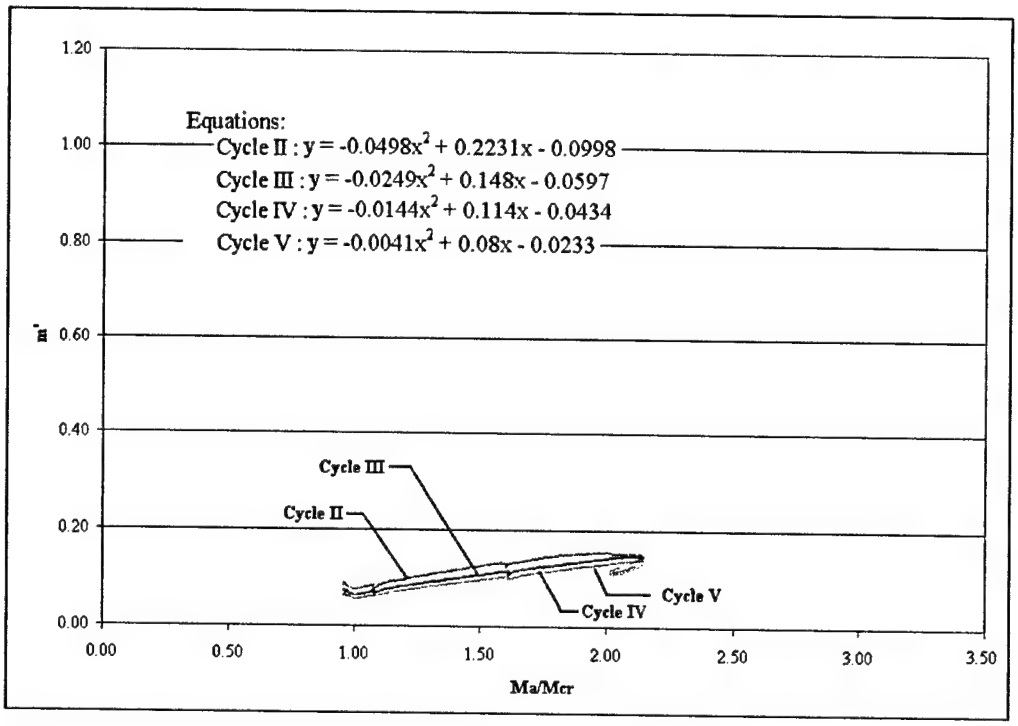

Figure C.9 - Exponent *m'* versus Applied Load (Specimen C3)

Appendix D
Cross Section Details and Sample Calculations

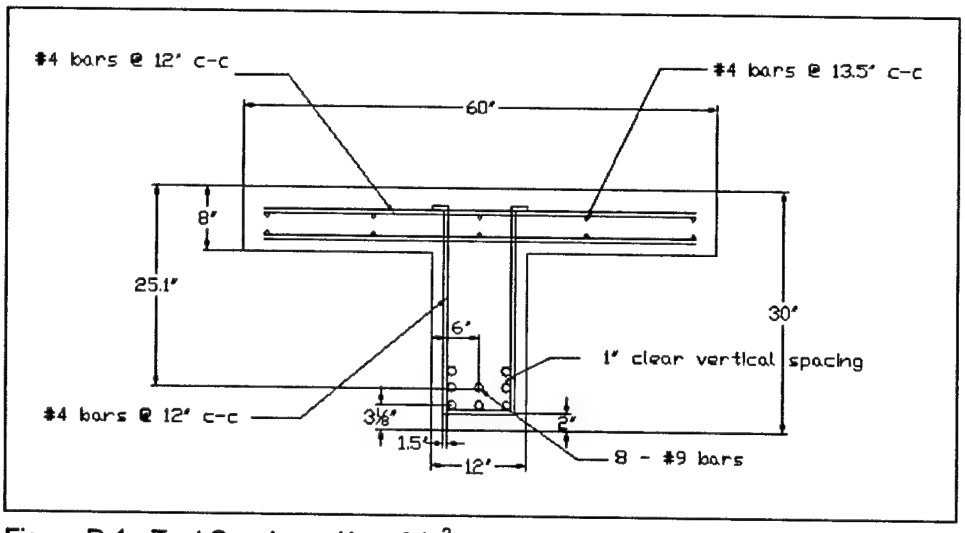

Figure D.1 - Test Specimen (A_s = 8 in^2)

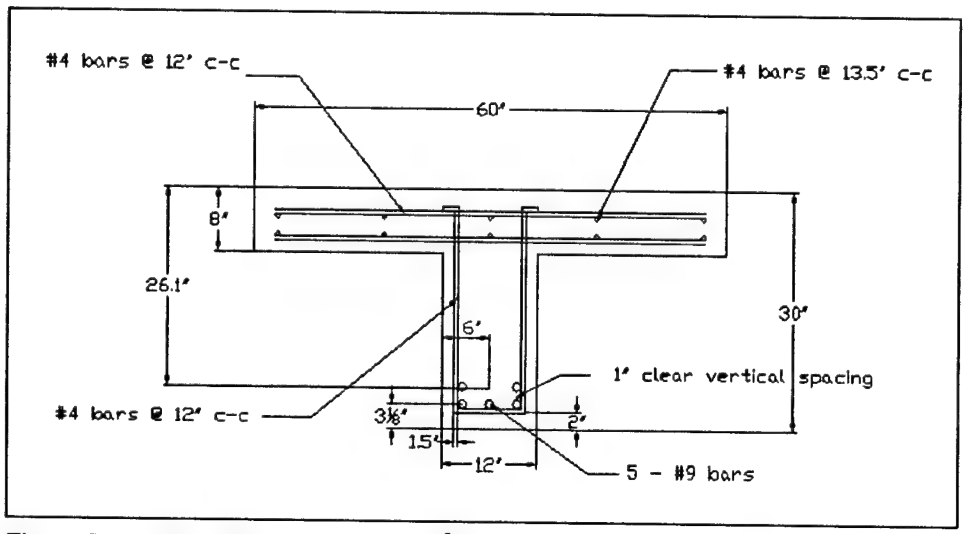

Figure D.2 - Test Specimen (A_s = 5 in^2)

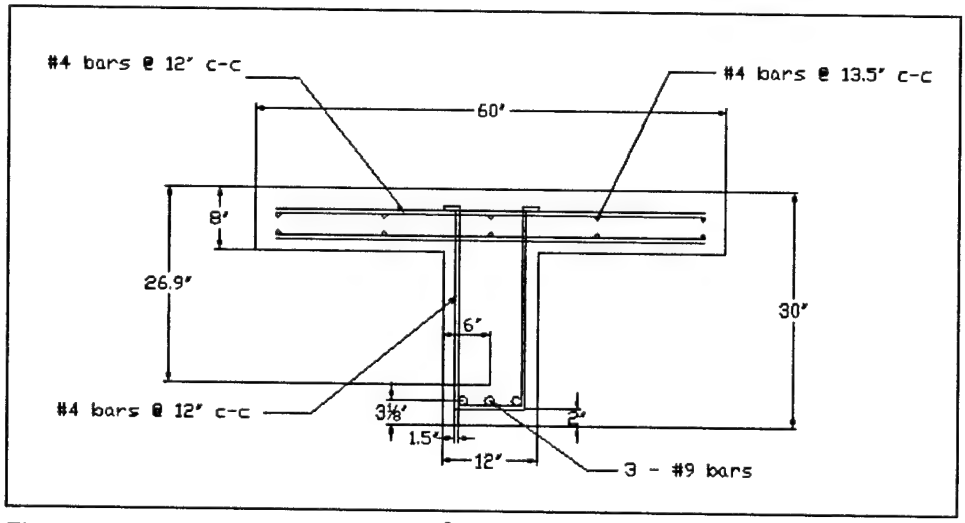

Figure D.3 - Test Specimen (A_s = 3 in^2)

Gross Cross-Section:

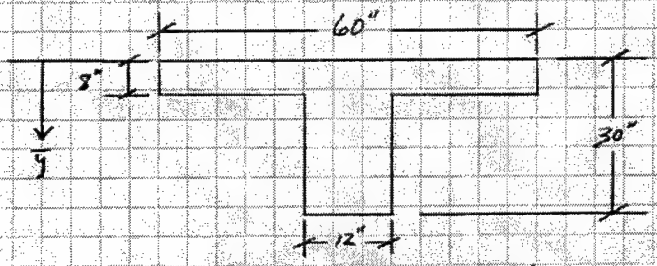

N.T.S.

Gross Section Properties:

- $A_c = (60" \times 8") + ((30"-8") * 12")$

$= 744\ in^2$

- Neutral Axis Depth:

$$\bar{y} = \frac{[60" * 8" * (8"/2)] + [(30"-8") * 12" * (8" + \frac{1}{2}(30"-8"))]}{[(60" * 8")] + [(30"-8") * 12"]}$$

$= 9.32"$

- Gross Moment of Inertia:

$$I_g = \left[\frac{60" * (8")^3}{12} + 60" * 8" * \left(9.32" - \left(\frac{8.0"}{2}\right)\right)^2\right] + \left[\frac{12" * (9.32" - 8.0")^3}{3}\right] + \left[\frac{12" * (30" - 9.32")^3}{3}\right]$$

$= 51530\ in^4$

Material Specific Calculations:

- for example:

$f'_c = 4000$ psi (Concrete Compressive Strength)

$f_y = 60\,000$ psi (Reinforcing Steel Yield Strength)

- Concrete Modulus of Elasticity

$E_c = 57000\sqrt{f'_c} = 3605$ ksi

- Concrete Modulus of Rupture

$f_r = 7.5\sqrt{f'_c} = 474$ psi

- Cracking Moment

$$M_{cr} = \frac{f_r I_g}{y_t} = \frac{474 \text{ psi} * 51530 \text{ in}^4}{(30" - 9.32")}$$

$= 98.5$ k·ft

- Modular Ratio

$$n = \frac{E_s}{E_c} = \frac{29000 \text{ ksi}}{3605 \text{ ksi}} = 8$$

Reinforcement Specific Calculations

- for example:

$A_s = 8.0\ in^2$ (Area of Steel Reinforcement)

- Effective Depth

$d = 25.1"$ (2" clear cover + #4 stirrup + ½(#9 bar))

- Reinforcement Ratio

$$\rho = \frac{A_s}{b * d} = \frac{8.0\ in^2}{12" * 25.1"} * 100 = 2.66\%$$

- Cracked Moment of Inertia

$$b * t_f * (t_f/2) = n A_s (d - t_f)$$

$$60" * 8" * (8"/2) = 8 * 8.0\ in^2 * (25.1" - 8")$$

$$1920\ in^3 > 1094\ in^3$$

$\therefore$ PNA in Flange

$$\Sigma M_{PNA} = 0$$

$$60" * \frac{y^2}{2} = 8 * 8.0\ in^2 * (25.1" - y)$$

$$30y^2 + 64y - 1606.4 = 0$$

$$y = 6.33"$$

$$I_{cr} = \frac{60" * (6.33")^3}{3} + 8 * 8.0\ in^2 * (25.1" - 6.33")^2$$

$$= 27621\ in^4 \quad (4)$$

· Minimum Reinforcement [ACI 1999]

$\phi M_n \geq 1.2 M_{cr}$

$\phi M_n \geq 1.2 * 98.5 \text{ k·ft} = 118.2 \text{ k·ft}$

$\therefore 118.2 \text{ k·ft} = A_{s(MIN)} * f_y * jd$

Assume $jd = 25.1"$

$A_{s(MIN)} = 0.94 \text{ in}^2$

· Maximum Reinforcement [McGregor 1999]

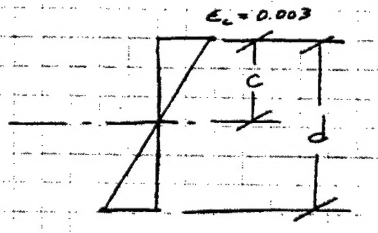

$\epsilon_y = \frac{60000 \text{ psi}}{29000 \text{ psi}} = 0.0207$

$\frac{C_b}{0.003} = \frac{25.1"}{0.003 + 0.0207}$

$C_b = 14.85"$

$a_b = 0.85 * 14.85" = 12.63"$ ∴ Compression In Flange

Maximum Reinforcement cont.' (Balanced Properties)

$A_{cb} = (60" * 8") + (12" * (12.63" - 8")) = 535.2 \text{ in}^2$

$C = 0.85 * 4 \text{ ksi} * 535.5 \text{ in}^2$

$= 1821^K$

$A_{sb} = \frac{1821^K}{60 \text{ ksi}} = 30.4 \text{ in}^2$

$A_{s(MAX)} = 0.75 A_{sb} = 22.8 \text{ in}^2$

REPORT DOCUMENTATION PAGE

Form Approved
OMB No. 0704-0188

1. REPORT DATE *(DD-MM-YYYY)*	2. REPORT TYPE	3. DATES COVERED *(From - To)*
August 2003	Final report	

4. TITLE AND SUBTITLE

A Study of Effective Moment of Inertia Models for Full-Scale Reinforced Concrete T-Beams Subjected to a Tandem-Axle Load Configuration

5a. CONTRACT NUMBER

5b. GRANT NUMBER

5c. PROGRAM ELEMENT NUMBER

6. AUTHOR(S)

Joseph E. Wickline, Thomas E. Cousins, Yazmin Seda-Sanabria

5d. PROJECT NUMBER

5e. TASK NUMBER

5f. WORK UNIT NUMBER
TE004

7. PERFORMING ORGANIZATION NAME(S) AND ADDRESS(ES)

Virginia Polytechnic Institute and State University
Blacksburg, VA 24061;

U.S. Army Engineer Research and Development Center
Geotechnical and Structures Laboratory
3909 Halls Ferry Road
Vicksburg, MS 39180-6199

8. PERFORMING ORGANIZATION REPORT NUMBER

ERDC/GSL TR-03-12

9. SPONSORING / MONITORING AGENCY NAME(S) AND ADDRESS(ES)

U.S. Army Corps of Engineers
Washington, DC 20314-1000

10. SPONSOR/MONITOR'S ACRONYM(S)

11. SPONSOR/MONITOR'S REPORT NUMBER(S)

12. DISTRIBUTION / AVAILABILITY STATEMENT

Approved for public release; distribution is unlimited.

13. SUPPLEMENTARY NOTES

14. ABSTRACT

This study focuses on some of the research efforts from the U.S. Army Engineer Research and Development Center (ERDC) in developing more accurate procedures for the estimation of the load-carrying capacity of in-service fixed bridges, in particular, of reinforced concrete T-beam bridges. This bridge type represents a stumbling block for U.S. Army field engineers whenever they are faced with unknown important parameters for load capacity estimation such as the amount and location of the flexural reinforcement in the T-beam girder cross sections.

Research personnel from the ERDC in collaboration with personnel from the Virginia Polytechnic Institute and State University worked in the development of a procedure that is potentially more accurate, can be quickly executed in the field, and is relatively easy to use by military engineers. The evaluation procedure presented herein provides a methodology for transition between the quantity of flexural reinforcement in a reinforced concrete T-beam and the member's actual moment of inertia.

This report is aimed at the evaluation of the accuracy of selected, effective moment of inertia models as a component in the proposed evaluation procedure. The accuracy of the selected models is evaluated using laboratory test data generated from an experimental program detailed herein, which included the load testing of full-scale reinforced concrete T-beams. The test specimens were subjected to a closely spaced, tandem-axle load configuration, which represents a typical load configuration in military equipment.

15. SUBJECT TERMS

Bridge
Effective Moment of Inertia
T-Beam
Reinforced Concrete

16. SECURITY CLASSIFICATION OF:			17. LIMITATION OF ABSTRACT	18. NUMBER OF PAGES	19a. NAME OF RESPONSIBLE PERSON
a. REPORT	b. ABSTRACT	c. THIS PAGE			19b. TELEPHONE NUMBER *(include area code)*
UNCLASSIFIED	UNCLASSIFIED	UNCLASSIFIED		101	